The Role of Specific JNK Isoforms in

Huntington's Disease Pathogenesis

BY

INA HAN LEE
B.A. (University of California, Berkeley) 1999

THESIS

Submitted in partial fulfillment of the requirements
for the degree of Doctor of Philosophy in Neuroscience
in the Graduate College of the
University of Illinois at Chicago, 2014

Chicago, Illinois

Defense Committee:
Larry Tobacman, Chair, Physiology and Biophysics
Scott T. Brady, Advisor
Jonathan Art
Karen Colley, Biochemistry and Molecular Genetics
Daniel Corcos, Kinesiology and Nutrition
John O'Bryan, Pharmacology

To my PuoPuo,

Wun May Lau,

who escaped foot-binding, was the first woman in her family to attend college,

and survived a world war to nurse her daughter's daughter back to life.

ACKNOWLEDGMENTS

I want to thank Matt, Sungkyong, Erin, and beloved Agnieszka. I thank my committee for their experience, wisdom, and patience. I thank those who fight the good fight, and do what is ethical and what is right. I thank the MSTP for all their support through these years. And I thank Kevin for everything.

PUBLICATION PERMISSIONS

Portions of Chapters 1, 2, and 5, including Figures 1 and 2, have been published previously in the Journal of Neurochemistry. Permissions have been obtained as documented in the Appendices.

TABLE OF CONTENTS

TABLE OF CONTENTS (continued)

LIST OF TABLES

LIST OF FIGURES

LIST OF ABBREVIATIONS

AR	androgen receptor
BDNF	brain-derived neurotrophic factor
cDNA	complementary deoxyribonucleic acid
DHC	dynein heavy chain
DIC	dynein intermediate chain
DLC	dynein light chain
HD	Huntington's Disease
Htt	huntingtin protein
IRES	internal ribosomal entry sequence
JIP	JNK interacting protein
JNK	c-Jun N-terminus Kinase
KHC	kinesin heavy chain
KLC	kinesin light chain
MAPK	mitogen activated protein kinase
MBO	membrane-bound organelle
MKK	mitogen activated protein kinase kinase
MLK	mixed lineage kinase
mRNA	messenger ribonucleic acid
MSN	medium spiny neuron
MT	microtubule
N2a	Neuro-2a
PolyQ	polyglutamine
qPCR	quantitative polymerase chain reaction
RNAi	RNA interference
SAPK	stress activated protein kinase
SBMA	spinal bulbar muscular atrophy
SCA	spinocerebellar ataxia
shRNA	short hairpin ribonucleic acid

SUMMARY

Huntington's disease (HD) is a devastating neurodegenerative disease caused by a mutation on the *IT15* gene coding for the *huntingtin* (Htt) protein [3]. The Htt mutation entails an expansion of a polymorphic polyglutamine (polyQ) tract located near the N-terminus of the protein. While the polyQ tract in wild-type, non-pathogenic Htt (wt-Htt) ranges from 6 to 35 glutamines, variants with 36 or more glutamines define a mutant allele encoding pathogenic Htt (polyQ-Htt) [4, 5]. HD is inherited in an autosomal-dominant manner with 100% penetrance, and typically presents with clinical symptoms in adulthood. These symptoms include deficits in both motor and cognitive functions that increase in severity throughout the duration of the patient's life [6]. Motor impersistence (the inability to maintain voluntary muscle contractions) represents a major clinical feature of HD that correlates well with disease progression [7]. Also, involuntary, arrhythmic limb movements termed "chorea" represent a common clinical motor phenotype in most, but not all, HD patients [8]. These dancelike movements were considered signature features in the original description of the disease as "Huntington's chorea" [9]. In addition to the progressive decline in motor function, non-motor disturbances such as cognitive impairments, personality changes, depression, and psychosis are commonly seen, and are often considered even more debilitating than the motor deficits [6]. Neurodegeneration in HD patients occurs mainly in the striatum [10], and likely manifests as the motor deficits in the disease. A significant degree of cortical degeneration is also present, to which the non-motor symptoms can likely be attributed [11, 12].

The preferential vulnerability of striatal neurons in HD sharply contrasts with the ubiquitous expression of Htt [13-15], suggesting that alterations in one or more cellular processes

particularly important for the function and survival of these neurons play a central role in HD pathogenesis. The unique morphology of neurons renders them distinctly vulnerable to deregulation of mechanisms underlying axonal function and maintenance, including the axonal transport of membrane-bound organelles (MBO) and kinase-based signaling mechanisms [16, 17]. PolyQ-Htt has been shown to inhibit MBO axonal transport in squid axoplasm [18] and mammalian cultures [19], but the molecular mechanism of polyQ-Htt induced inhibition on axonal transport is still unclear. Various independent reports showed activation of the c-Jun N-terminus kinase (JNK) pathway by polyQ-Htt, and a protective effect of JNK inhibition in cellular and animal HD models. Previous data from our lab identified axon-autonomous effects of polyQ-Htt on JNK activity and impaired axonal transport of MBO [18]. Studies using a knock-in HD mouse revealed differential phosphorylation of specific JNK isoforms [20]. Perfusion of active recombinant JNKs and pharmacological inhibitors in squid axoplasm also suggested different degrees of participation from specific JNK isoforms in polyQ-Htt induced axonal transport deficits. Furthermore, mass spectrometry studies found that recombinant JNK3 directly phosphorylates kinesin-1 on Ser176, which lies within the microtubule-binding region of kinesin-1. Reductions in kinesin-based axonal transport have been shown to cause a dying-back pattern of degeneration of axons resulting in disease in humans [21], which is characteristic of the neurodegeneration in HD [22-24]. These data strongly suggest that specific JNK isoforms play a role in the axonal transport deficits observed in HD. However, due to the nature of the pharmacological agents used, off-target effects were inevitable [25-28], and any observations from the previously mentioned studies could not conclusively be attributed to any single JNK isoform.

In the research presented here, we proposed that polyQ-Htt induced activation of JNK3, but not JNK1, is a critical pathogenic event underlying axonal degeneration in HD. In order to overcome the non-specific nature of pharmacological agents, we generated a mammalian cell model using target-specific RNA interference (RNAi) technology to evaluate the roles of specific JNK isoforms in polyQ-Htt induced axonal pathology. Lentiviral delivery of isoform-specific JNK shRNAs was used to knock down either JNK1 or JNK3 in mouse neuroblastoma cells stably expressing wt- or polyQ-Htt. To evaluate the contribution of single JNK isoforms to polyQ-Htt induced axonal transport deficits, we analyzed differentiated cells under each set of test conditions by neurite outgrowth analysis and mitochondrial density. Our results yielded statistically significant evidence that JNK3, and not JNK1, mediates polyQ-Htt induced deficits in both outgrowth and mitochondrial transport of neurites.

At present, there are no treatments for HD that are effective in reversing, halting, or even slowing disease progression [29]. Current treatment consists of symptom management with anti-seizure and antipsychotic medications, and lifestyle management, and HD patients typically die within 20 years of diagnosis from various complications such as accidents, aspiration and dysphagia [6]. While a definitive link between the Htt gene mutation and disease was established nearly 20 years ago, the molecular mechanisms underlying HD pathogenesis remain elusive. It is our hope that our contribution here may help advance the understanding of this devastating disease towards a meaningful therapy.

CHAPTER 1

INTRODUCTION AND AIMS

Huntington's Disease (HD) is caused by expansion of a polyglutamine (polyQ) tract in the *huntingtin* (Htt) protein. The polymorphic polyQ stretch in wild-type, non-pathogenic Htt (wt-Htt) ranges from 6 to 35 Qs, whereas Htt variants with 36 or more Qs define an HD allele (polyQ-Htt) [30]. Expression of polyQ-Htt results in adult onset degeneration of selected neuronal populations, particularly in the striatum [10]. Pathological observations from HD patients indicate that neurons affected in HD undergo a "dying back" pattern of degeneration, which is characterized by early alterations in synaptic and axonal function prior to neuronal cell death [31]. However, mechanisms underlying axonal degeneration in HD remain unknown.

The preferential vulnerability of striatal neurons in HD sharply contrasts with the ubiquitous expression of Htt [13-15], suggesting that alterations in one or more cellular processes particularly important for the function and survival of these neurons play a central role in HD pathogenesis. The unique morphology of neurons renders them distinctly vulnerable to alterations in mechanisms underlying axonal function and maintenance, including the axonal transport of membrane-bound organelles (MBO) and kinase-based signaling mechanisms [16, 17]. PolyQ-Htt has been shown to inhibit MBO axonal transport in squid axoplasm [18] and mammalian cultures [19], but the molecular mechanism of polyQ-Htt induced inhibition on axonal transport is still unclear. Aberrant patterns of protein phosphorylation have been found in association with HD, and led to studies demonstrating abnormal polyQ-Htt induced activation of protein kinases and kinase-dependent alterations in MBO axonal transport. Various independent

reports showed activation of c-Jun N-terminus kinase (JNK) pathway by polyQ-Htt, and a protective effect of JNK inhibition in cellular and animal HD models. Specifically, these studies indicate that JNK plays a role in polyQ-Htt induced impairment of MBO axonal transport. Findings from these studies also suggest that neuron-specific JNK isoform 3 (JNK3), and not ubiquitous JNK1, mediates polyQ-Htt induced axonal degeneration through impairment of axonal transport. *Based on these findings, we propose that polyQ-Htt induced activation of JNK3, but not JNK1, is a critical pathogenic event underlying axonal degeneration in HD*. Work proposed here will address the following aims:

Aim 1. To generate a mammalian cell model for the evaluation of specific JNK isoforms in polyQ-Htt induced axonal transport dysfunction. Previous data from our laboratory identified axon-autonomous effects of polyQ-Htt on JNK activity and impaired axonal transport of MBO [18, 20]. Specifically, perfusion of recombinant active JNK3 into squid giant axoplasm impaired both anterograde and retrograde transport rates, mimicking the effects of polyQ-Htt, while JNK1 did not. The perfusion of various pharmacological inhibitors confirmed participation of the JNK pathway, and further suggested differential roles of JNK isoforms, in polyQ-Htt induced pathology. However, due to the nature of the pharmacological agents used, off-target effects were inevitable [25-28], and any observations made could not conclusively be attributed to any single JNK isoform. In order to overcome the non-specific nature of pharmacological agents, we aim to generate a mammalian cell model using target-specific RNA interference (RNAi) technology to evaluate the roles of specific JNK isoforms in polyQ-Htt induced pathology.

Aim 2. To evaluate the role of specific JNK isoforms in polyQ-Htt induced axonal degeneration. Studies using a knock-in HD mouse revealed differential phosphorylation of specific JNK isoforms induced by polyQ-Htt [20]. Perfusion of active recombinant JNKs and pharmacological inhibitors also suggested different degrees of participation from specific JNK isoforms in polyQ-Htt induced axonal transport deficits. Furthermore, mass spectrometry studies found that recombinant JNK3 directly phosphorylates kinesin-1 on Ser176, which lies within the microtubule-binding region of kinesin-1. Reductions in kinesin-based axonal transport have been shown to cause a dying-back degeneration of axons resulting in disease in humans [21], which is characteristic of the neurodegeneration in HD [22-24]. Based on these findings, we hypothesize that JNK3, but not JNK1, mediates polyQ-Htt induced impairment of axonal transport, resulting in axonal dysfunction. The use of RNAi to selectively knock down specific JNK isoforms in polyQ-Htt expressing mammalian neuroblasts will allow us to discern the contribution of different JNK isoforms to polyQ-Htt induced axonal degeneration.

CHAPTER 2

BACKGROUND AND LITERATURE REVIEW

2.1 HUNTINGTON'S DISEASE

2.1.1 OVERVIEW

Huntington's disease (HD) is a devastating neurodegenerative disease caused by a mutation on the *IT15* gene coding for the huntingtin (Htt) protein [3]. The Htt mutation entails an expansion of a polymorphic polyglutamine (polyQ) tract located near the N-terminus of the protein. While the polyQ tract in wild-type, non-pathogenic Htt (wt-Htt) ranges from 6 to 35 glutamines, variants with 36 or more glutamines define a mutant allele encoding pathogenic Htt (polyQ-Htt) [4, 5]. HD is inherited in an autosomal-dominant manner with 100% penetrance, and typically presents with clinical symptoms in adulthood. These symptoms include deficits in both motor and cognitive functions that increase in severity throughout the duration of the patient's life [6]. Motor impersistence (the inability to maintain voluntary muscle contractions) represents a major clinical feature of HD that correlates well with disease progression [7]. Also, involuntary, arrhythmic limb movements termed "chorea" represent a common clinical motor phenotype in most, but not all, HD patients [8]. These dancelike movements were considered signature features in the original description of the disease as "Huntington's chorea" [9]. In addition to the progressive decline in motor function, non-motor disturbances such as cognitive impairments, personality changes, depression, and behavioral disturbances are commonly seen, and are often considered even more debilitating than the motor deficits [6]. Neurodegeneration in HD patients occurs mainly in the striatum [10], and likely manifests as the motor deficits in the disease. A significant degree of cortical degeneration is also present, to which the non-motor

symptoms can likely be attributed [11, 12]. At present, there are no treatments for HD that are effective in reversing, halting, or even slowing disease progression [29]. Current treatment consists of symptom management with anti-seizure and antipsychotic medications, and lifestyle management, and HD patients typically die within 20 years of diagnosis from various complications such as accidents, aspiration and dysphagia [6]. While a definitive link between the Htt gene mutation and disease was established nearly 20 years ago, the molecular mechanisms underlying HD pathogenesis remain elusive.

2.1.2. Cell Types Affected in HD

The basal ganglia comprise a set of subcortical brain structures involved in various aspects of motor control and cognition [32, 33]. Within the basal ganglia, the neurodegenerative process characteristic of HD typically begins in the striatum [10], which serves to integrate and filter multiple input pathways originating in different cortical regions [33]. Information processed in the striatum ultimately returns to the cerebral cortex to complete the corticobasal ganglia-thalamocortical loop [34].

Within the striatum, signs of pathology initially appear in the caudate nucleus, with reactive gliosis and neurons showing neuritic dystrophy. As the disease progresses, these alterations advance along the caudal-rostral, and dorsal-ventral direction towards the putamen [35]. The prominent reduction in the size of the caudate nucleus and the secondary enlargement of the lateral ventricles typical of advanced HD patients results from degeneration of neurons within these brain structures. Although less marked than in the striatum, a significant loss of

neurons is also observed in the cerebral cortex of HD patients, including frontal, parietal, and temporal regions [36, 37].

At the cellular level, HD is characterized by differential vulnerability of specific neuronal subpopulations within the striatum and the cerebral cortex (see Figure 1). The striatum represents the major input stage of the basal ganglia, being mainly composed of projection neurons (up to 95% of total striatal neurons) and a much smaller number of interneurons (approximately 5%). Golgi staining methods and electron microscopic studies identified and classified various subtypes of projection neurons and interneurons with unique morphological and biochemical characteristics[38-40]. Striatal projection neurons are all GABAergic and morphologically characterized by a long axon, medium-sized cell bodies, and spiny dendrites, hence the commonly used term *medium spiny neurons* (MSNs) [38, 39, 41]. MSNs project their axons over long distances to the globus pallidus (GP) and the substantia nigra pars reticulata (SNr), which are the main "output" structures of the basal ganglia (see Figure 1). Striatal interneurons represent key elements of the local striatal circuitry, displaying a wide range of morphological and biochemical heterogeneity [40, 42]. Striatal interneurons have short axons, medium to very large-sized cell bodies, and display extensive dendritic arborization, making abundant synaptic contacts with multiple MSNs [43, 44]. Intriguingly, MSNs represent the main and earliest cell type affected in HD, whereas striatal interneurons are typically unaffected or only mildly affected at late stages of the disease, despite their smaller numbers in the striatum.

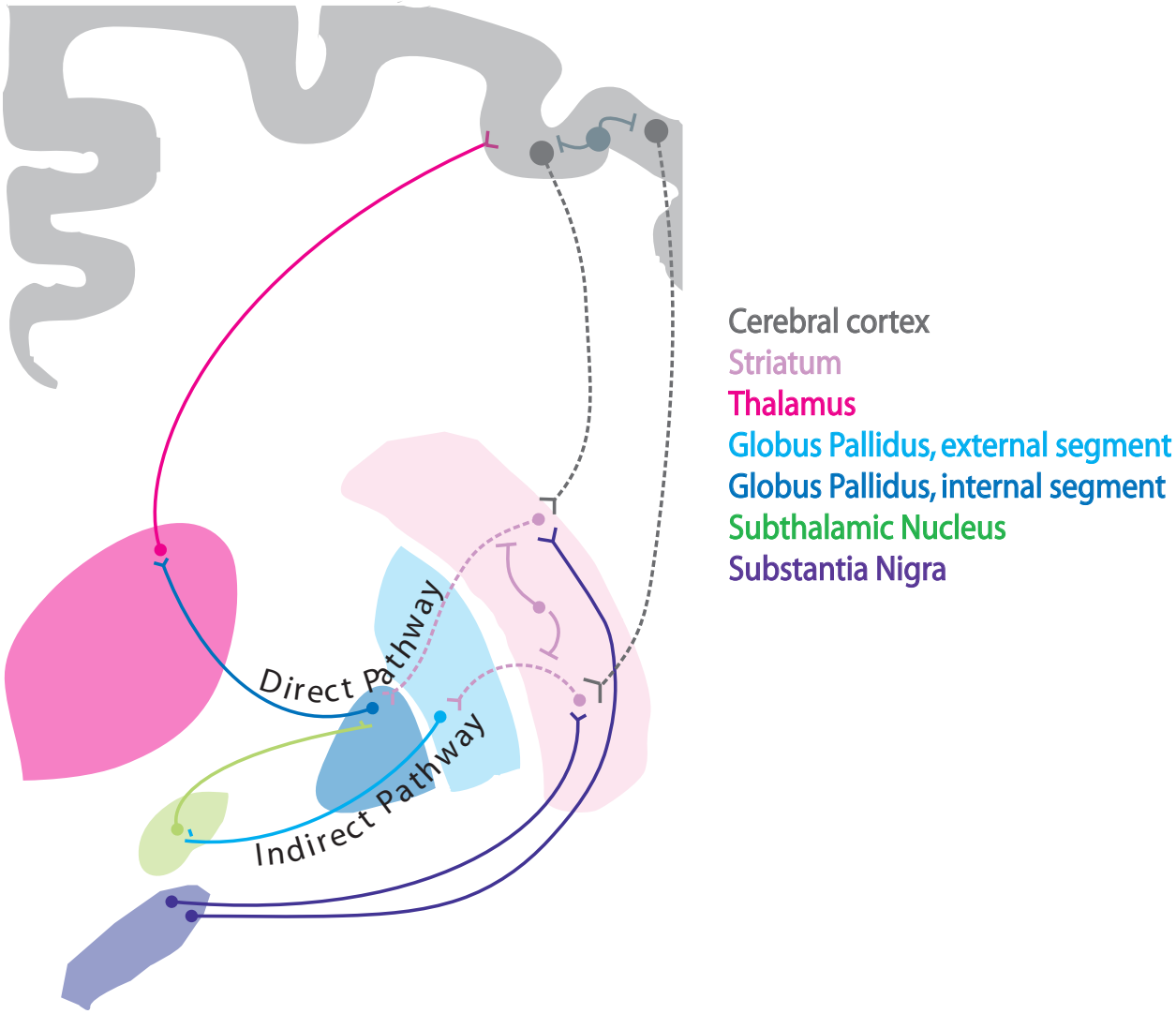

Figure 1. Overview of cell types affected in HD. A subset of projection neurons in the striatum and the cortex (represented by dashed lines) are particularly vulnerable in HD. These include medium spiny neurons (MSNs, pink dashed lines) of the striatum and large pyramidal projection neurons in cortical layers V, VI and III of the cerebral cortex (gray dashed lines). MSNs in the *indirect pathway* of the basal ganglia project to the external segment of the globus pallidus (GPe) and are affected early in the course of the disease. As HD progresses, MSNs projecting to the internal segment of the globus pallidus (GPi) via the *direct pathway* and cortical pyramidal cells projecting to the striatum are also impaired. Remarkably, most interneurons in both the striatum (pink solid lines) and the cerebral cortex (gray solid lines) are largely spared. This morphological and functional difference has been proposed to play a role in the differential vulnerability of neurons observed in HD [1], as well as other neurodegenerative diseases [45, 46]. Abbreviations: medium spiny neuron (MSN); subthalamic nucleus (STN); internal segment of the globus pallidus (GPi); external segment of the globus pallidus (GPe); substantia nigra (SN).

The increased vulnerability of MSNs within the HD striatum further extends to specific MSNs subtypes, as defined by their projection targets and neurochemical content [33]. Based on their projection targets, MSNs in the striatum can be divided into two main groups: *a*) MSNs in the "direct" (or striatonigral) pathway, which project their axons monosynaptically to the internal segment of the GP (GPi) or to the SNr [47]; and *b)* MSNs in the "indirect" (or striatopallidal) pathway, which project axons that polysynaptically contact the external segment of the GP (GPe). Intriguingly, MSNs in the "indirect pathway" are affected at earlier stages and to a greater extent than MSNs in the "direct pathway" [11, 48, 49]. Early functional abnormalities in the indirect pathway have been associated with development of the chorea-like movements in HD [50, 51]. Degeneration of MSNs of the direct pathway late in the course of HD manifests as rigidity and bradykinesia [52] reminiscent of symptoms seen in Parkinson's disease, another neurodegenerative disease that affects the basal ganglia.

Albeit less pronounced than in the striatum, differential vulnerability and loss of selected neuronal populations is also readily observed in the cerebral cortex of HD patients. Specifically, large pyramidal projection neurons in cortical layers V, VI and to a lesser extent, layer III, are preferentially lost [53, 54]. Axons emanating from cortical projection neurons in layers V and VI innervate the striatum. As in the striatum, there is remarkable preservation of cortical interneurons in HD [53, 55].

2.1.3. Differential Vulnerability of Affected Cell Populations in HD

The earlier and more pronounced degeneration of specific neuronal populations within the striatum and cortex observed in HD fueled the use of the words *"selective neuronal*

vulnerability" by many investigators[56-58] . However, the unique cellular topography of HD pathology does not mean that the toxic effects of polyQ-Htt are *limited* to selected neuronal populations. Supporting this idea, a large body of pathological and experimental evidence demonstrates that polyQ-Htt expression can elicit toxic effects in additional neuronal cell types and even in some non-neuronal cells. Pathological examination in advanced HD patients revealed degeneration of neurons in other areas of the basal ganglia, as well as the hippocampus, the angular gyrus in the parietal lobe, and the lateral tuberal nuclei of the hypothalamus [10, 59-61]. Further, pronounced neuronal loss has been observed in the cerebellum of patients with juvenile HD onset [62, 63]. Although some of these neuronal losses may reflect secondary neuronal damage due to deafferentation, experiments involving tissue-specific overexpression of polyQ-Htt *in vivo* demonstrated that polyQ-Htt expression can promote functional abnormalities in many neurons not typically affected in HD [64, 65]. Additionally, various non-neuronal tissues, including skeletal muscle and pancreatic islet cells, appear to be affected in peripheral tissues of HD patients and animal HD models [66]. Finally, a plethora of studies document functional abnormalities and decreased cell survival associated with the expression of pathogenic polyQ-Htt constructs across a range of cultured cell types including mouse [67, 68] and human [69] neuroblastoma, African green monkey kidney (COS-7)[70]) and PC12 cells [71], among others. Taken together, these observations indicate that the toxic effects of polyQ-Htt do not *selectively* affect specific neuronal populations. Instead, cell type-specific features might *differentially* render specific cell populations increasingly vulnerable to polyQ-Htt-induced toxicity.

2.1.4. DYING BACK NEURODEGENERATION

A discussion of potential pathogenic mechanisms and cellular features modulating polyQ-Htt toxicity requires a revision of the sequence of pathogenic events in neurons affected. Historically, our understanding of the neurodegenerative process in HD was limited to the study of brain tissue harvested from HD patients *post mortem*. The marked loss of neurons observed in these tissues logically focused research efforts into cell death-related mechanisms [72, 73], and the development of HD animal models based on acute intoxication and induction of cell death in the striatum. More recently, the development of various knock-in rodent HD models revealed important information on earlier pathogenic events [24]. These animal models accurately reproduced the autosomal dominant pattern of inheritance as well as the major pathological characteristics of HD, including formation of Htt aggregates, the development of motor and behavioral symptoms, and the differential vulnerability of discrete neuronal populations [74]. Variations in disease onset and severity among HD models can be attributed to differences in length of the polyQ tract, promoters driving transgene expression, and size of the exogenous Htt transgene introduced [24, 74, 75]. Regardless of these variations, a common theme emerged from detailed pathological, electrophysiological and behavioral analysis of these animals. All models analyzed thus far have shown various degrees of behavioral and motor abnormalities well before apparent neuronal loss [22-24]. For example, motor defects reminiscent of the HD human phenotype (i.e., increased motor activity, gait abnormalities, and altered stride length) were observed in HD transgenic mice models expressing truncated polyQ-Htt constructs, including R6/2 mice [76-78], N171-82Q mice [79], and a transgenic rat model expressing a truncated Htt with 51 glutamine repeats [80]. Similar findings have been reported in various knock-in HD

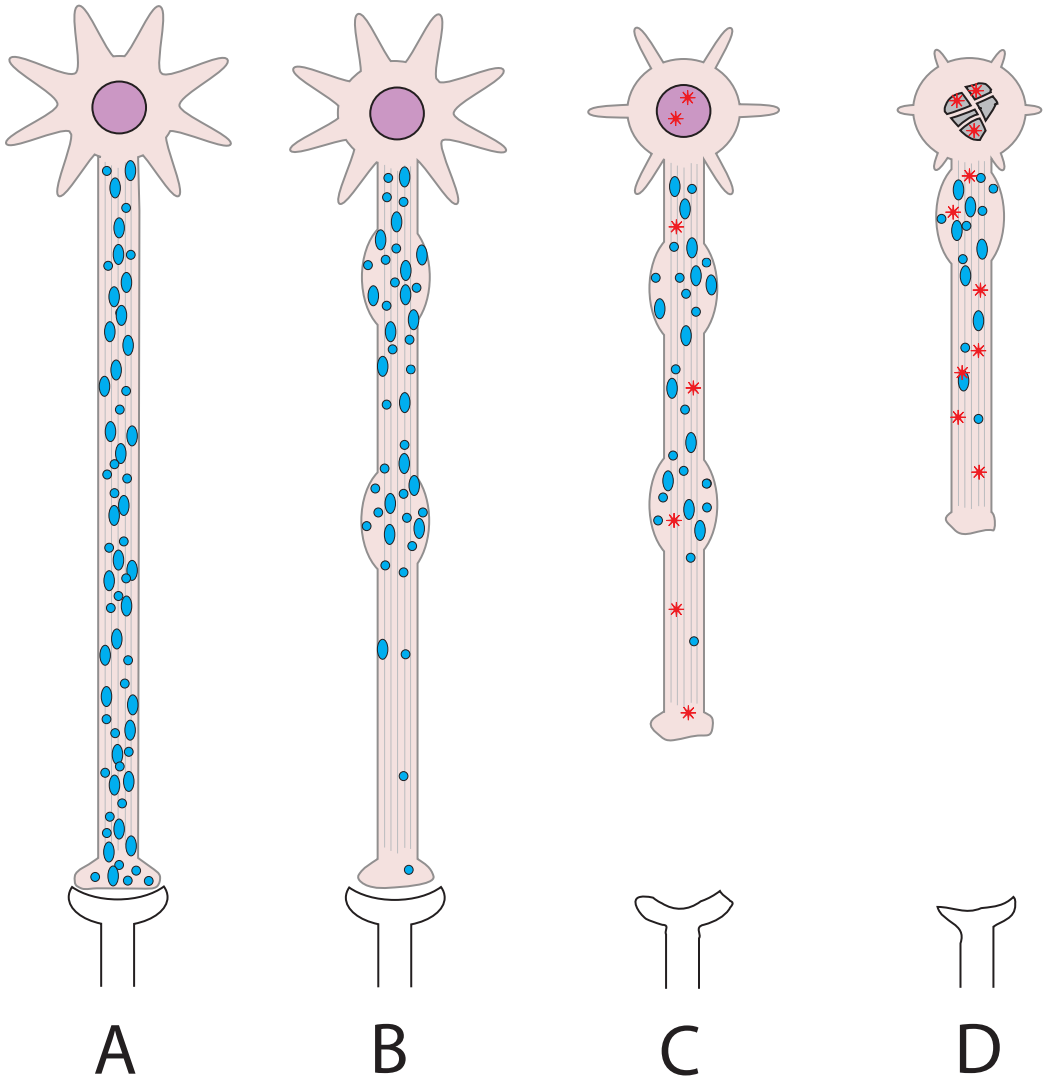

Figure 2. Dying back pattern of neuronal degeneration in HD. A) Neurons undergo normal development, retaining normal connectivity and functionality prior to disease state. B) Affected neurons begin to exhibit signs of synaptic and axonal alterations early in the disease process, including abnormalities in the phosphorylation of axonal proteins, abnormal accumulation of membrane-bounded organelles (blue circles) in axons [81-84], and loss of synaptic proteins [85]. These changes correspond to functional impairments in synaptic function that appear very early on, even in presymptomatic stages [22, 86]. C) Axonal degeneration steadily advances in a retrograde fashion, and nuclear/neuritic Htt aggregates (red stars) become evident. As HD progresses, dysfunction of striatal and corticostriatal projection neurons manifest in clinical symptoms such as motor deficits and cognitive decline long before evidence of cell death [87]. D) Disruption of functional synaptic connectivity and eventual loss of appropriate trophic support [2] ultimately result in cell death, likely by apoptosis-related mechanisms [88].

animal models expressing polyQ-Htt at endogenous levels in its appropriate genomic context [24]. Remarkably, the behavioral abnormalities in knock-in HD animal models were detected in the absence of neuronal loss [24] or formation of polyQ-Htt aggregates. The relevance of these observations to HD is highlighted by functional MRI imaging studies that reveal early changes in neuronal function in presymptomatic HD patients [89], and studies indicating that early manifestation of motor deficits in HD patients results from neuronal dysfunction and not cell loss [90].

Providing a structural basis for the early alterations in neuronal function described above, histopathological studies documented a marked reduction in the number of axonal fibers and synaptic proteins early in the course of HD [11, 22, 85, 91]. Alterations in axonal connectivity and synaptic function were consistent with the progressive electrophysiological disturbances reported in association with polyQ-Htt expression [92-95]. Diffusion tensor imaging studies further demonstrated early signs of axonal degeneration in white matter of presymptomatic HD patients [96, 97]. Together, these observations suggested the existence of critical pathogenic events affecting neuronal functionality *prior* to cell death in HD.

The accumulated evidence indicates that alterations in neuronal connectivity play a major role in HD pathology, and that neurons affected in HD follow a dying back pattern of degeneration[31, 91, 98, 99] (see Figure 2). In sum, neurons undergo normal development, establishing and retaining functional connectivity into adulthood. Affected neurons then develop signs of synaptic and axonal dysfunction early in the disease process, including abnormal phosphorylation of axonal proteins and accumulation of organelles [81-84], as well as loss of synaptic proteins [85]. These axonosynaptic deficits manifest as clinical motor and cognitive

symptoms long before evidence of cell death [87]. Axonal degeneration steadily progresses and ultimately, loss of functional connectivity and appropriate target-derived trophic [2]support results in cell death, likely by apoptosis [88].

2.2 Proposed Mechanisms of HD Pathogenesis

Htt is ubiquitously expressed throughout the body, and this also holds true for polyQ-Htt in the disease state [13-15]. Despite the presence of polyQ-Htt in every tissue of the body in HD patients, degeneration has only been found in neuronal tissue, suggesting that specific properties of neurons render them vulnerable to the affects of polyQ-Htt. The ubiquitous distribution of Htt and the lack of sequence homology with other proteins reveals little information on the normal physiological function of this protein, which remains poorly understood. There is some evidence that Htt participates in development and neurogenesis [100, 101], and is also necessary for neural maintenance in adulthood [102]. Htt is mostly found in the cytoplasm, and associates with vesicular structures and microtubules, suggesting a role in intracellular transport of membrane-bound organelles along microtubules [103]. Along these lines, a growing number of studies demonstrate that polyQ-Htt leads to impairments in axonal transport.

The autosomal dominant heritability of HD, coupled with huntingtin knockdown and knockout experiments confirm that mutant-Htt causes disease by a gain of function mechanism. Deletion of Htt in mice results in embryonic lethality, suggesting a critical, yet unidentified role of Htt during normal development [104, 105]. In contrast, various knock-in mouse models expressing pathogenic, polyQ-expanded versions of full-length Htt at endogenous levels are viable, displaying a late onset phenotype with pathological features reminiscent of HD [24].

Viability of these knock-in mice indicate that aspects of Htt functionality relevant to embryonic development are not compromised by polyQ tract expansion. The precise contribution that potential decreases in normal Htt function play in HD pathogenesis remains unclear, but the autosomal dominant pattern of HD inheritance and other genetic evidence strongly indicate that the polyQ expansion confers a toxic gain of function [31, 106]. Consistent with this idea, several lines of experimental evidence showed polyQ-Htt expression induces alterations in critical cellular processes including transcriptional regulation, cell survival, intracellular signaling, mitochondrial function, and axonal transport, among others.

2.3 Cellular Factors Influencing PolyQ-Htt Toxicity

Projection neurons in the striatum and the cerebral cortex are major targets of the HD pathology, whereas interneurons within these structures are largely unaffected by the neurodegenerative process [11, 48, 49]. In addition, MSNs in the indirect pathway succumb earlier and to a larger extent than MSNs in the direct pathway. Differences in biochemical content, morphology and connectivity among these subpopulations could provide clues towards an explanation of their differential vulnerabilities in HD. In the case of striatal neurons, it is reasonable to speculate that one or more unique characteristics of MSNs could exacerbate the toxic effects of polyQ-Htt in these cells, and allow the insult to overcome compensatory mechanisms. Alternately, a different combination of characteristics might confer protection upon striatal interneurons against the toxic effects of polyQ-Htt. Similar supposition may apply to projection neurons and interneurons in the cortex, but mechanisms underlying the differential vulnerability of cortical neurons are rarely addressed [22, 107].

Because a molecular basis for the toxic gain of function associated with polyQ-Htt remains unknown, the contribution of cell type-specific traits in the modulation of polyQ-Htt-induced toxicity can only be speculative. However, while keeping in mind the differential vulnerability of various populations and the dying back pattern of neurodegeneration, a thorough review of cell type-specific factors in HD and HD models may reveal patterns to discern secondary pathology from primary pathogenic events.

2.3.1 HTT DISTRIBUTION, EXPRESSION LEVELS, AND SOMATIC INSTABILITY

In some familial forms of human diseases, the increased vulnerability of cell types affected can be explained by differential expression of the pathogenic gene product. Following the discovery of the Htt gene, multiple studies aimed to determine whether heterogeneities in Htt mRNA and/or protein expression could underlie the increased vulnerability of MSNs and cortical neurons in HD. However, extensive mRNA and protein expression analyses indicated that Htt is ubiquitously expressed in nearly all tissues [13, 108, 109]. Moreover, Htt expression levels were comparable in normal and HD patients[14, 110]. Immunochemical studies showed widespread distribution of Htt protein throughout the brain [111], with no evidence of increased Htt expression in brain regions most affected in HD [112, 113]. In fact, detailed studies showed that striatal interneurons, largely unaffected in HD, express higher levels of Htt than MSNs [110], strongly suggesting that differences in mutant Htt expression levels do not account for the increased vulnerability of MSNs.

Several studies in HD patients and animal models showed that the mutant CAG repeat tract in the Htt gene can undergo both inter- and intra-generational variability in expansion size[114, 115]. Studies on end-stage human HD autopsy material indicated that approximately

10% of sampled striatal cells contained hyperexpansions of over 200 repeats [116]. Further, age-dependent instability of Htt was observed in the striatum and the cerebral cortex of knock-in HD mice [115, 117]. These findings led to the proposal that increased instability of Htt's CAG expansion might contribute to the marked vulnerability of striatal neurons in HD [114]. However, increased instability of CAG repeats in the striatum was observed in other polyQ-expansion diseases, and displayed little or no striatal pathology [118, 119]. Moreover, observations from a bacterial artificial chromosome-based HD mouse model expressing polyQ-Htt with a stable CAA-CAG tract is inconsistent with a role of somatic repeat instability in HD pathogenesis [120]. More recently, comparable repeat instability in liver and striatum was shown in a HD knock-in mouse model [121], yet degeneration is not observed in the livers of HD animal models or patients. These observations argue against a direct correlation between somatic CAG expansion mosaicism and the increased vulnerability of striatal MSNs. Collectively, the evidence indicates that neither heterogeneities in Htt expression levels nor somatic instability of the Htt gene play a role in the differential vulnerability of striatal neurons affected in HD.

2.3.2. HTT AGGREGATION

Following the discovery of the Htt gene, the generation of antibodies mapping to different Htt epitopes [122] revealed that N-terminal fragments of polyQ-Htt accumulate to form microscopically visible aggregates in both the nucleus [83] and neurites [123] of some, but not all, neurons affected in HD patients [83, 124]. These aggregates are also found in a number of HD rodent models [57, 125], and have thus come to represent a major histopathological feature of HD.

Initial focus on polyQ-Htt aggregates as a pathogenic agent of HD was fueled by biochemical findings suggesting that elongated polyQ stretches form insoluble structures toxic to cells [126, 127]. Earlier work in cellular HD models based on overexpression of truncated polyQ-Htt constructs proposed a positive correlation between the abundance of polyQ-Htt aggregates and cellular toxicity [128, 129]. However, Htt toxicity and aggregation were experimentally dissociated in both cellular [130] and animal [131] HD models, and that aggregates were even predictive of decreased neuronal death [130]. At present, it remains unclear whether polyQ-Htt aggregates promote neuronal dysfunction and death, or whether polyQ-Htt aggregation represent the result of endogenous cellular mechanisms conferring protection against soluble, toxic polyQ-Htt species[132, 133].

Despite the vast body of research on polyQ-Htt aggregates, little evidence exists linking these structures to the preferential degeneration of MSNs and cortical neurons characteristic of HD. As observed in SBMA [134] and other polyQ diseases [135], a poor correlation was found between polyQ-Htt aggregation and neuronal vulnerability [136]. Moreover, the presence of polyQ-Htt aggregates in the surviving neurons of advanced HD patient brains suggested these structures might promote neuronal survival [132]. Experiments in cellular [130] and animal [131] HD models further supported this view. Finally, prominent polyQ-Htt aggregates have been reported in striatal interneurons [124], and in brain regions largely spared in HD such as the hippocampus [137, 138]. While the precise contribution of polyQ-Htt aggregation to HD pathogenesis remains unknown, no evidence definitively shows that the formation and abundance of polyQ-Htt aggregates causes cell death in HD.

2.3.3 Alterations in Gene Expression

Major advances in molecular biology and computer technology have allowed for the screening of large numbers of candidate genes in an unbiased fashion. This has facilitated numerous gene studies in transgenic HD models and HD human tissue describing polyQ-Htt-induced transcriptional alterations [139, 140]. Specifically, microarray studies screened HD-related changes in the expression levels of thousands of RNAs encoding molecular components involved in various cellular processes including calcium homeostasis, intracellular signaling, energy metabolism and the transcriptional machinery.

Several lines of evidence suggest that abnormally long polyQ repeats in HD may interfere with the normal function of cellular proteins by altering gene transcription, either by intranuclear aggregate formation or by sequestering key transcription factors [141, 142]. It has been shown that transcription factors including CREB-binding protein (CBP), TATA-binding protein (TBP), and specificity protein 1 (SP1) can be recruited to intranuclear aggregates, supporting the hypothesis that transcriptional deregulation may possibly play a role in HD pathogenesis. Interestingly, each of these transcription factors themselves contain a glutamine-rich domain which can regulate their activity [143, 144]. Indeed, it is an abnormally expanded polyglutamine tract in the androgen receptor (AR), a known nuclear transcription factor, which causes Spinal Bulbar Muscular Atrophy (SBMA). From this line of evidence, it has been proposed that the toxic gain of function conferred by polyQ-Htt may be due to an ability to mimic transcription factors, or the involvement of transcription factors in aberrant protein-protein interactions. Expanded polyQ tracts might enable polyQ-Htt to act as a repressor by

binding DNA or sequestering transcriptional factors. Conversely, they might interact with repressors to activate normally silent genes [141].

CREB binding protein (CBP) has been widely found to be sequestered by nuclear inclusions in cells expressing polyQ-expanded mutant proteins that cause DRPLA, SBMA, and SCA-3 [145-147], leading to the theory that nuclear recruitment of transcription factors by polyglutamine inclusions downregulates the expression and function of those transcription factors. There is also some evidence that CRE-regulated genes are downregulated in HD patients [148]. In mice, the conditional knockout of CREB resulted in progressive neurodegeneration in the hippocampus and striatum [149]. But contrary to this, in vivo studies of double-transgenic mice expressing polyQ-Htt and a CRE-α-galactosidase reporter construct showed an increase in phosphorylated CREB and CRE–mediated transcription [150].

Like CBP, TATA-binding protein (TBP) can be recruited into polyQ-Htt aggregates in vitro and in the brains of HD patients [151], and abnormal expansion of its polyQ region results in Spinocerebellar Ataxia-17 (SCA-17), another polyQ expansion neurodegenerative disease [152]. Specificity protein 1 (SP1)-mediated transcription is likewise disrupted by sequestering SP1 into polyQ-Htt aggregates. Furthermore, there is abnormally enhanced interaction between polyQ-Htt and SP1 in brain extracts from asymptomatic HD patients, and the association of SP1 with its coactivator $TAF_{II}130$ is decreased in comparison to healthy brains [153]. The enhanced binding of polyQ-Htt to SP1 blocked the binding of SP1 to its promoter region, thereby downregulating SP1-mediated transcription of genes known to be diminished in HD patients with HD, including the dopamine-D2-receptor gene. Overexpression of both SP1 and $TAF_{II}130$

in combination, but not either one alone, ameliorated polyQ-Htt inhibition of dopamine-D2-receptor gene expression.

In contrast, studies have also found that CBP, SP1, TBP in symptomatic HD mice were not sequestered or reduced by polyQ-Htt nuclear inclusions [154]. Also, altered expression did not correlate with the formation of nuclear inclusions in HD mice [155], and was found to occur in PC12 cells in the complete absence of nuclear inclusions [156, 157], suggesting that polyQ-Htt could alter gene expression by a mechanism other than nuclear aggregation. It has been shown that soluble polyQ-Htt can bind a number of transcription factors including CBP and SP1 [146, 147, 153]. Additionally, there is a compelling body of work demonstrating that wt-Htt normally regulates BDNF by binding repressor elements in the cytoplasm, and that polyQ-Htt fails to bind this repressor element resulting in suppression of BDNF expression [158], resulting in neurodegeneration due to lack of trophic support [2]. These studies implicate soluble polyQ-Htt, and not aggregated polyQ-Htt, as the more likely culprit. While altered gene expression no doubt contributes to the disease pathology, it is unclear whether changes in gene expression identified thus far play a direct role on HD pathogenesis or represent a secondary response to primary pathogenic events. Changes in the levels of specific genes could result from compensatory mechanisms, making difficult to establish the relevance of such changes to HD pathogenesis. Additionally, most gene expression studies screened for transcriptional changes in the striatum or cortex, but few established quantitative comparisons between the most affected MSNs or pyramidal neurons and mildly affected or unaffected cells such as striatal and cortical interneurons. Currently, the evidence linking transcriptional alterations of specific genes to the differential vulnerability of affected cell populations in HD remains largely inconclusive. A

proposed mechanism involving regulation of BDNF expression by Htt, however, sheds light on both the function of wt-Htt, and a mechanism that may in part explain the preferential degeneration of striatal neurons.

2.3.4. ABNORMALITIES IN BDNF

Brain-derived neurotrophic factor (BDNF) is normally synthesized by neurons in the cortex and the SN, then transported along axons to the striatum, where it supports the acquisition of normal dendritic morphology and survival of MSNs [159, 160]. Abnormalities in BDNF signaling have been proposed to contribute to the preferential vulnerability of striatal neurons in HD [2]. Supporting this idea, reductions in BDNF levels have been demonstrated in a number of cellular and animal HD models, as well as in HD patients [2].

A compelling body of work shows that wild-type huntingtin can regulate the activity of genes that contain neuron-restrictive silencer elements (NRSEs) by modulating NRSE-binding transcription factors that normally recruit NRSEs from the cytoplasm to the nucleus [161]. Specifically, wild-type Htt was shown to bind to repressor-element-1 transcription factor–neuron-restrictive silencer factor (REST–NRSF) in the cytoplasm, thereby reducing the availability to nuclear NRSE-binding sites and ultimately promoting the transcription of neuronal genes governed by NRSEs. Aberrant polyQ-Htt fails to interact with REST-NRSF, leading to increased levels in the nucleus, suppression of transcription of NRSE-regulated genes, and the loss of BDNF [162, 163]. This raises the possibility that reductions in striatal BDNF levels might result from polyQ-Htt-induced transcriptional changes in the cortex. Alternatively, these

reductions could result from polyQ-Htt-induced reductions in anterograde axonal transport of BDNF in cortical neurons [18, 164, 165], decreased BDNF endocytosis by MSNs [19], or both.

While mechanisms underlying BDNF deficits remain a matter of debate, current evidence does indicate that deficits in BDNF signaling contributes to pathologic changes specific to cells affected in HD. Of note, an extensive expression profile study showed that striatal profiles from forebrain-specific BDNF knockout mice were more similar to striatal profiles of HD patients than other HD mouse models, including the most well-characterized and widely used R6/2 HD mouse model [166]. While a growing number of studies lend credence to the loss of BDNF contributing to HD pathology, a number of non-neuronal BDNF-dependent tissues in the body, such as lung [167] and bone [168], are unaffected in HD patients. This indicates that polyQ-Htt-mediated loss of BDNF per se is not likely to be the pathogenic mechanism underlying the differential cell death seen in HD, but could possibly confer cell-specific vulnerability in conjunction with another cell-type factor, such as morphology.

2.3.5. MITOCHONDRIAL INVOLVEMENT

Mitochondria are the chief cellular producers of chemical energy and regulators of metabolism, as well as crucial modulators of intracellular signaling and survival [169] . Evidence of disturbances in cellular metabolism in HD implicate mitochondrial impairment as a component of HD pathology. Profound weight loss despite normal to increased caloric intake is observed in a significant number of HD patients [170]. Postmortem studies on HD brain tissue showed decreased activity in complex II, III, and IV of the mitochondrial respiratory chain [171]. Subsequent in vivo studies in HD patients employing live imaging techniques report region-

specific alterations in metabolic markers. Specifically, reductions in glucose usage [172-174] and creatine [174] and increases in lactate [173] strongly suggest a mitochondrial component in HD pathology. Of importance, these same signs of mitochondrial deficits were seen in presymptomatic HD carriers [175-178], suggesting that mitochondrial defects are present early on in the disease process, and may be involved in HD pathogenesis. This idea stems from observations that mitochondrial inhibitors could create pathologic phenotypes reminiscent of HD. Accidental ingestion of the irreversible mitochondrial inhibitor 3-nitropropionic acid (3-NP) by humans causes chorea, dystonia, and basal ganglia degeneration [179]. Likewise, systemic administration of 3-NP in rats [180] and primates [181] selectively caused striatal lesions with accompanying motor deficits. Electrophysiological studies in animals models further demonstrated that MSNs were adversely effected by mitochondrial inhibition of 3-NP, while striatal interneurons were not [182, 183], providing indirect evidence that mitochondrial involvement may cause preferential vulnerability of MSNs.

In comparison to all other cell types, neurons require enormous amounts of energy. Indeed, while the brain accounts for only 2% of a person's total body weight, it accounts for 25% of the body's total glucose consumption [184]. The highly specialized regions of neurons, such as synapses and Nodes of Ranvier, have especially high mitochondrial demands [185]. Coupled with the extensive lengths of projection neurons, the complex logistics of shuttling and maintaining mitochondria to where they are most needed becomes an exceptional challenge as well as a great vulnerability. While the relative length of striatal MSNs may explain why they, and not their neighboring interneurons, might be highly susceptible to intraneuronal misregulation of mitochondria, it can not explain the preferential vulnerability of the striatal

projection neurons in relation to much longer projection neurons throughout the nervous system. Experiments using SOD1 mutant ALS mice have demonstrated that misfolded mutant SOD1 binds selectively to mitochondrial membranes, and that this binding is restricted to the spinal cord, which is preferentially affected in ALS [186]. Taken together with insight from studies mentioned above, this precedence lends the possibility of region-specific association of polyQ-Htt to mitochondria as a component of HD pathology.

Mutant Htt may cause damage to mitochondrial membrane signaling, trafficking, and Ca^{2+} regulation by abnormal binding to mitochondrial membrane components [187, 188]. Additionally, a progressive increase in mitochondrial DNA damage as ascertained by qPCR was observed in striatum and cerebral cortex of R6/2 mice between 7 and 12 weeks of age [189], corroborating previous findings of early mitochondrial impairment in HD mouse striatal cells[190-193]. Although results from these studies were in line with mitochondrial breakdown as a component of HD pathogenesis, comparative gene expression profiles argue against mitochondrial dysfunction as a primary event in HD. Using human striatal HD gene profiles as the reference, striatal profiles of multiple mitochondrial dysfunction animal models (3-NP-treated rats, MPTP-treated mice, and *PGC-1* knock-out mice) failed to yield the same reductions in striatum-enriched mRNAs associated with MSN disturbances as seen in HD tissues, and were more indicative of astrocytosis and apoptosis [166] . Furthermore, a study detailing changes in gene expression patterns in 3-NP striatal cells versus polyQ-Htt expression in STHdh$^{Q111/Q111}$ cells revealed that, while both conditions caused significant changes associated with metabolism, expression of nine mitochondrial genes was greatly reduced in the 3-NP treated cells, but unchanged in the polyQ-Htt-treated cells [194]. While this argues against decreased

mitochondrial gene expression as a likely pathogenic event in HD, it does not contraindicate mitochondrial involvement in HD pathogenesis. Disturbances in cellular energetics may be caused by both loss of function of wt-Htt, and by gain of function of polyQ-Htt, via their interactions with other proteins that regulate mitochondria. For example, binding of wt-Htt to HAP1 regulates HAP1 interactions with molecular motors such as kinesin [195], which play a role in microtubule-mediated transport of mitochondria. Interestingly, a HAP1 homolog in drosophila moderates distribution of mitochondria throughout axons [196, 197]. It's also been shown that both loss of wt-Htt and overexpression of polyQ-Htt result in impaired axonal transport of mitochondrial in drosophila [198]. Trushina and others confirmed that expression of full-length polyQ-Htt impaired fast axonal transport of mitochondria both in mammalian cell culture and in animals in vivo [165]. These decrements in transport were found early on prior to detectable mitochondrial damage, formation of Htt aggregates, or neurological deficits. More recently, soluble N-terminal polyQ-Htt fragments were shown to interact with mitochondria, and interfere with associations between microtubule-based transport proteins and mitochondria in vitro [199]. This study also demonstrated impaired distribution and transport of mitochondria within neuronal processes in vitro, as well as decreased levels of ATP in synaptosomal fractions from the forebrains of *Hdh*(CAG)150 knock-in mice, elaborating on the idea that positional misregulation of mitochondria within neurons could lead to detrimental energetic imbalances in neuronal microenvironments.

2.3.6. NEUROCHEMICAL CONTENT

Based on their neurochemical content, MSNs can be classified as part of the "striosomes" (also referred to as "patches" or "striatal bodies") or as part of the "matrix compartment" (also known as "extrastriaosomal matrix") [32, 200]. Projection MSNs represent the main cell type present in striosomes, while striatal interneurons are the dominant cell type at the matrix compartment. According to this classification, MSNs in the striosomal compartment are among the first to degenerate in HD [201]. Various biochemical markers have been identified showing differential expression between the striosomal and the matrix compartments, including neuropeptides and neurotransmitter receptors. Microarrays for HD mouse brains suggest that there is specific altered expression in a number of genes that are important for neuronal function and survival such as neurotransmitter receptors, including glutamate and dopamine receptors [202, 203].

Neuropeptide and calcium-binding proteins: While all MSNs express the neurotransmitter GABA, striosomal MSNs express higher levels of various neuropeptides including enkephalin (ENK, a pentapeptide endorphin derived from the proenkephalin gene), dynorphin (DYN, a class of opioid peptides derived from the precursor protein prodynorphin), substance P (SP), and neurotensin (NT, a 13 amino acid neuropeptide) among others [204, 205]. Interestingly, the expression of specific neuropeptides correlates with the increased vulnerability of MSN subtypes. For example, MSN neurons in the "direct pathway" express DYN and/or SP, whereas MSNs in the indirect pathways express ENK[206]. However, it remains unclear whether expression of DYN and/or SP exacerbates polyQ-Htt toxicity, nor is clear whether ENK expression would provide a protective effect. Similarly, interneurons expressing nitric oxide

synthase (NOS), somatostatin and neuropeptide Y[207] are particularly resistant in HD, but mechanisms of how these proteins could confer neuroprotection are indeterminate.

A positive association between the level of expression of some calcium-binding proteins (i.e., calbindin) and the survival of interneurons in HD [208] led to the proposal that higher levels of calcium-binding proteins in striatal interneurons may protect these cells from glutamate-mediated excitotoxic mechanisms [209]. However, calbindin is detected throughout both the MSN-enriched striosomal and interneuron-enriched patch compartments [210, 211]. Conversely, hippocalcin was found to be significantly decreased in the brains of HD mice and patients, leading to the hypothesis that decreased expression of hippocalcin and other calcium sensor proteins in MSNs contribute to the increased vulnerability of these cells in HD [202]. However, functional experiments demonstrated that overexpression of hippocalcin did not decrease vulnerability of striatal neurons to polyQ-Htt [212].

Glutamate-related factors: Glutamate is the most abundant excitatory brain neurotransmitter in mammals, activating both N-methyl-D-aspartate (NMDA) and non-NMDA ionotropic glutamate receptors (i.e., AMPA and kainate receptors) [213]. Abnormally sustained stimulation of NMDA receptors by glutamate can lead to prolonged increases in intracellular calcium, triggering various intracellular events including activation of kinases and phosphatases, calcium-dependent proteases, synthesis of nitric oxide synthase (NOS), generation of reactive oxygen species, mitochondrial dysfunction, and activation of apoptotic pathways [214]. Both striatal MSNs and cortical neurons receive a rich supply of excitatory glutamatergic inputs [215]. Striatal MSNs in particular are constantly stimulated by these inputs, remaining hyperpolarized much of the time [216], leading to suggestions that increased exposure of MSNs to cortical

glutamate stimulation could render these cells more vulnerable to excitotoxic damage.

Experimental evidence using intrastriatal injection of agonists for NMDA (i.e., quinolinic acid) and non-NMDA (i.e. kainic acid) receptors in rodent and non-primate animals demonstrated increased vulnerability of MSNs to glutamate-induced excitotoxicity, compared to striatal interneurons [217, 218]. However, these experiments did not provide a mechanistic relationship linking the differential vulnerability of these neuronal subtypes to polyQ-Htt expression. Despite this, various HD models have been proposed based on the administration of glutamate receptor agonists [217, 218]. While these models generally resemble the HD phenotype of striatal dysfunction, the acute induction of cell death induced in these models contrasted sharply with the dying back pattern of degeneration observed in HD (see Figure 2). Further, some studies showed that the pattern of striatal neuron degeneration resulting from systemic quinolonic acid injection differs significantly from that of HD [219], suggesting different pathogenic mechanisms. Since the neurological symptoms in HD reflect loss of functional connections made by affected neurons, any treatment that disrupted these synaptic relationships would be expected to exhibit similar clinical symptoms, without necessarily involving the same underlying pathogenic mechanisms. Relevant HD animal models needs to replicate the sequence of changes in neuronal connections and neuronal populations seen in the disease, including the dying back pattern of neuronal degeneration.

A molecular basis underlying the differential vulnerability of striatal neurons to glutamate excitotoxicity is currently unknown, but alterations in glial function, levels of calcium-binding proteins, and heterogeneous expression of NMDA receptor subtypes have been proposed [33]. NMDA glutamate receptors exist as heteromeric dimers of NR1 and NR2 (A, B, C and D)

subunits [220]. In the brain, levels of NR1 expression greatly exceeded that of the other subunits combined, whereas NR2A, B, C and D subunits varied widely [221]. NR1 subunits are essential for NMDA receptor function, but heteromerization with NR2 subunits increases both the permeability of the channel (over 100 fold), and its deactivation time [222]. Significantly, differential expression of NMDA subunits have been observed among striatal neurons [1], with MSN projection neurons reportedly expressing higher levels of the NR2B subunit, and striatal interneurons predominantly expressing NR2D [223, 224]. While differences in NMDA receptor subtype expression might help explain the increased vulnerability of MSNs over striatal interneurons to NMDA agonists, they do not explain the minimal HD pathology observed in the hippocampus and olfactory bulb, which show levels of NR2B expression as high or higher than in the striatum [221, 225]. Overlooking these discrepancies, evidence that glutamate excitotoxicity could kill striatal neurons and manifest in motor deficits reminiscent of HD was deemed sufficient rationale for the use of NMDAR antagonists in HD patients [226-228], but these treatments showed no beneficial effects [228]. Despite the extensive efforts that have been focused on glutamate toxicity in HD [33, 56, 229], a plausible mechanism by which polyQ-Htt expression causes differential dying back neuropathy by glutamate imbalances has yet to emerge.

Dopamine signaling: Like glutamate, dopamine (DA) is a key neurotransmitter in multiple CNS circuits, and the striatum is heavily innervated by dopaminergic afferents from the SN [230]. Changes in DA signaling in the basal ganglia is known to cause motor deficits in neurodegenerative disease; indeed it is loss of dopaminergic neurons in the substantia nigra pars compacta (SNc) that causes Parkinson's disease. In addition to motor control, DA also

participates in regulation of emotion and cognition via the mesolimbic and mesocortical pathways, in which DA dysregulation could possibly explain the HD psychocognitive changes.

Analysis of autopsied tissue from HD patients reveals that both D1 and D2 receptors in the striatum are reduced [231-234]. PET studies confirmed these findings in HD patients in vivo [235, 236]. Importantly, decreases in striatal D1 and D2 levels, as well as decreases in striatal metabolism, were observed in asymptomatic HD gene carriers [237-239]. Furthermore, the degree of decreases in DA receptor binding correlated with the patient's number of CAG repeats [237]. Interestingly, the striatal DA content exhibits a dorsal to ventral gradient [240] that is consistent with the progression of pathology in HD [35]. Based on these observations, and additional findings on DA signaling deregulation in HD models and patients [241], it has been proposed that disturbances in DA signaling contribute to the differential vulnerability in the HD striatum [242].

DA in the striatonigral circuit exerts excitatory signals by activation of D1 receptors, and inhibitory signals by activation of D2 receptors [230] . MSNs of the "indirect pathway" express high levels of D2, in contrast with the MSNs in the "direct pathway", which express high levels of D1 [243], suggesting that differences in DA-induced signaling could modulate the toxic action of polyQ-Htt. More recent research has expanded on this, revealing that D1 and D2 are G-protein-coupled receptors that activate downstream effector proteins such as PKA and DARPP-32 to manipulate the response of MSNs to glutamate by phosphorylation of ion channels [244], as well as numerous other striatal targets [245]. In line with this, early MSN-specific electrophysiological and biochemical changes in DA signaling have been demonstrated in presymptomatic R6/2 HD mice, in the absence of cell loss [93].

There is evidence that targeted vulnerability may result from multiple neurotransmitters acting in concert. As just mentioned, DA can act synergistically with glutamate pathways to increase vulnerability of MSNs to apoptosis by potentiating Ca2+, and that DA inhibitors were useful in ameliorating cell death [241]. Also, DA exacerbates polyQ-Htt effects on JNK activation, Htt aggregation, and cell death in a synergistic manner [246], suggesting that polyQ-Htt could exert its toxic effects both directly and indirectly through DA signaling. Of note, the aggregation and cell death in this study were attenuated by D2 inhibition, but not with D1 inhibition. It has also been shown that indirect pathway MSNs express the A2a adenosine receptor subtype [247] that can specifically modulate activity of D2 receptors [248], while MSNs of the direct pathway lack these A2a receptors. As decreases in both D1 and D2 receptors are observed, it is unlikely that the dorsal to ventral DA gradient acting on progressively decreasing numbers of DA receptors could alone account for the differential vulnerability between MSNs of the direct and indirect pathways. It is entirely possible, however, that the DA gradient could act in concert with a D2 receptor-specific factor resulting in a preferential vulnerability to changes in DA.

2.4. AXONAL TRANSPORT AND HD

A common biochemical feature has yet to be found among the most vulnerable neuronal cell types in HD, but an analysis of their morphological characteristics does reveal a common theme. Neurons affected in HD within the striatum and the cortex are all projection neurons [1]. MSNs and cortical neurons affected in HD project their axons to anatomically distant target structures outside the striatum and the cortex, respectively (see Figure 1). In contrast, the striatal

and cortical interneurons that are largely spared in HD possess short axons that remain within the boundaries of their originating brain structures. This morphological and functional difference has been proposed to play a role in the differential vulnerability of neurons observed in HD [1] as well as other neurodegenerative diseases [20, 45, 46].

The continuous distribution of cargoes such as synaptic vesicles, mitochondria, and even RNAs to where they are needed along the axon is vital to the development, function, and maintenance of neurons. This process depends on the ability of motor proteins to properly carry and release the correct cargo, correctly bind and unbind to the microtubules they travel along, and to deliver these cargoes to the right place at the right time. Components synthesized in the cell body but required distally are transported by kinesins in the anterograde direction [249, 250], and cargoes such as endosomes and neurotrophic signals that need to be brought to the cell body are transported largely by dyneins in the retrograde direction [251], although some kinesins have been shown to be bi-directional. Conventional kinesin, or kinesin-1, is the most abundant kinesin motor. The first kinesin to be discovered, it was shown to be a microtubule-based anterograde molecular motor enriched in the nervous system [252, 253]. Kinesin-1 holoenzyme is a heterotetramer, consisting of two heavy chains and two light chains. Kinesin-1 heavy chains (KHC) possess a microtubule (MT)-binding domain and an ATP-dependent force-generating region, which drives the mechanical motion of kinesin along microtubules. Kinesin light chains (KLC) are involved in the specification and binding of cargoes [254, 255]. Cytoplasmic dynein is a macromolecular complex consisting of a heavy chain (DHC), variable intermediate chains (DIC), and light chains (DLC) [256, 257]. The DIC and DLC help specify the intracellular location of the dynein and regulate its motor activity. Like KHC, DHC contains the ATPase and

MT-binding region that allow for the transduction of chemical energy into mechanical force. The complete reliance of the axonosynaptic compartment on the delivery of materials from the cell body render neurons uniquely vulnerable to deficits in axonal transport [20, 46, 258]. Evidence linking loss of function mutations in kinesin [21, 259], dynein [260], and other components of transport machinery [249, 250] to neurodegerative diseases illustrates the absolute dependence of neuronal function and axonal maintenance on axonal transport.

Multiple independent studies provided evidence of axonal transport deficits in HD. Ultrastructural observations first showed reduced number of synaptic vesicles, and abnormal membrane-bound organelle (MBO) profiles within axons of affected neurons [91, 123, 125]. Experiments in cultured cells [19, 164] and Drosophila neurons [261, 262] similarly documented reductions in axonal transport and accumulation of axonal vesicle cargos in association with polyQ-Htt expression. Live imaging in the nerves of whole mount transgenic Drosophila larvae expressing polyQ-Htt showed abnormalities in both anterograde and retrograde axonal transport [198]. In a similar HD Drosophila model, cargoes in nerves of larvae expressing polyQ-Htt stalled for longer and more often than controls, but when stalling events were excluded, mean cargo velocities between the groups were not different [261]. These findings were confirmed in a mouse model of HD [165]. In this study, transport of vesicles and mitochondria in striatal cells from HD mice was impaired in both anterograde and retrograde directions. Also, these MBOs displayed more frequent stopping, and shorter distances traveled between stops, than in wt controls. Axonal transport deficits were also demonstrated in vivo, and that these deficits occurred before onset of any symptoms. Furthermore, in the same study, conditional knockout animals deficient in wt-Htt also demonstrated axonal transport impairment, indicating that wt-Htt

is necessary for normal physiologic transport function. Interestingly, expression of one copy of polyQ-Htt in the conditional knockout animals partially restored axonal transport function, demonstrating that polyQ-Htt at least in part retains normal function, supporting that the polyQ expansion does not cause disease through a loss of function mechanism, but rather a pathogenic gain of function. While a a partial loss of function of polyQ-Htt can not be discounted, and toxic gain of function may or may not be related to the physiologic function of the affected protein, this study provided evidence that both wt and polyQ-Htt possess axonal transport related functions. The authors of the aforementioned studies hypothesized that deficits in transport were due to a decrease in available functioning kinesin and dynein due to sequestration of these molecular motors to polyQ-Htt aggregates [165, 198, 261]. However, a number of studies demonstrated polyQ-Htt induced transport deficits in the absence of aggregates.

In striatal cells cultured from HD knock-in mice, transport of both APP and BDNF were impaired in the absence of any aggregates or observable disruption to molecular motor complexes, indicating that deficits in transport are not due to depletion or disruption of molecular motor complexes, but perhaps altered regulation of intact transport complexes [19]. In another study using knock-in HD mice, brain lysates showed decreased association of both anterograde and retrograde molecular motors with mitochondria compared to wt controls [199]. This study also used live-cell imaging to observe polyQ-Htt expressing striatal cultures, and found impaired transport of mitochondria in both directions, and that the distribution of mitochondria to neurites was substantially reduced. In these findings, no aggregation was detected. Perfusion of polyQ-Htt in squid axoplasm also inhibited axonal transport in both directions [18]. This too occurred in the absence of any aggregates, and importantly, the final concentration of recombinant polyQ-

Htt was sub-nanomolar, while the concentration of kinesin in squid axoplasm is 0.5μM. These findings indicated that polyQ-Htt exerts it toxic effects on transport by an catalytic mechanism as opposed to sequestering molecular motors to aggregates or direct inhibition of kinesins and dyneins. Of particular relevance, immunoprecipitation studies on brain lysates from knock-in HD mice demonstrated that polyQ-Htt did not co-precipitate with KHC, KLC, DHC, nor DIC, demonstrating the lack of association between polyQ-Htt and molecular motor components [20].

Coupled with the absolute reliance of neurons on appropriate axonal transport and the dying back pattern of neurodegeneration, these observations suggest that axonal transport deficits represent a major pathogenic event underlying the increased vulnerability of projection neurons in HD [20].

2.5 JNK AND HD

The c-Jun N-terminal kinases (JNKs) "are members of the evolutionarily conserved mitogen-activated protein kinase (MAPK) family. The JNK subfamily consists of three related genes: *Jnk1*, *Jnk2,* and *Jnk3*. In mammals, the JNK1 and JNK2 proteins are ubiquitously expressed, whereas JNK3 is found almost exclusively in the brain and testis" [274]. JNKs, appropriately also known as stress-activated protein kinases(SAPKs), are activated in response to both internal and external stressors, including heat shock, UV irradiation, and inflammatory cytokines. JNKs are activated through phosphorylation by upstream kinases, mitogen activated protein kinase kinase (MKK) 4 and MKK7 [263-265], which must first themselves be activated through phosphorylation by various MAPKKKs, including mixed lineage protein kinases (MLKs) [266]. JNKs are additionally regulated spatially by a variety of scaffold proteins such as

JNK interacting protein (JIP) 1, JIP2, and JIP3 [267-269], which organize the assembly of complexes that comprise a MAPKKK, MAPKK, and MAPK. The precise combination of kinases and locale produce a highly directed signal by way of temporal, spatial and kinase specificity. For example, JIP1 binds to MKK7 but not to MKK4, which restricts signal transduction downstream of the JIP1/MKK/JNK assembly to appropriate targets [270].

All JNKs can phosphorylate c-Jun on Ser63 and/or Ser73, which in turn binds AP-1 sites in DNA [271, 272]. While c-Jun is the namesake substrate of JNKs, it is but one in a number of nuclear and cytoplasmic targets [273-275] including "various apoptotic proteins, and microtubule-associated proteins (MAPs). Through phosphorylation of these substrates, JNKs regulate gene expression governing stress responses as well as the normal physiological processes of cell proliferation, apoptosis, differentiation, and cell migration" [274]. Knockout mice lacking specific JNK isoforms have provided insight on the vital contributions each isoform makes to the development and maintenance of neural tissue. JNK1 is required for dendrite formation and neural migration during brain development, and also for axonal maintenance [276-278]. In adulthood, JNK1 seems to have a role in regulating metabolism [279-281]. Evidence implies that JNK2 and JNK3 play a role in stress-induced cell death. JNK2 and JNK3 knockout mice are resistant to MPTP neurotoxicity, and double JNK2/3 knockouts display an even higher resistance against MPTP-induced neuronal death [282]. JNK3 knockout mice are also resistant to cell death induced by kainic acid excitotoxicity [283], ischemia [284, 285], Alzheimer's disease-related protein β-amyloid [286], and 6-hydroxydopamine toxicity [287]. JNK3 has also been implicated in non-pathogenic processes such as brain development [288], neurite formation and plasticity [289, 290], and cognitive functions such as memory and learning

[287, 291]. A more recent study reinforces the importance of JNKs' influence in early stages of neurite outgrowth [292]. This study used isoform specific JNK knockout mice coupled with pharmacological JNK inhibitors to demonstrate delay of neuritogenesis by lack of JNK2 and JNK3, but not JNK1, whereas JNK1 and JNK2 were required for sustained neurite elongation. Of interest, JIP1 was required for both neuritogenesis and elongation of DRG neurons, underscoring its importance as a regulator of JNKs.

PolyQ-Htt induces a stress response involving the JNK pathway [293, 294], which has been corroborated by numerous studies both in vitro and in vivo. More specifically, inhibition of JNK in striatal cultures expressing polyQ-Htt by selective JNK pathway inhibitor SP600125 ameliorate neurite retraction [295] as well as DA-exacerbated cell death [246]. Protection from cell dysfunction and death by inhibition of the JNK pathway was confirmed by use of additional inhibitors, CEP-11004 and CEP-1347, in a number of different cell lines [296, 297]. Furthermore, subcutaneous injection of a JNK pathway inhibitor was able to mitigate progression of motor deficits and restore serum and cortical BDNF levels in the R6/2 HD mouse [297]. More recently, in a lentiviral rat HD model, dominant negative MEKK1 and dominant negative JIP1 were able to attenuate loss of MSNs, while dominant negative ASK1 or dominant negative c-Jun could not [131]. This indicates that polyQ-Htt activates JNKs via upstream MLK activators that can be phosphorylated by MEKK1, but not ASK1. It also indicates that although polyQ-Htt expression can increase phosphorylation of c-Jun [294, 295], polyQ-Htt induced JNK activation does not exert its toxic effects through activation of c-Jun, but through phosphorylation of a different substrate. While this does not rule out the possibility that c-Jun activation contributes to the overall phenotype of HD, it makes it an unlikely candidate as an

underlying pathogenic event. It has been shown that JIPs bind directly to kinesin [25, 298] and that compromised JIPs can result in impaired axonal transport [25], suggesting that localization of JNK cascades play an important role in the regulation of molecular motor components.

2.6. JNK AND AXONAL TRANSPORT IN HD

Axonal transport is highly dependent on regulation by kinases and phosphatases. Research from our lab has found evidence that a number of kinase pathways influence molecular motors through phosphorylation, resulting in transport deficits that might underly population-specific dying back neuropathy in a number of neurodegenerative diseases [16, 18, 20, 31, 46, 299-301]. For example, glycogen synthase kinase 3beta (GSK3ß) inhibits anterograde transport in isolated squid axoplasm, and additional findings in human cell lines demonstrated that GSK3ß phosphorylates KLCs, resulting in the release of cargoes from kinesin-1 [300]. Subsequent studies revealed that a mutant presenilin-1 (PS1), a protein that causes Alzheimer's disease (AD), increases GSK3ß activity and therefore KLC phosphorylation [16]. Binding of kinesin-1 to MBOs was reduced, and transport of synaptophysin, syntaxin-I, amyloid precursor protein (APP), and mitochondria were found to be impaired. This suggests that mutant PS1 could mediate AD pathogenesis via phosphorylation of KLC by GSK3ß. More recent studies provide evidence that polyQ-Htt may mediate HD pathogenesis through a similar mechanism.

Reductions in axonal transport observed in various HD experimental models raised the question of how polyQ-Htt might inhibit axonal transport. Aberrant patterns of phosphorylation of neurofilaments [85, 302] and synapsin [303], as well as increased activation of kinases [295, 296, 304], represent well-established features in HD features. Additionally, there is a growing body of evidence that polyQ-Htt causes impairments in axonal transport (see SECTION 2.4

Axonal Transport and HD). These well-documented phenomena suggest that transport deficits in HD may result from abnormal phosphorylation of molecular motor proteins mediated by polyQ-Htt [31, 46]. It has also been established that JNK interacting proteins (JIPS), scaffolding proteins that assemble JNKs and their upstream activators, also bind to kinesin-1 [305-307]. In newly plated primary cortical neurons, JIP1 localizes to a single neurite and continues to accumulate as that neurite becomes an emerging axon [308]. Disruption of JIP1 binding impairs outgrowth of the emerging axon, suggesting JIP1 is important in the regulation of axonal development and maintenance. This also implies that the JNK cascade assembled by JIP1 may also play an important role in axonal formation and survival. Biochemical analysis revealed that activation of drosophila homologs for dual leucine zipper-bearing kinase (DLK) and MKK7, both upstream activators in the JNK pathway, disrupts binding between kinesin-1 and drosophila JIP1. This suggests that activation of JNKs could impair kinesin-based transport by dissociating kinesin regulatory components [25].

Studies in isolated squid axoplasm and a knock-in mouse model provided evidence that polyQ-Htt inhibits axonal transport through a mechanism involving activation of the JNK pathway and phosphorylation of the molecular motor protein conventional kinesin [18, 20]. Perfusion of recombinant polyQ-Htt protein constructs into squid axoplasm significantly impaired both anterograde and retrograde vesicle velocity [18]. As mentioned above (see SECTION 1.3 Axonal Transport and HD), this occurred in the absence of any aggregates, and importantly, the final concentration of recombinant polyQ-Htt was in the range of 0.1-0.2nM, while the concentration of kinesin in squid axoplasm was ~ 0.5M [309, 310]. These findings indicated that polyQ-Htt exerts it toxic effects on transport by an enzymatic mechanism as

opposed to sequestering molecular motors to aggregates or direct inhibition of kinesins and dyneins. Subsequent studies using knockin HD mice confirmed this idea by showing that neither wt-Htt nor polyQ-Htt co-precipitated with KHC, KLC, DHC, nor DIC, demonstrating the lack of association between polyQ-Htt and molecular motor components [20]. This same study also put forth evidence that polyQ-Htt impairment of axonal transport is mediated by JNKs, specifically the JNK3 isoform. Co-perfusion of polyQ-Htt into squid axoplasm with two different JNK inhibitors were able to prevent inhibition of transport in both directions, and analysis of mouse neuroblastoma cells expressing polyQ-Htt showed decreased binding of KHC to microtubules. Biochemical analysis of the polyQ-Htt expressing neuroblastoma cells and striatal lysates from knock-in HD mice showed differential increases in phosphorylation of individual JNK isoforms, with significant increases corresponding to JNK2 and JNK3, but not JNK1. Perfusion of squid axoplasm with active recombinant JNK3, but not JNK2, accurately mimicked the anterograde and retrograde deficits seen previously when axoplasm was perfused with polyQ-Htt. Furthermore, liquid chromatography tandem mass spectrometry (LC/MS/MS) showed that JNK3 could phosphorylate KHC at serine residue 176 (Ser176), while JNK1 could not. Ser176 is located in the microtubule-binding region of KHC [311], corroborating the aforementioned decrease in binding of KHC to mirotubules. Collectively, these data strongly suggest that polyQ-Htt induced deficits in axonal transport are, at least in part, caused by phosphorylation of KHC by JNK3.

CHAPTER 3

MATERIALS AND METHODS

3.1 CELL CULTURE

3.1.1. N2a Cells

Neuro-2a (N2a)(Cat#CCL-131, American Type Culture Collection, Manassas, VA) cells are derived from a Mus musculus neuroblastoma, and display neuronal characteristics such as neuronal cell morphology and expression of neuronal cellular products when differentiated by serum deprivation and retinoic acid [312]. They have long been used as a model of axonal phenomena [313], and of specific importance to the work presented here, have been validated to be good models of neurite outgrowth influenced by the pathogenic effects of mutant huntingtin protein constructs [67]. N2a cells are cultured and maintained in DMEM (Cat#11995, Life Technologies, Grand Island, NY) with 5%FBS (Cat#35-101-CV, lot FB10516, CellGro, Manassas, VA) at 37°C with 5%CO_2. In preparation for analysis by Western Blot or quantitative PCR, cells are plated into 6-well plates at a density of 100,000 cells/well. When applicable, N2a cells were differentiated no more than 24h post-plating with 10μM all-trans retinoic acid (Cat# R2625, Sigma-Aldrich, St. Louis, MO) in serum-free DMEM.

3.1.2. ibidi μ-Slides

ibidi® μ-Slides VI $^{0.4}$ (Cat# 80606, ibidi LLC, Verona, WI) are coated with poly-L-lysine (100μg/ml) for at least 1h at room temperature. Channels are then rinsed with ultrapure water. Water was then removed, and channels were coated with laminin (Cat#23017-15, Invitrogen, Grand Island, NY) .(10μg/ml) for at least 30 minutes at room temperature. Channels are rinsed with ultrapure water, then 60μl of complete medium are added per channel. Ibidi slides are

allowed to equilibrate for 30 minutes in cell culture growth conditions (37°C with 5%CO_2). Cells are added to ibidi slides at 1500 cells in a volume of 60µl complete medium. Cells are differentiated in serum-free medium with 10µM all-trans retinoic acid no more than 24h post-plating, and maintained in differentiation medium until processed for neurite outgrowth or mitochondrial distribution.

3.2. Expression of Htt in N2a Cells

3.2.1. Htt Plasmids

Plasmids expressing huntingtin protein constructs were a kind gift from Dr. John O'Bryan (see TABLE I). Plasmids express exon 1 of human huntingtin with the polyglutamine repeat region containing 23Q, 65Q, or 148Q repeats. Expression cassettes were cloned into the pECFP N1 vector (Clontech, Mountain View, CA, and therefore have a CFP reporter and G418

Name	Source	Description	Usage
N171Q23-pECFP N1	Dr. John O'Bryan	mammalian expression vector with a CMV promotor for expression of N-terminus 171aa of huntingtin with a 23Q polyglutamine repeat, and CFP reporter	Stable transfection of N2a cells for the expression of a non-pathogenic Htt protein fragment.
N171Q65-pECFP N1	Dr. John O'Bryan	mammalian expression vector with a CMV promotor for expression of N-terminus 171aa of huntingtin with a 65Q polyglutamine repeat, and CFP reporter	Stable transfection of N2a cells for the expression of a pathogenic Htt protein fragment.
N171Q148-pECFP N1	Dr. John O'Bryan	mammalian expression vector with a CMV promotor for expression of N-terminus 171aa of huntingtin with a 148Q polyglutamine repeat, and CFP reporter	Stable transfection of N2a cells for the expression of a pathogenic Htt protein fragment.

TABLE I

Huntingtin protein expressing plasmids.

selection genes. All three plasmids were used in initial transfections and validation, but only 23Q and 148Q were used in neurite outgrowth and mitochondrial density experiments.

3.2.2. Transfection of N2a Cells with Htt plasmids

N2a cells were transfected with Htt-CFP expressing plasmids using X-tremeGENE 9 DNA transfection reagent (Cat# 06 365 779 001, Roche, Indianapolis, IN) per vendor recommendations. Briefly, N2a cells were plated into 6-well plates at a density of 100,000 cells/ well. Twenty-four hours post-plating, transfection complex (per well) was made by combining 100µl serum-free media, 6µl X-tremeGENE transfection reagent, and 2µg plasmid DNA. Transfection complex was incubated for 30 min at RT. Complete media was removed from cells, 500µl serum-free media was added to each well, then transfection complex was added to cells drop by drop. Cells are switched to G418 selection medium (600µg/ml) 24h post-transfection.

3.2.3. Htt Expression Validation

N2a cells transfected with Htt plasmids were evaluated by WB (see section 3.4 Western Blot below) using EM48 anti-huntingtin antibody (Cat#mAb 5374, Millipore, Billerica, MA)(see TABLE IV) and qPCR analysis using human-specific Htt primers (see TABLE V).

3.3. ISOFORM-SPECIFIC KNOCKDOWN OF JNK

Knockdown of JNK1 and JNK3 were achieved by infection of N2a cells using lentiviruses encoding isoform-specific shRNAs (see TABLE II). JNK1shRNA containing lentiviruses were created and produced in-house, and JNK3shRNA lentiviruses were obtained commercially.

Name	Target protein	NCBI Accession Number	Gene target sequence
non-targeting shRNA	non-targeting	N/A	ATCTCGCTTGGGCGAGAGTAAG
JNK1shRNA1	JNK1	NM_016700	GGAAAGAACTGATATACAA
JNK1shRNA2	JNK1	NM_016700	GAAGCAAACGTGACAACAA
JNK3shRNA1	JNK3	NM_009158 NM_001081567	CAATAAAGATGGAAACTAA
JNK3shRNA2	JNK3	NM_009158 NM_001081567	CACATTGAGGGAAAGATGA

TABLE II

Lentiviruses expressing isoform-specific JNK shRNAs.

3.3.1. JNK1 Isoform-Specific Knockdown: Lentivirus Expressing JNK1-Specific shRNAs

Lentivirus encoding JNK1-specific shRNA (see TABLE II) was produced by calcium phosphate triple-transfection (see Figure 3) in 293T HEK cells (Cat#CRL-11268, American Type Culture Collection, Manassas, VA). Expression of specific JNK isoforms were knocked down with isoform-specific shRNAs (see TABLE II) delivered by a LentiLox3.7 (pLL3.7) lentiviral construct [314] that effectively deliver small-hairpin loop RNAs (shRNAs) in neurons [315]. The pLL3.7 lentiviruses contain the mouse U6 promoter upstream of a CMV–GFP expression cassette, resulting in a vector that simultaneously produces shRNAs and a reporter fluorescent protein [316] (see Figure 4A) . On day 1, low passage 293T cells (<p10) were plated at 50% confluency into six 15 cm^2 dishes (per transgene) in DMEM (Cat# 11995-065, Gibco, Grand Island, NY) with 5% FBS. On day 2, media was removed and 20ml of new media was added to each dish.

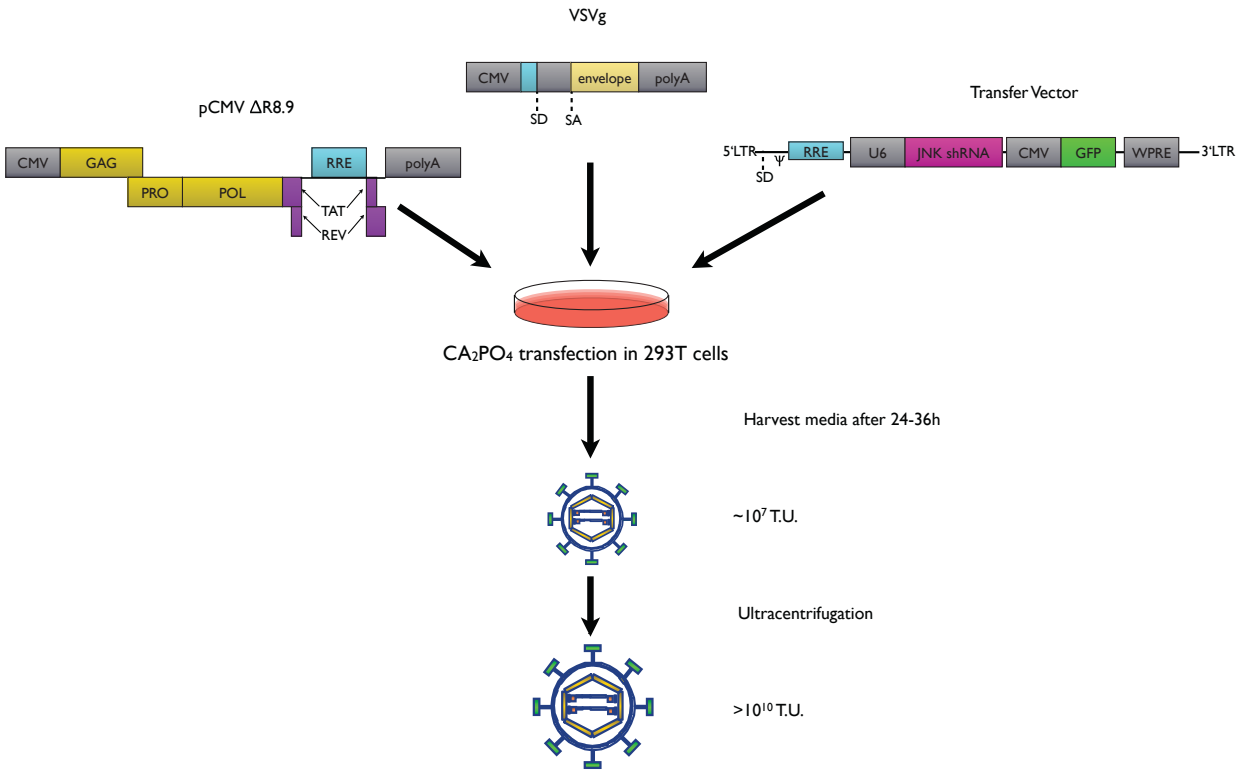

Figure 3. Production of high titer lentivirus for JNK1 knockdown. 293T HEK cells were calcium phosphate triple transfected with helper plasmids RΔ8.9 and VSVg, and expression vector pLL3.7-mm-JNK1-I or pLL3.7-mm-JNK1-II (see TABLE III). Viral supernatant underwent ultracentrifugation, and viral titer was assessed and calculated.

In a 50ml conical tube, 6ml of 0.1X T.E was combined with 3 ml of sterile water in a 50 ml falcon tube. Then either pLL3.7-mm-JNK1-I or pLL3.7-mm-JNK1-II transgene plasmid (see TABLE III) was added in combination with VSVg and ΔR8.9 helper plasmids (see TABLE III) was added in a ratio of 2:1:1 moles for a total of 186 µg/plate. After adding 900µl of 2.5M $CaCl_2$, the solution was pipetted thoroughly to mix, then incubated at RT for 5min. Lastly, 9 ml of 2X HBS was added drop by drop while vortexing. Three mL of mixture was immediately added per dish while gently rocking.

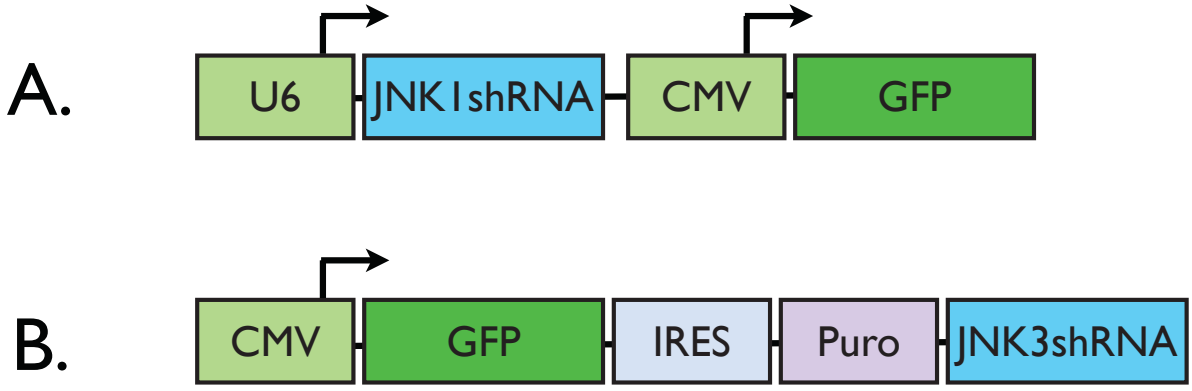

Figure 4. Schematics of JNKshRNA expression vectors. A) Knockdown of JNK1. One of two JNK1-specific shRNA sequences is driven by an upstream mouse U6 promoter. Expression of a GFP reporter protein is driven by a CMV promoter [314]. B) Knockdown of JNK3. One of two JNK3-specific shRNA sequences contained in an expression cassette with upstream GFP reporter gene, and puromycin resistance selection gene preceded by an internal ribosomal entry sequence (IRES), is driven by an upstream CMV promoter [317].

Transfected cells were incubated at growth conditions for 14-16h, and media was changed to 3% FBS in DMEM on day 3. Cells were assessed by microscopy for presence of fluorescent reporter protein 24h later on day 4. Viral supernatant was harvested and concentrated on day 5. The supernatant was filtered using a 0.45µm low-protein binding vacuum filter (Cat#SCHVU05RE, Millipore, Billerica, MA). Thirty ml of cleared viral supernatant was then layered over a a 5ml cushion of 20% sucrose in 1X TNE buffer in each ultracentrifuge tube, and centrifuged at 20,000g for 4h at 4°C. The media and sucrose cushion were then carefully aspirated, and viral pellet was resuspended in 400µl Mg^{2+}- and Ca^{2+}- free sterile 1X PBS (pH=7.4). Concentrated virus was then aliquoted and stored at -80°C until use.

To determine the titer of concentrated lentivirus, 293T cells were plated into into 6 well plates at a density of 200,000 cells/well. 10µl of concentrated virus was then added to 990µl complete media for a dilution factor of 10^{-2}. Serial ten-fold dilutions were then made from the 10^{-2} dilution, down to a 10^{-7} dilution. 900µl of each dilution was added to a designated well, and the plate was incubated under growth conditions for 72 hours. Infected cells were then examined by fluorescent microscopy. Images from at least 5 random fields were acquired and florescent cells were counted, with each fluorescing cell considered to represent one active viral particle. The concentration of viral particles per 10µl aliquot was then back-calculated using the number of fluorescing cells, the surface area of each field, and the total surface area of one well of a 6-well plate.

Effective multiplicity of infection (MOI) in N2a cells was determined by infecting cultured N2a cells with serially diluted virus of known titer in the same fashion as used in titer determination, then assessing for JNK1 knockdown by WB.

Name	Source	Description	Usage
VSVg	Dr. Anita Szodorai	helper plasmid expressing VSVg viral envelope protein	lentivirus production
RΔ8.9	Dr. Anita Szodorai	helper plasmid expressing gag (group antigens) pol (reverse transcriptase)	lentivirus production
pLL3.7-mm-JNK1-I	Drs. Dongyan Huang and Gerardo Morfini	U6 promoter-driven expression of shRNA targeting mus musculus JNK isoform 1 followed by CMV-GFP	isoform-specific knockdown of JNK by lentiviral shRNA expression
pLL3.7-mm-JNK1-II	Drs. Dongyan Huang and Gerardo Morfini	U6 promoter-driven expression of shRNA targeting mus musculus JNK isoform 1 followed by CMV-GFP	isoform-specific knockdown of JNK by lentiviral shRNA expression

TABLE III

Plasmids used in JNK1shRNA lentivirus production.

3.3.2. JNK3 Isoform-Specific Knockdown: Lentivirus Expressing JNK3-Specific shRNAs

While successful production and validation of lentiviruses encoding JNK3-specific shRNAs were initially performed in-house, loss of starting materials required that an alternative be found. Ultimately, for the isoform-specific knockdown of JNK3, lentivirus was commercially obtained.

Two high titer lentiviruses using the OpenBiosystems GIPZ lentivirus system encoding shRNA sequences targeting JNK3 were obtained (Cat#VGM5524-98727594 cloneV2LMM_175620 and Cat#VGM5524-98694857 cloneV2LMM_175625, Thermo Scientific, Lafayette, CO) (see Figure 4B). Proprietary informatics software was used to design

JNK3 shRNA sequences (TABLE II) to maximize target specificity and minimize off target effects. Similar to our in-house lentiviruses, the GIPZ lentiviruses express a GFP marker. Additionally, they contain a puromycin selection gene, facilitating the creation of cell populations with more consistent knockdown of the target gene by reducing the necessary amount of virus and eliminating non-expressing cells.

Effective multiplicity of infection (MOI) in N2a cells was determined by infecting cultured N2a cells with serially diluted virus of known titer in the same fashion as used in titer determination, then assessing for JNK3 knockdown by WB.

3.3.3 Infection of N2a cells

N2a cells were infected with JNK1shRNA lentiviruses at MOI = 18,500, or JNK3shRNA lentiviruses at MOI = 100. Cells were plated at 20,000 cells/well into 24-well plates in complete medium. Twenty-four hours post-plating, complete medium was removed and lentivirus was added to cells in serum-free medium in a total volume of 300µl/well. Six hours post-infection, 500µl complete medium was added per well. Cells infected with JNK3shRNA lentiviruses were switched to puromycin selection medium (3µg/ml) 24h post-transfection.

3.3.4. Validation of isoform-specific JNK knockdown

N2a cells infected with shRNA lentiviruses were evaluated by WB using JNK1 (Cat#551196, BD Pharmingen, San Jose, CA), JNK3 (Cat#55A8, Cell Signaling, Danvers, MA), and H2 antibodies (Brady Laboratory) (see TABLE IV) and qPCR analysis using mouse-specific primers for JNK1, JNK3, and GAPDH (see TABLE V).

3.4. WESTERN BLOT

Cell lysates for all test groups were validated at the protein level for 1) presence of Htt expression and/or 2) isoform-specific knockdown of JNK by Western Blot analysis.

3.4.1. Sample Collection and Preparation

Cells were lysed and harvested in 20mM HEPES with 1%SDS and sonicated on ice. Samples were not pelleted to avoid potential loss of aggregated Htt. Total protein concentrations of lysates were determined by BCA assay (Cat#23235, Thermo Fisher Scientific, Rockford, IL) and normalized.

3.4.2. Sample Analysis

Cell lysates were normalized, and a total of 20μg protein was loaded per well. Samples were resolved using NuPAGE® Novex 4–12% Bis-Tris Midi Gel in 1X MOPS buffer (Invitrogen, Grand Island, NY) at a constant 50mA. Proteins were then transferred to PVDF membranes in 1X Towbin buffer using Hoefer transfer apparatus (Hoefer, Inc., Hollistan, MA) at 4°C for 2h at 400mA. Membranes were blocked in 1% milk in 1X TBS buffer for 1h at RT, then incubated in 1°Ab (see TABLE ???) diluted into 1%BSA in 1X PBS overnight at at 4°C. The next day, membranes were washed 3x10min in 1X TBS buffer with 0.1%Tween20 (TBST), then incubated in HRP-conjugated 2°Ab diluted into TBST with 1% milk for 1h at RT. Membranes were then washed 3x10min in 1X TBS, and immunoreactivity was visualized using Immobilon Western Chemiluminescent HRP Substrate (Cat#WBKLS0500, Millipore, Billerica, MA).

Name	Vendor	Catalog#	Host Species	Dilution for WB	Dilution for ICC
EM48(Htt)	Chemicon	MAB5374	mouse	1:1000	
JNK1	BD Pharmingen	551196	mouse	1:10,000	
JNK3	Cell Signaling	55A8	rabbit	1:2000	
H2 (KHC)	in-house, Brady Laboratory	N/A	mouse	1:1,000,000	
DM1a (α-tubulin)	Sigma-Aldrich	T 9026	mouse		1:1000

TABLE IV

Antibodies used for Western Blot and Immunocytochemistry.

3.5. QUANTITATIVE PCR

3.5.1. Primer Design and Optimization

An initial search for primers targeting genes of interest were performed on http://primerdepot.nci.nih.gov/. If none were available, primers were designed using MacVector software. All primer sequences were validated using MacVector software (MacVector, Inc., Cary, NC). Primers for qPCR were designed to 1) span exon-exon junctions to preclude recognition of genomic DNA, 2) maximize terminal G/C content to enhance complete binding, 3) generate an amplicon between 50 and 200bp for optimal PCR efficiency, and 4) minimize unwanted secondary structures such as primer dimers and hairpins that could interfere with PCR efficiency.

primer name	sequence (5' to 3')	NCBI Accession Number	NCBI gene name(s)
JNK1.for	TTTGCTTCTGCTCAT GATGG	NM_016700	Official Symbol: Mapk8; Official Full Name: mitogen-activated protein kinase 8; Also known as JNK, JNK1, Prkm8, SAPK1, AI849689, Mapk8
JNK1.rev	GCTACGGGCTTCCAG GTC	NM_016700	Official Symbol: Mapk8; Official Full Name: mitogen-activated protein kinase 8; Also known as JNK, JNK1, Prkm8, SAPK1, AI849689, Mapk8
JNK3.for	TCACATCCAAGGTTG GTTCA	NM_009158 NM_001081567	Official Symbol: Mapk10; Official Full Name: mitogen-activated protein kinase 10; Also known as JNK3, Serk2, JNK3B1, JNK3B2, p493F12, p54bSAPK, SAPK(beta), C230008H04Rik, Mapk10
JNK3.rev	AGGCAAGACGCTGTT GAGTT	NM_009158 NM_001081567	Official Symbol: Mapk10; Official Full Name: mitogen-activated protein kinase 10; Also known as JNK3, Serk2, JNK3B1, JNK3B2, p493F12, p54bSAPK, SAPK(beta), C230008H04Rik, Mapk10
HTT-hs.for	GCTACCAAGAAAGAC CGTGTGAATC	NM_002111.6	Official Symbol: HTT; Official Full Name: homo sapiens huntingtin; Also known as Htt, IT15
HTT-hs.rev	ACCATCCTGACATCT GACTCTGCG	NM_002111.6	Official Symbol: HTT; Official Full Name: homo sapiens huntingtin; Also known as Htt, IT15
mGAPDH.for	ACCCAGAAGACTGTG GATGG	NM_008084	Official Symbol: Gapdh; Official Full Name: glyceraldehyde-3-phosphate dehydrogenase [Mus musculus]; Also known as Gapd
mGAPDH.rev	GACATTGGGGGTAGG AACAC	NM_008084	Official Symbol: Gapdh; Official Full Name: glyceraldehyde-3-phosphate dehydrogenase [Mus musculus]; Also known as Gapd

TABLE V

Primers used in quantitative PCR.

3.5.2. RNA Isolation and cDNA Synthesis

Cells were lysed and harvested in TRI REAGENT® - RNA / DNA / Protein Isolation Reagent (Cat# TR 118, Molecular Research Center, Inc., Cincinnati, OH) and RNA was isolated using the Direct-zol RNA miniprep kit (Cat# R2050, Zymo Research, Irvine, CA) per vendor protocols. Normalized RNA was then used to synthesize cDNA using the iScript cDNA kit (Cat#170-8890, BioRad, Hercules, CA) per vendor protocol.

3.5.3. Quantitation of mRNA Transcript Expression

Quantitative PCR was performed on samples using the iQ5 thermocyler apparatus and software (Bio-Rad Laboratories, Hercules, CA) in conjunction with iQ™ SYBR® Green Supermix (Cat#170-8880, BioRad, Hercules, CA). Briefly, each qPCR reaction consisted of 1µg sample cDNA, forward and reverse primer (see TABLE V) at a final concentration of 150nM, and iQ™ SYBR® Green Supermix at a final concentration of 1X, all in a total volume of 20µl. Samples were run in triplicate, and a melting curve was performed on each plate to validate amplification of correct PCR products.

Quantitative PCR data was analyzed using the delta-delta calculation method [318] to determine relative expression of the mRNA transcript of interest as normalized to GAPDH.

3.6. NEURITE OUTGROWTH ANALYSIS

Cells grown in ibidi slides were differentiated for 5 days in serum-free media with 10µM all-trans retinoic acid. Cells were fixed with 4%PFA in 1xPBS for 20min at RT, then washed 3x5min in 1xPBS. Cells were then permeabilized and blocked in 5%NGS in 0.25% TritonX100 in PBS for 1h at RT, and washed 3x5min in 1xPBS. Cells were incubated in DM1A anti-tubulin

antibody (Sigma Aldrich T9026) at 4°C overnight. The next day, cells were rinsed 3x5min in 1xPBS, then incubated in a secondary antibody (AlexaFluor594, Cat# A-11032, Invitrogen, Grand Island, NY) for 1h at RT. After rinsing 3x5min in 1xPBS, 30µl of Vectashield mounting media with DAPI (VectorLabs, H-1200) was added to each channel. Images were acquired using a Zeiss Axiovert 200M with OpenLab software (Perkin Elmer) using 40x, 1.3 N.A., 20x, 0.5 N.A., and 10x, 0.3 N.A. objectives. Neurite length was measured for at least 250 cells per group using NIH ImageJ image analysis software. Cells with neurites less than 1.5x the diameter of the cell in length were excluded. Outcomes were determined by MANOVA followed by post-hoc Tukey's HSD analysis, with the level of significance set at 0.05.

3.7. MITOCHONDRIAL DISTRIBUTION ANALYSIS

Cells grown in ibidi slides were differentiated for 5 days in serum-free media with 10µM all-trans retinoic acid, then stained with MitoTracker® Red CMXRos (Cat# M7512, Invitrogen, Grand Island, NY), a fluorescing dye that selectively accumulates in active mitochondria, according to vendor recommendations. Briefly, cells were incubated in MitoTracker® Red CMXRos diluted in differentiation medium at a final concentration of 100nM for 45min at 37°C with 5%CO_2. Cells were then fixed in 4%PFA in medium for 15min at 37°C. After rinsing 3x5min in 1xPBS, cells were incubated in ice-cold acetone for 5min to improve signal-to-background ratio, per vendor recommendation. After rinsing 3x5min in 1xPBS, 30µl of Vectashield mounting media with DAPI (VectorLabs, H-1200) was added to each channel. Images were acquired using a Zeiss Axiovert 200M with OpenLab software (Perkin Elmer) using a 40x, 1.3 N.A. objective. Images were then analyzed for MitoTracker® Red CMXRos

fluorescence in the cell bodies and in neurites measured as mean gray pixel intensity per traced area using NIH ImageJ software. For each cell of interest, the entire cell body or the entire neurite was traced and measured, as well as an adjacent non-cell-containing area for background. For each group, 60 cells were measured, and mean cell body and neurite values were corrected for background. Cells with neurites less than 1.5x the diameter of the cell in length were excluded. Outcomes were determined by MANOVA followed by post-hoc Tukey's HSD analysis, with the level of significance set at 0.05.

CHAPTER 4

RESULTS

4.1. Generation and Validation of an In Vitro Test Model for the Role of Specific JNK Isoforms in PolyQ-Htt Mediated Axonal Dysfunction

In order to examine the effect of individual JNK isoforms on polyQ-Htt induced axonal deficits, we created a cell model with concurrent expression of wt- or polyQ-Htt and knockdown of JNK1 or JNK3. Due to the extended half life of JNKs (~8h) [319], we chose to use lentiviral delivery of JNK shRNAs. This would facilitate knockdown of JNKs in 2 ways: 1) lentiviral delivery would result in stable integration of the expression cassette into the host genome, and 2) shRNAs can silence multiple copies of their target mRNAs, as opposed to single use siRNAs. N2a cells were selected as our host for a number of reasons. They are derived from neural tissue, and are easily differentiated with robust polarization and neurite outgrowth, and have long been used as a model of axonal phenomena [313]. Additionally, neurite outgrowth in N2a cells has been shown to be inhibited by polyQ-Htt, but not wt-Htt [67]. N2a cells have also been shown to express JNK1, JNK2, and JNK3 at the mRNA and protein level [320]. We also confirmed expression of all three JNK isoforms in

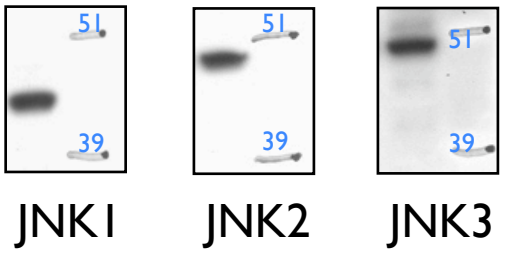

Figure 5. Differentiated N2a cells express all 3 isoforms of JNK. Western blot of N2a cells differentiated for 5d and probed with isoform-specific JNK antibodies demonstrate expression of all 3 JNK isoforms at the protein level.

differentiated N2a cells by WB (see Figure 5). Before the creation of cell lines expressing both Htt construct and JNK shRNAs, we produced cell lines expressing a single characteristic to validate the efficacy of transduction.

4.1.1. Stable Expression of 23Q-Htt or 148Q-Htt in N2a Cells

Htt expressing cell lines were initially generated by infection of N2a cells with lentivirus encoding either a wt- or polyQ-Htt exon1 construct. The use of lentivirus allowed for the integration of the Htt expression cassette into non-dividing cells (i.e. differentiated neurons), not only facilitating the stable expression of Htt constructs in our target host population, but also for future use in vivo. Infections of N2a cells from the original productions of wt-Htt and polyQ-Htt lentivirus resulted in the successful expression of both Htt constructs, as verified by WB (See Appendix B). Unfortunately, subsequent productions of the polyQ-Htt lentivirus failed to yield detectable levels of polyQ-Htt in N2a lysates. In order to bypass this obstacle we switched to stable transfection of N2a cells with Htt construct expressing plasmids (a kind gift from Dr. John O'Bryan). These plasmids encode the first 171aa of the N-terminus of Htt exon1, with a 23Q, 65Q, or 148Q polyglutamine stretch in the polymorphic expansion region (from this point on referred to as 23Q-, 65Q-, or 148Q-Htt, respectively), and an enhanced CFP fused to the C-terminus (see TABLE I). Additionally, the plasmids encode a G418 resistance gene to allow for selection.

Lysates of N2a cells transfected with plasmids encoding 23Q-, 65Q-, and 148Q-Htt were analyzed by WB using an anti-Htt antibody (EM48, Millipore) that recognizes an epitope in the

C-terminus of exon1 adjacent to the proline-rich region (PRR) [321]. Lysates were harvested 6 days post-transfection, and after cells had undergone 5 days of differentiation without G418

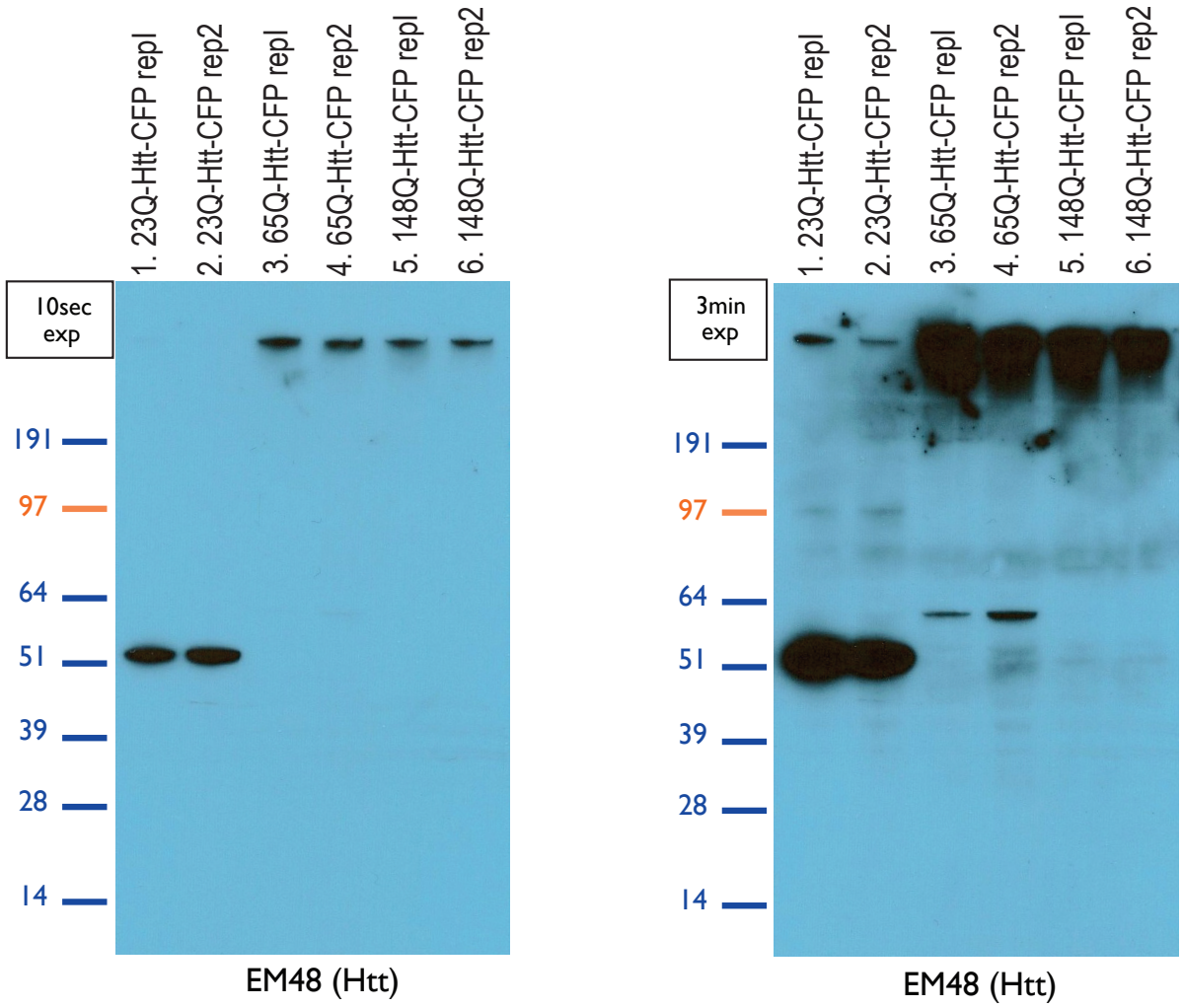

Figure 6. Expression of Htt-CFP in N2a cells. N-terminus fragments of human Htt containing polyQ expansions of 23Q, 65Q, or 148Q were expressed in N2a cells and analyzed by Western blot. Left panel: EM48 anti-Htt Ab reveals immunoreactive bands corresponding to 23Q (~51kDa) in lanes 1&2, 65Q (>191kDa) in lanes 3&4, and 148Q-Htt (>191kDa) in lanes 5&6. 65Q-Htt and 148Q-Htt bands did not show significant migration from loading well, most likely due to prevention of migration through gel matrix due to aggregation. Right panel: Longer exposure of the membrane in the left panel reveals bands for non-aggregated 65Q-Htt (~64kDa) in lanes 3&4, as well as endogenous mouse Htt (343kDa) in lanes 1&2. Endogenous Htt bands are masked by 65Q-Htt and 148Q-Htt in rows 3-6.

selection. EM48 immunoreactive bands were present in all samples (see Figure 6). A short exposure time (10 sec, left panel) revealed that N2a cells trasfected with 23Q-Htt yields a band at ~51kDa (lanes 1&2) and both 65Q- and 148Q-Htt lysates yield a high molecular weight (HMW) band (lanes 3-6). A longer exposure time (3 min, right panel) revealed that N2a cells transfected with 65Q-Htt yielded 2 bands, a weakly immunoreactive band at ~64kDa, and second HMW band (lanes 3&4). The ~64kDa band represents linearized soluble 65Q-Htt, slightly larger than the 23Q-Htt band (lanes 1&2) as accounted for by the longer polyQ stretch. The HMW bands from 65Q- and 148Q-Htt samples (lanes 3-6) did not migrate any appreciable distance from the loading well, likely due to decreased ability to migrate through the gel matrix. This could possibly be due to aggregation during sample preparation, as SDS and sonication have been shown to cause aggregation of proteins containing alpha helices and beta sheets, which structures that elongated polyQ stretches are known to form [322, 323]. Longer exposure time also revealed a weakly immunoreactive HMW band in the 23Q-Htt lysate (right panel, lanes 1&2), representing endogenous mouse Htt (343kDa). The HMW bands present in 65Q- and 148Q-Htt samples are likely a mixture of exogenous constructs and endogenous mouse Htt (lanes 3-6), but it is possible that the increased HMW immunoreactivity in 65Q- and 148Q-Htt samples compared to HMW bands in 23Q-Htt samples is due to upregulation of endogenous Htt expression. To address this issue, several steps can be taken to increase the likelihood that the HMW bands contain exogenous Htt constructs. Corresponding qPCR data indicates that 148Q-Htt expression was much lower than 23Q-Htt (see Figure 7). Equal amounts of total protein were loaded for each sample, but it is possible that levels of linearized 148Q-Htt within samples were too low to be detected by the methods used. Running more total protein may reveal 148Q-

Htt bands of the expected molecular weight. The next step would be to re-analyze the samples using CFP antibody to detect the CFP tag on exogenous Htt constructs. Presence of both increased EM48 immunoreactivity and CFP immunoreactivity migrating to the same molecular weight would increase the likelihood that the HMW EM48 immunoreactive bands contains the exogenously expressed 65Q- and 148Q-Htt. Also, the samples had been resolved using a NuPAGE® Novex 4–12% Bis-Tris Midi Gel, and running the samples on a lower % gel would allow for higher molecular weight proteins to migrate more easily, and might improve resolution between endogenous mouse Htt and exogenously expressed Htt. Further, new samples could be prepared using a different detergent such as Cetyltrimethylammonium bromide [324], which serves as an alternative to SDS where protein aggregation by SDS is suspected. Preparation procedures could also be modified to disrupt cell membranes by running samples through needles of decreasing diameter in lieu of sonication. This may result in less thorough disruption of cell membranes, but would also decrease the potential of aggregate formation.

Htt constructs were also validated at the qPCR level, using human-specific Htt primers that only recognize the exogenous Htt constructs. Cells used for qPCR validation of Htt had undergone G418 selection and, as with the samples used for WB analysis, were differentiated for 5 days before harvesting and processing. From this point forward, we opted to use only the 148Q-Htt construct to represent pathogenic Htt, as pathological phenotype is proportional to polyQ length [325]. cDNA synthesized from both 23Q-Htt and 148Q-Htt samples yielded detectable amounts of exogenous Htt (see Figure 7), validating the presence of the constructs at the mRNA level. The positive control used was previously validated lysate from N2a cells

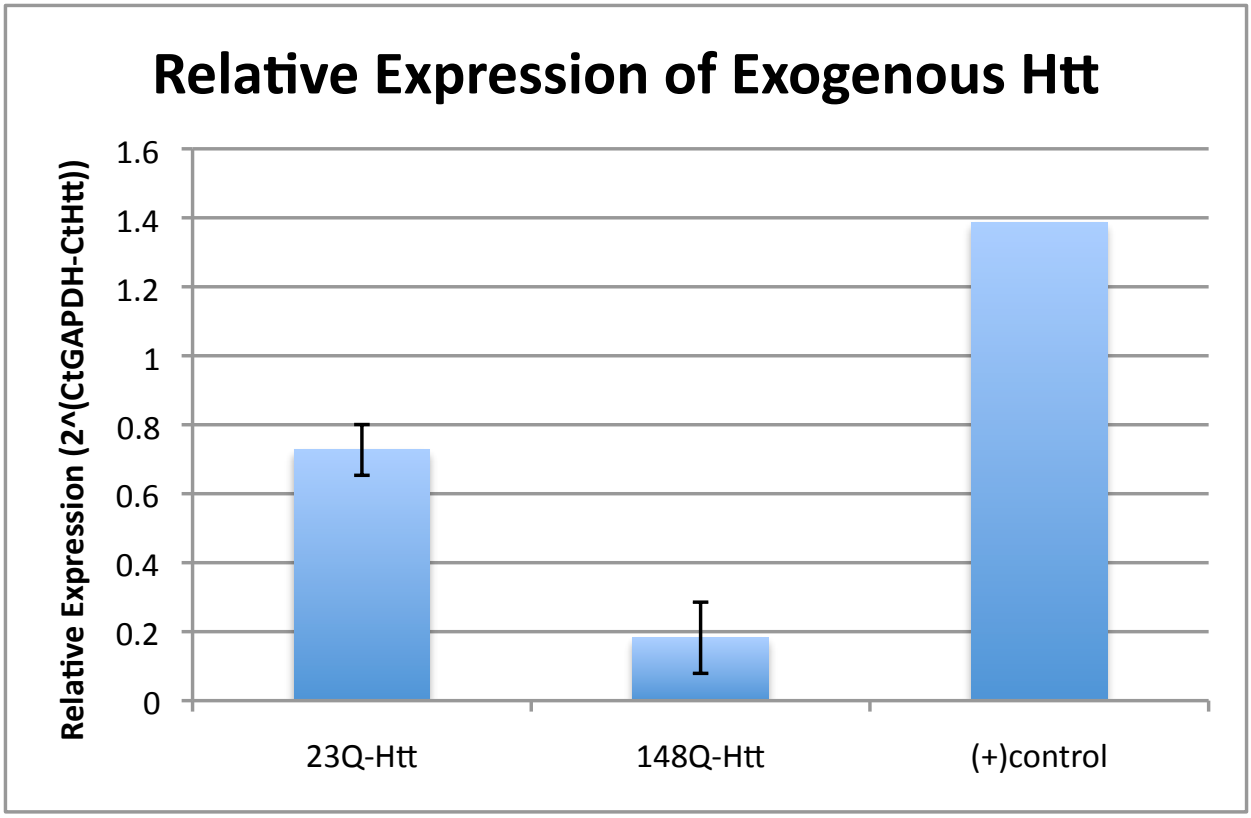

Figure 7. Expression of exogenous Htt constructs. cDNA synthesized from mRNA harvested from N2a cells stably expressing either 23Q-Htt or 148Q-Htt was analyzed by qPCR using human-specific Htt primers. Relative expression of exogenous Htt was calculated using the ΔΔCt method, normalized to mouse GAPDH. Positive control was from N2a cells infected with lentivirus encoding 23Q-Htt previously validated for Htt expression. Error bars indicate ± SEM.

infected with lentivirus encoding 23Q-Htt (see Appendix B). Of note, the 148Q-Htt expression is lower than 23Q-Htt. However, G418 selected 148Q-Htt populations still showed detectable 148Q-Htt at the mRNA and protein level, detectable CFP reporter by fluorescent microscopy (see Figure 16I), and an obvious difference in phenotype compared to 23Q-Htt expressing cells (see Figure 19A&G). Importantly, there were no microscopically detectable aggregates in neurites as assessed by CFP fluorescence in either 23Q-Htt or 148Q-Htt cells (see Figures 16C&I) after G418 selection.

4.1.2. Stable Isoform-Specific Knockdown of JNK1 or JNK3

JNK knockdown was achieved through the use of lentiviral delivery of expression cassettes encoding isoform-specific shRNA sequences (see Figure 4 and TABLE II). High titer lentiviruses encoding JNK1-specific shRNAs were successfully produced and validated in house. Initial productions for in house JNK3 shRNA encoding lentiviruses were also successful, but due to unforeseeable adverse events in material transfer, subsequent productions were not successful. Alternately, comparable commercially available lentiviruses were obtained from OpenBiosystems.

For the knockdown of JNK1 and JNK3 isoforms, a total of 5 cell lines were created. For each JNK isoform of interest, N2a cells were infected with one of two lentiviruses expressing different shRNA sequences targeting the same gene (see TABLE II). This was done to overcome any spurious sequence-specific effects as to ensure that any significant observations made were based on actual knockdown of a single JNK isoform. As a negative control for knockdown, a fifth lentivirus encoding a non-targeting shRNA was used. Fluorescent microscopic assessment

of GFP reporter protein encoded by all 5 lentiviruses was present and stable over time (see Figure 16D&J for representative images).

Isoform-specific knockdown of JNKs were confirmed by WB (Figures 8&10) and qPCR (Figures 9&11) analysis. H2 antibody (Brady Laboratory), which recognizes KHC, was used as a loading control. There were no appreciable differences in H2 immunoreactivity across all samples analyzed within individual experiments, indicating loading of equivalent amounts of total protein. Cells infected with JNK1shRNA1 (see Figure 8, top panel, lanes 1&2) and JNK1shRNA2 (lanes 3&4) showed decreased JNK1 immunoreactivity in JNK1 size-specific bands (46kDa) as compared to non-targeting shRNA controls (lanes 5&6). In contrast, neither JNK1shRNA sample (see Figure 8, bottom panel, lanes 1-4) showed a decrease in JNK3 immunoreactivity at JNK3 size-specific bands (54kDa) compared to non-targeting shRNA controls (lanes 5&6). The significant reduction in JNK1 immunoreactivity and lack of reduction in JNK3 immunoreactivity validates the effective and specific knockdown of JNK1 by JNK1shRNA1 and JNK1shRNA2 at the protein level. This was confirmed at the RNA level by qPCR (Figure 9). Relative expression of JNK1, as normalized to the housekeeping gene GAPDH, was reduced to less than 30% in cDNA samples synthesized from cells expressing JNK1shRNA1 and JNK1shRNA2 as compared to non-targeting controls. And as with WB results, there were no significant differences in JNK3 expression across all samples. This validates at the mRNA level that there is significant and specific knockdown of JNK1 by JNK1shRNA1 and JNK1shRNA2. Conversely, WB and qPCR analysis of cells expressing JNK3shRNAs showed no knockdown of JNK1, but effective knockdown of JNK3.

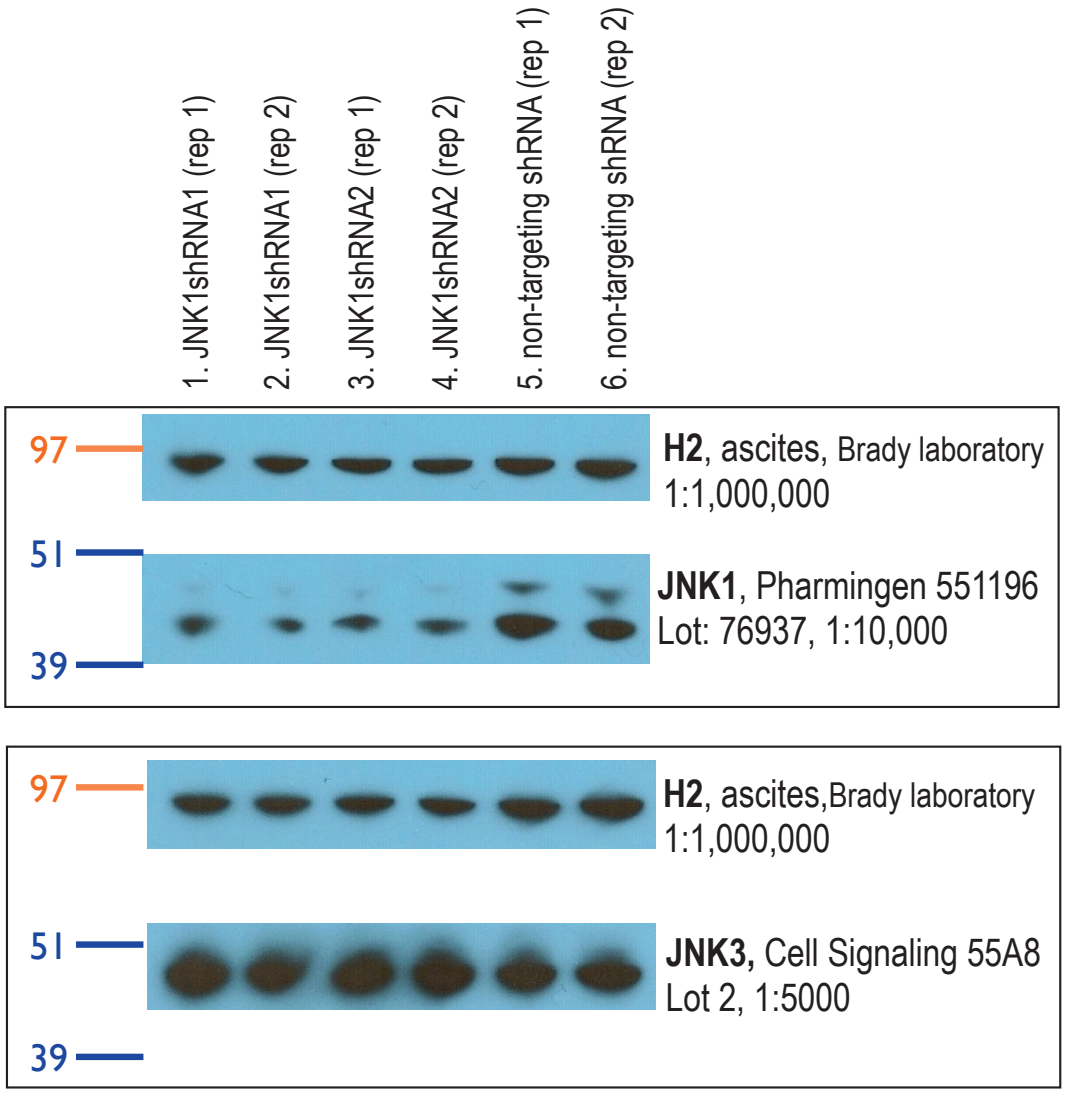

Figure 8. Isoform specific knockdown of JNK1 in N2a cells. N2a cells were infected with lentivirus encoding one of two JNK isoform 1 specific shRNAs, or a non-targeting shRNA (see TABLE II) then analyzed by Western blot. Top panel: N2a cells expressing JNK1shRNA1 (lanes 1&2), and JNK1shRNA2 (lanes 3&4) show JNK1 size-specific bands with reduced JNK1 immunoreactivity as compared to cells expressing non-targeting shRNA (lanes 5&6). Kinesin heavy chain (H2) was used as a loading control, and yielded bands of similar immunoreactivity across all groups. Bottom panel: Samples showed no reduction in immunoreactivity of JNK3 size-specific bands when probed for JNK3 across all groups. This indicates that JNK1shRNA1 and JNK1shRNA2 are effective and specific in knocking down JNK1 in N2a cells at the protein level.

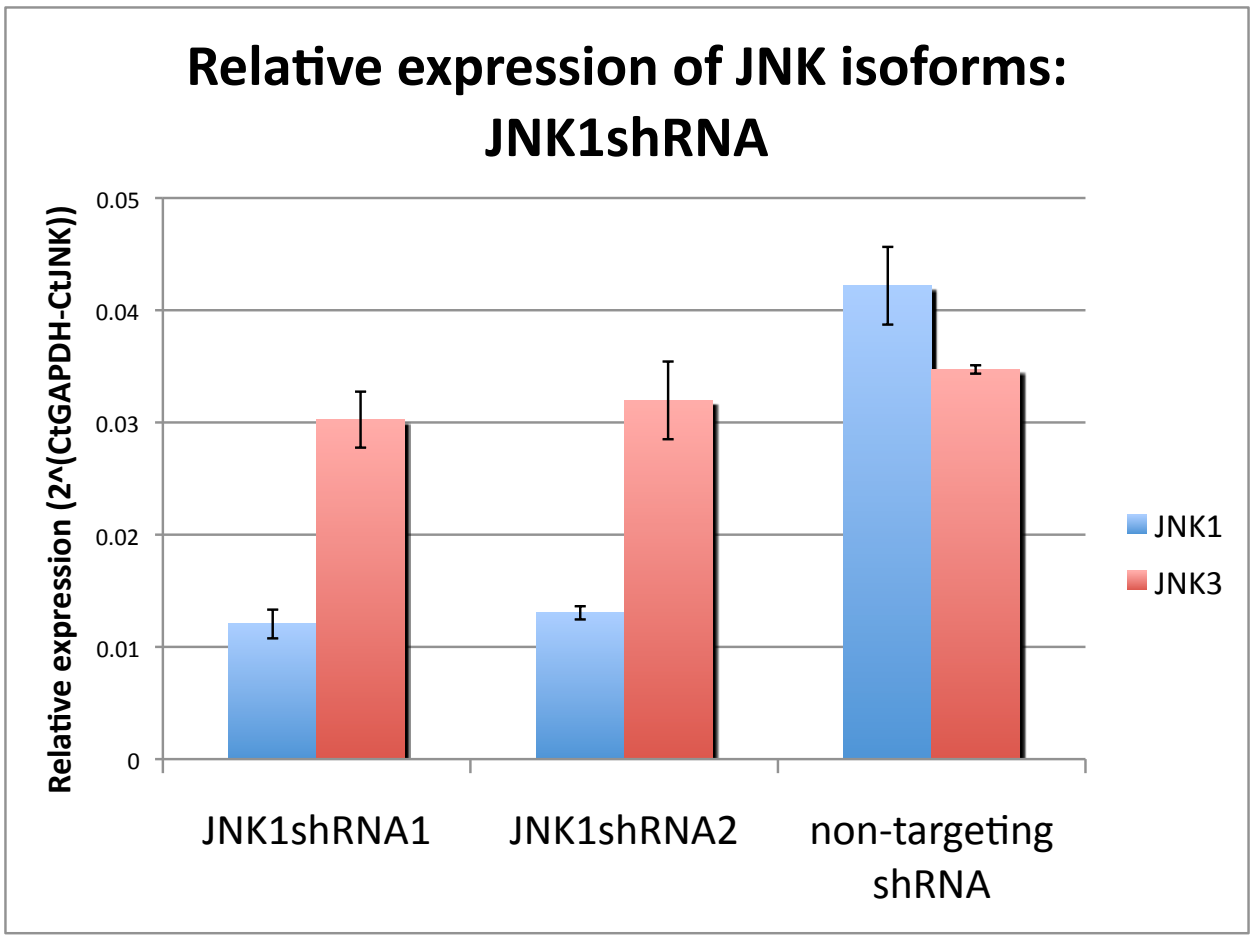

Figure 9. Expression of JNK1 in N2a cells with isoform specific knockdown of JNK1. cDNA synthesized from mRNA harvested from N2a cells stably expressing JNK1shRNA1, JNK1shRNA2, or non-targeting shRNA was analyzed by qPCR using mouse JNK1 and JNK3 specific primers. Relative expression of each JNK isoform was calculated using the ΔΔCt method, normalized to mouse GAPDH. JNK1shRNA1 and JNK1shRNA2 decreased the amount of detectable JNK1 cDNA while having no effect on JNK3 cDNA, as compared to non-targeting shRNA controls. This indicates that JNK1shRNA1 and JNK1shRNA2 are effective and specific in knocking down JNK1 in N2a cells at the mRNA level. Error bars indicate ± SEM.

Cells infected with JNK3shRNA1 (see Figure 10, bottom panel, lanes 3-6) and JNK3shRNA2 (lanes 7-9) showed decreased JNK3 immunoreactivity in JNK3 size-specific bands (54kDa) as compared to non-targeting shRNA controls (lanes 1-3). In contrast, neither of the JNK3shRNA samples (see Figure 10, top panel, lanes 4-9) showed a decrease in JNK1 immunoreactivity at JNK1 size-specific bands (46kDa) compared to non-targeting shRNA controls (lanes 1-3). The significant reduction in JNK3 immunoreactivity and lack of reduction in JNK1 immunoreactivity validates the effective and specific knockdown of JNK3 by JNK3shRNA1 and JNK3shRNA2 at the protein level. This too was confirmed at the RNA level by qPCR (see Figure 11). Relative expression of JNK3, as normalized to the housekeeping gene GAPDH, was reduced to less than 25% in cDNA samples synthesized from cells expressing JNK3shRNA1 and JNK3shRNA2 as compared to non-targeting controls. And as with WB results, there were no significant differences in JNK1 expression across all samples. This validates at the mRNA level that there is effective and isoform specific knockdown of JNK3 by JNK3shRNA1 and JNK3shRNA2.

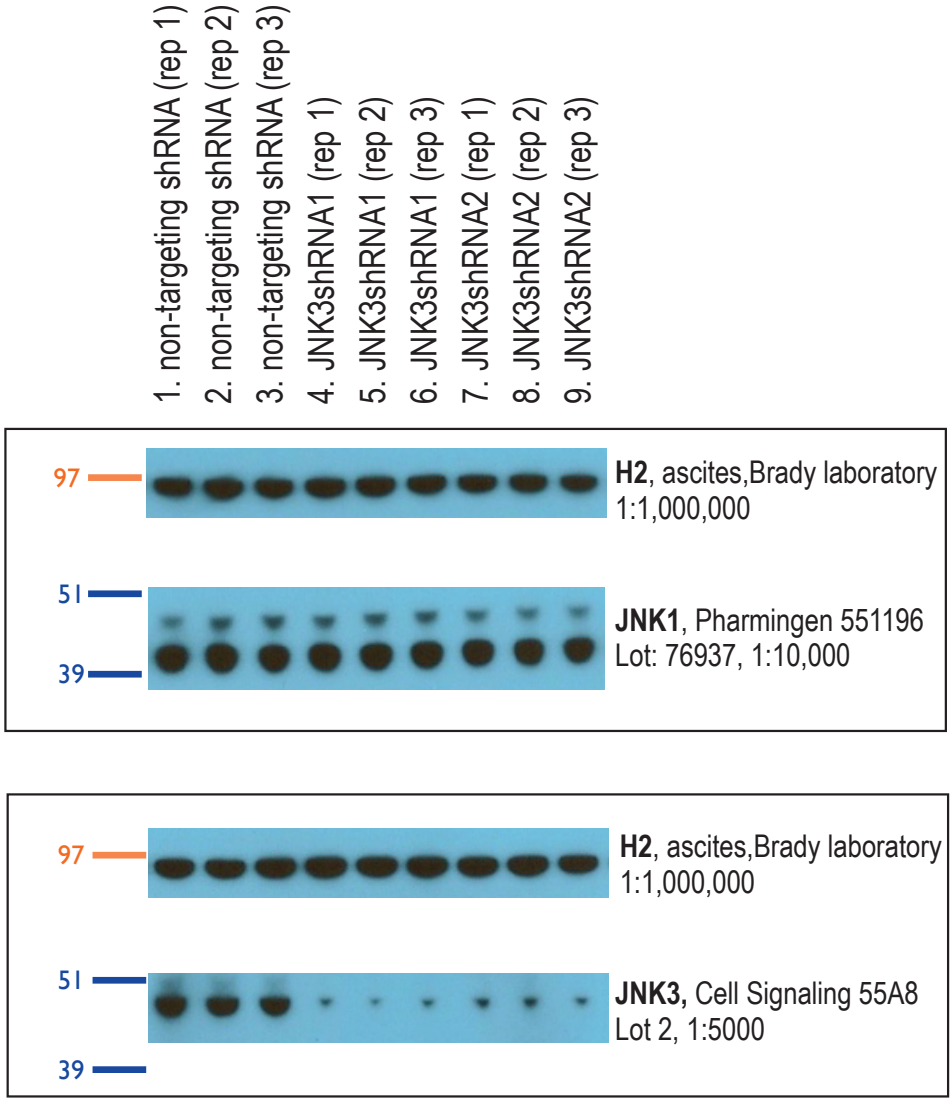

Figure 10. Isoform specific knockdown of JNK3 in N2a cells. N2a cells were infected with lentivirus encoding one of two JNK isoform 3 specific shRNAs, or a non-targeting shRNA (see TABLE II) then analyzed by Western blot. Top panel: N2a cells expressing JNK3shRNA1 (lanes 4-6) or JNK3shRNA2 (lanes 7-9) show JNK1 size-specific bands with similar JNK1 immunoreactivity as compared to cells expressing non-targeting shRNA (lanes 1-3). Kinesin heavy chain (H2) was used as a loading control, and yielded bands of similar immunoreactivity across all groups. Bottom panel: N2a cells expressing JNK3shRNA1 (lanes 4-6) or JNK3shRNA2 (lanes 7-9) show JNK3 size-specific bands with reduced JNK3 immunoreactivity as compared to cells expressing non-targeting shRNA (lanes 1-3). This indicates that JNK3shRNA1 and JNK3shRNA2 are effective and specific in knocking down JNK3 in N2a cells at the protein level.

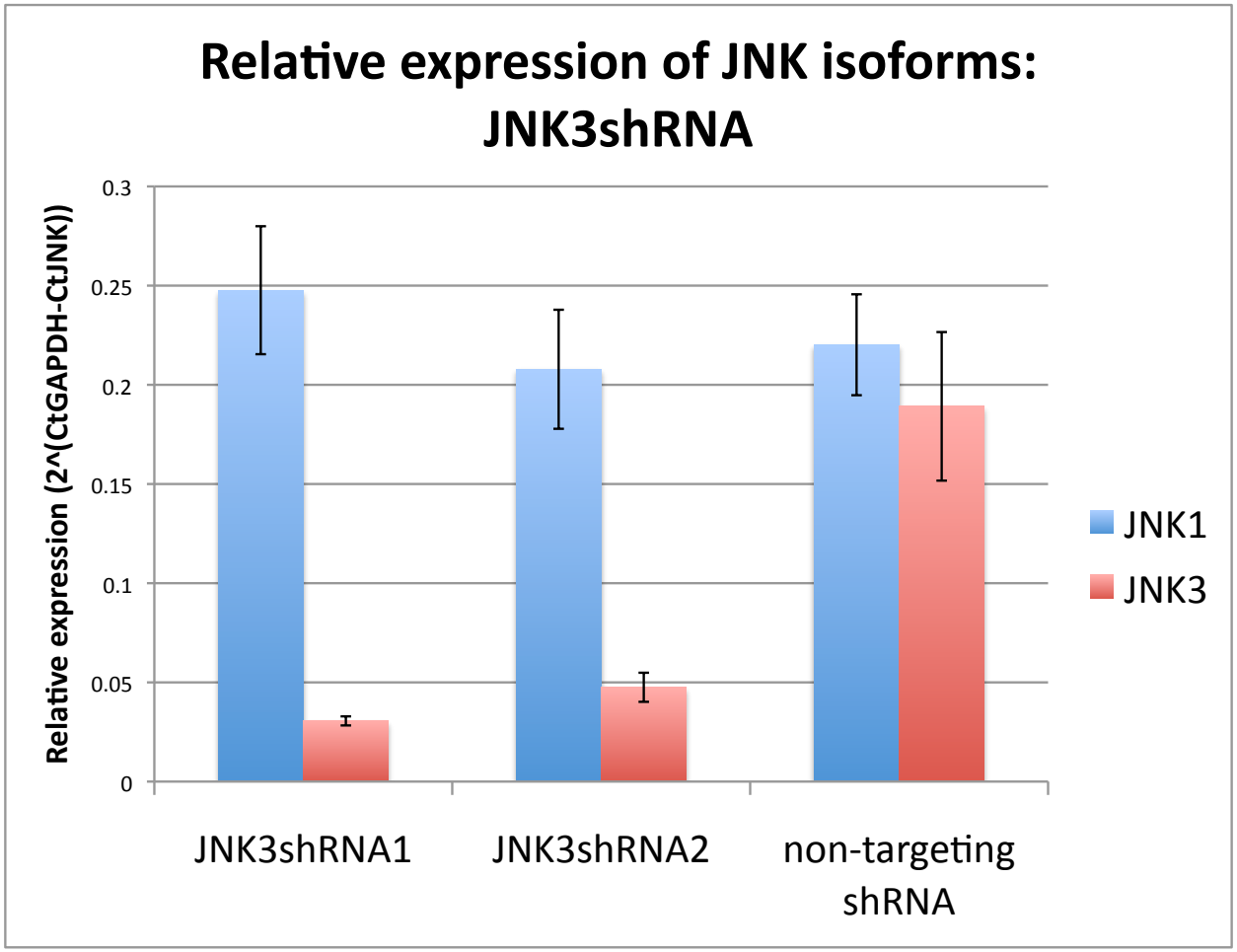

Figure 11. Expression of JNK3 in N2a cells with isoform specific knockdown of JNK3. cDNA synthesized from mRNA harvested from N2a cells stably expressing JNK3shRNA1, JNK3shRNA2, or non-targeting shRNA was analyzed by qPCR using mouse JNK1 and JNK3 specific primers. Relative expression of each JNK isoform was calculated using the ΔΔCt method, normalized to mouse GAPDH. JNK3shRNA1 and JNK3shRNA2 decreased the amount of detectable JNK3 cDNA while having no effect on JNK1 cDNA, as compared to non-targeting shRNA controls. This indicates that JNK3shRNA1 and JNK3shRNA2 are effective and specific in knocking down JNK3 in N2a cells at the mRNA level. Error bars indicate ± SEM.

4.1.3. Stable Htt Expression with JNK Knockdown

At this juncture, expression of normal and pathogenic Htts, and knockdown of JNK1 and JNK3, had been validated. In order to test the effects of each JNK isoform in polyQ-Htt mediated axonal dysfunction, we created N2a cell lines expressing 1) 23Q- or 148Q-Htt, with simultaneous expression of 2) JNK1shRNA1, JNK1shRNA2, JNK3shRNA1, JNK3shRNA2, non-targeting shRNA, or no shRNA, for a total of 12 different cell lines. Due to the limited amount of lentivirus encoding shRNAs, we used cells in which isoform-specific knockdown had been validated and transfected them with the 23Q-Htt or 148Q-Htt plasmids, as opposed to the reversed order. Concurrently infected (for shRNA expression) and transfected (for Htt expression) cells underwent G418 and puromycin double selection, and were validated for continued expression of Htt constructs and knockdown of JNKs by WB.

Cells expressing both 23Q-Htt and isoform-specific JNK shRNAs were cultured, differentiated, and harvested in the same manner as above. WB analysis of 23Q-Htt/ JNK1shRNA cells (see Figure 12) confirmed that the cells continued to express 23Q-Htt (bottom panel, all lanes), as well as have efficient knockdown of JNK1 (top panel, lanes 1-6) in the absence of any JNK3 knockdown (middle panel, lanes 1-6) compared to non-targeting controls (top and middle panels, lanes 7-9). WB analysis of 23Q-Htt/JNK3shRNA cells (see Figure 13) likewise confirmed that all samples continued to express 23Q-Htt (bottom panel, all lanes), and that compared to non-targeting controls (top and middle panels, lanes 1-3), JNK3 was effectively knocked down (middle panel, lanes 4-9) but JNK1 was not (top panel, lanes 4-9). This data confirms the generation of N2a cells expressing 23Q-Htt with concomitant isoform specific knockdown of either JNK1 or JNK3.

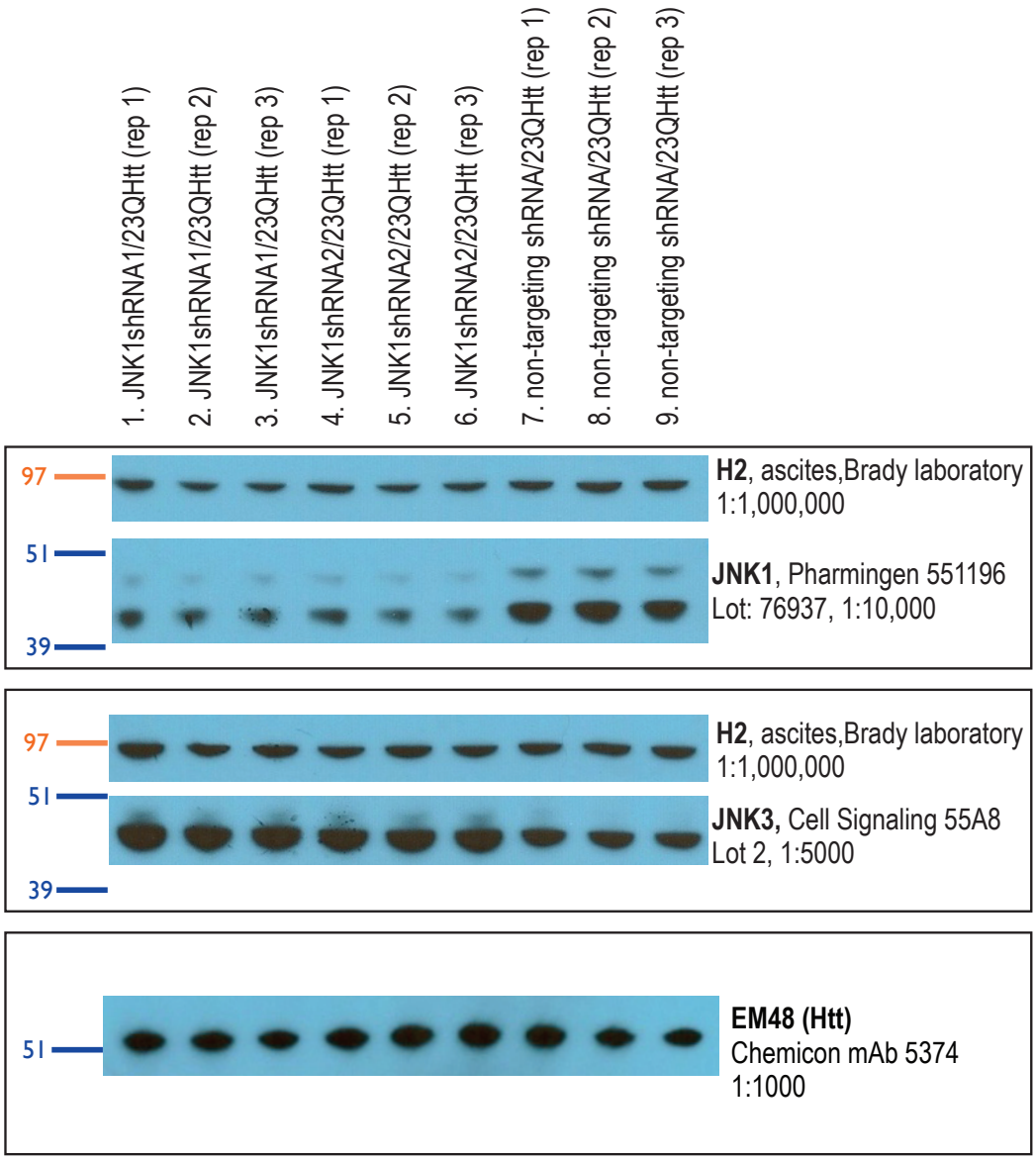

Figure 12. JNK knockdown and Htt expression in 23Q-Htt/JNK1shRNA cells. N2a cells stably expressing 23Q-Htt and JNK1 specific shRNAs were validated for isoform-specific JNK knockdown and expression of Htt. Top panel: N2a cells stably expressing 23Q-Htt in conjunction with JNK1shRNA1 (lanes 1-3) or JNK1shRNA2 (lanes 4-6) showed significant reductions in JNK1 immunoreactivity as compared to 23Q-Htt cells with non-targeting shRNA (lanes 7-9). Kinesin heavy chain (H2) was used as a loading control, and yielded bands of similar immunoreactivity across all groups. Middle panel: There was no decrease in JNK3 immunoreactivity in 23Q-Htt cells expressing JNK1shRNA1 (lanes 1-3) or JNK1shRNA2 (lanes 4-6) as compared to 23Q-Htt cells with non-targeting shRNA (lanes 7-9). Bottom panel: All samples expressed 23Q-Htt size-specific bands with similar immunoreactivity. These results indicate that N2a cells expressing both 23Q-Htt and a JNK1 specific shRNA maintain expression of exogenous Htt and isoform specific knockdown of JNK1 at the protein level.

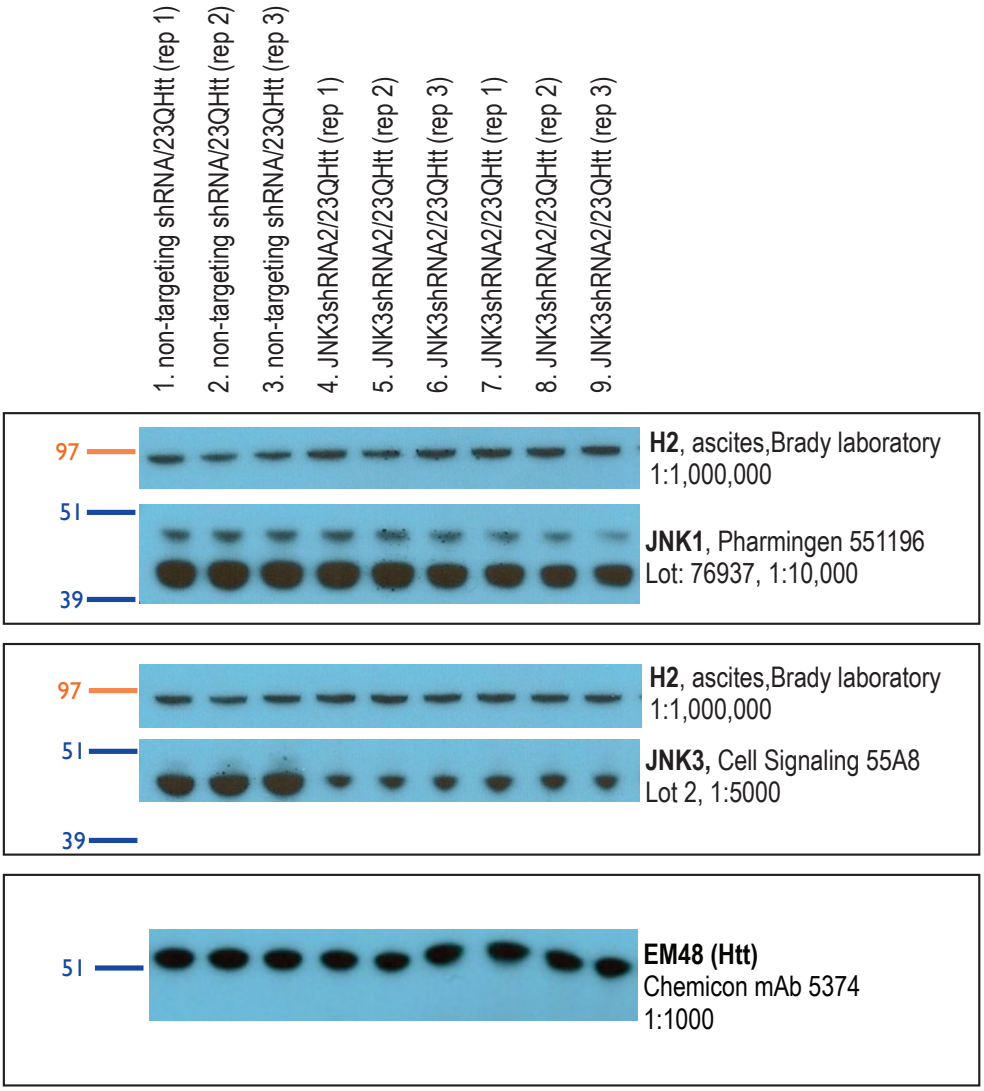

Figure 13. JNK knockdown and Htt expression in 23Q-Htt/JNK3shRNA cells. N2a cells stably expressing 23Q-Htt and JNK3 specific shRNAs were validated for isoform-specific JNK knockdown and expression of Htt. Top panel: N2a cells stably expressing 23Q-Htt in conjunction with JNK3shRNA1 (lanes 4-6 or JNK3shRNA2 (lanes 7-9) showed no differences in JNK1 immunoreactivity as compared to 23Q-Htt cells with non-targeting shRNA (lanes 1-3). Kinesin heavy chain (H2) was used as a loading control, and yielded bands of similar immunoreactivity across all groups. Middle panel: There were significant reductions in JNK3 immunoreactivity in 23Q-Htt cells expressing JNK3shRNA1 (lanes 4-6) or JNK3shRNA2 (lanes 7-9) as compared to 23Q-Htt cells with non-targeting shRNA (lanes 1-3). Bottom panel: All samples expressed 23Q-Htt size-specific bands with similar immunoreactivity. These results indicate that N2a cells expressing both 23Q-Htt and a JNK3 specific shRNA maintain expression of exogenous Htt and isoform specific knockdown of JNK3 at the protein level.

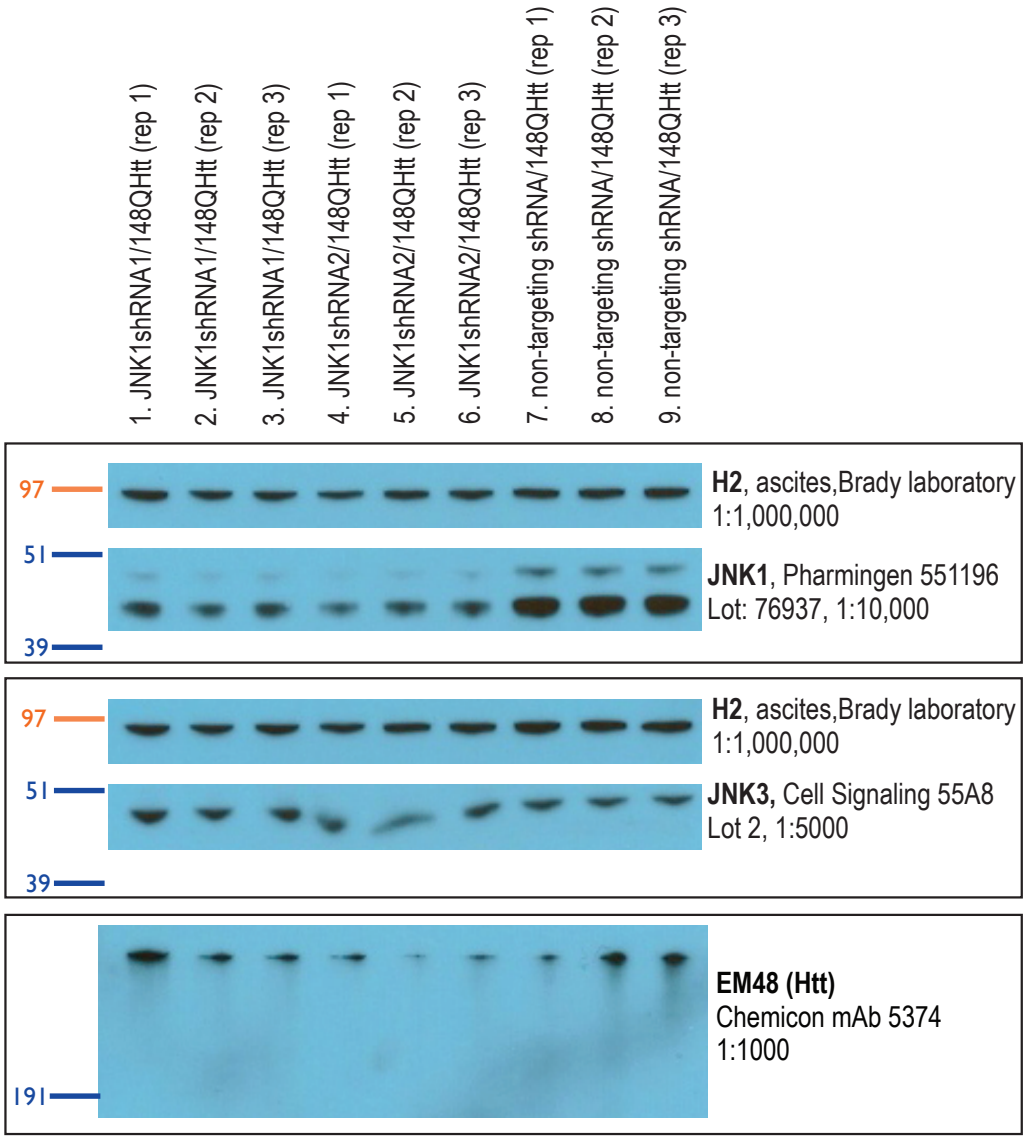

Figure 14. JNK knockdown and Htt expression in 148Q-Htt/JNK1shRNA cells. N2a cells stably expressing 148Q-Htt and JNK1 specific shRNAs were validated for isoform-specific JNK knockdown and expression of Htt. Top panel: N2a cells stably expressing 148Q-Htt in conjunction with JNK1shRNA1 (lanes 1-3) or JNK1shRNA2 (lanes 4-6) showed significant reductions in JNK1 immunoreactivity as compared to 148Q-Htt cells with non-targeting shRNA (lanes 7-9). Kinesin heavy chain (H2) was used as a loading control, and yielded bands of similar immunoreactivity across all groups. Middle panel: There was no significant decrease in JNK3 immunoreactivity in 148Q-Htt cells expressing JNK1shRNA1 (lanes 1-3) or JNK1shRNA2 (lanes 4-6) as compared to 148Q-Htt cells with non-targeting shRNA (lanes 7-9). Bottom panel: All samples expressed 148Q-Htt size-specific bands with appreciable immunoreactivity. These results indicate that N2a cells expressing both 148Q-Htt and a JNK1 specific shRNA maintain expression of exogenous Htt and isoform specific knockdown of JNK1 at the protein level.

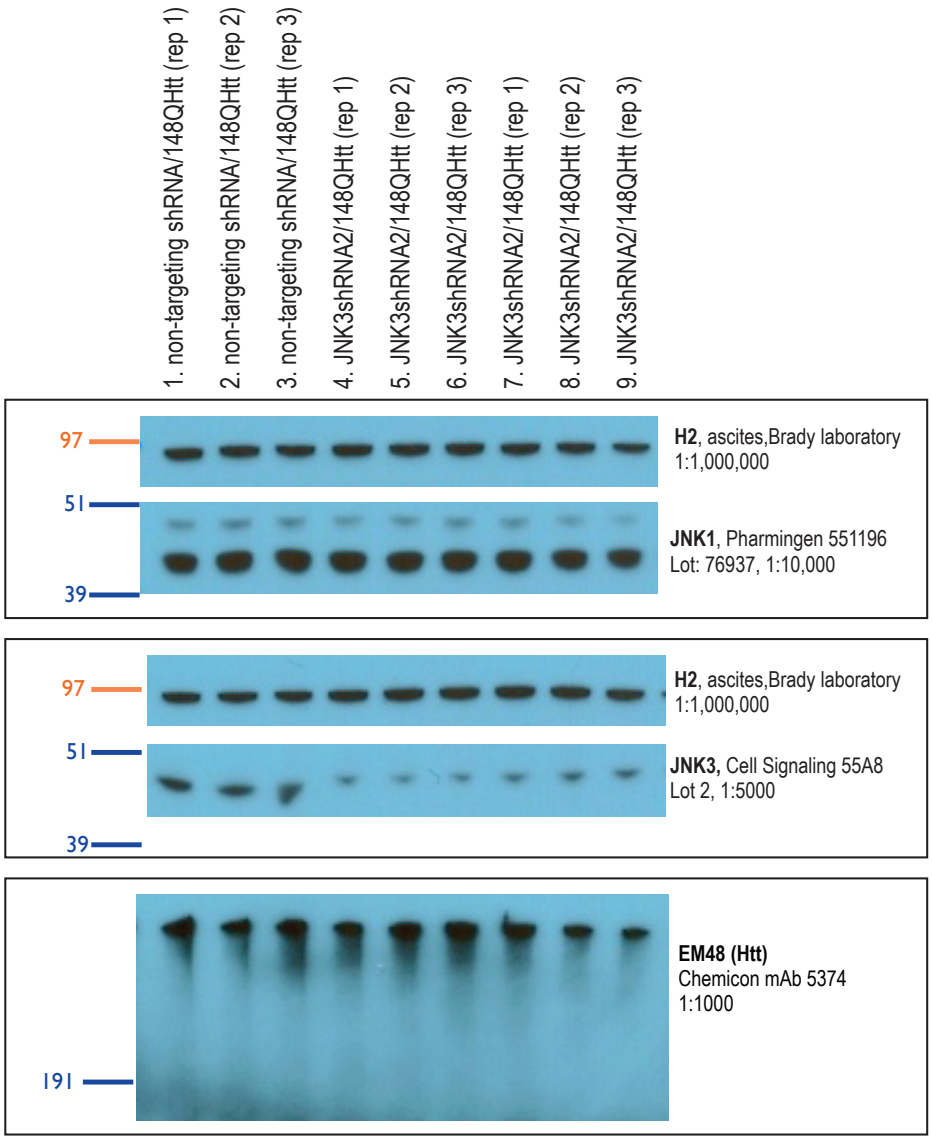

Figure 15. JNK knockdown and Htt expression in 148Q-Htt/JNK3shRNA cells. N2a cells stably expressing 148Q-Htt and JNK3 specific shRNAs were validated for isoform-specific JNK knockdown and expression of Htt. Top panel: N2a cells stably expressing 148Q-Htt in conjunction with JNK3shRNA1 (lanes 4-6) or JNK3shRNA2 (lanes 7-9) showed no differences in JNK1 immunoreactivity as compared to 148Q-Htt cells with non-targeting shRNA (lanes 1-3). Kinesin heavy chain (H2) was used as a loading control, and yielded bands of similar immunoreactivity across all groups. Middle panel: There was a significant reduction in JNK3 immunoreactivity in 148Q-Htt cells expressing JNK3shRNA1 (lanes 4-6) or JNK3shRNA2 (lanes 7-9) as compared to 148Q-Htt cells with non-targeting shRNA (lanes 1-3). Bottom panel: All samples expressed 148Q-Htt size-specific bands with similar immunoreactivity. These results indicate that N2a cells expressing both 148Q-Htt and a JNK3 specific shRNA maintain expression of exogenous Htt and isoform specific knockdown of JNK3 at the protein level.

Cells expressing both 148Q-Htt and JNK shRNAs yielded parallel results. WB analysis of 148Q-Htt/JNK1shRNA cells (see Figure 14) confirmed that all samples continued to express 148Q-Htt (bottom panel, all lanes), and that JNK1 was effectively knocked down (top panel, lanes 1-6) but JNK3 was not (middle panel, lanes 1-6) compared to non-targeting controls (top and middle panels, lanes 7-9). Lastly, 148Q-Htt/JNK3shRNA cells (see Figure 15) were verified to express 148Q-Htt (bottom panel, all lanes), and show reduced JNK3 (middle panel, lanes 4-9) but not JNK1 (top panel, lanes 4-9) as compared to non-targeting controls (top and middle panels, lanes 1-3). As with the aforementioned 23Q-Htt/JNKshRNA cell lines, these data validate the generation of N2a cells expressing 148Q-Htt with concomitant isoform specific knockdown of either JNK1 or JNK3.

4.1.4. 148Q-Htt Decreases Neurite Length and Neurite Mitochondrial Density in the Absence of Htt Aggregates

All validated cell lines were maintained in selection media, and continued expression of Htt constructs and shRNAs were monitored closely over time by fluorescence of CFP and GFP, respectively (see Figure 16 for representative images). As noted above, CFP fluorescence revealed no detectable aggregates in neurites of any of the generated cell lines. Preliminary examination of 23Q-Htt and 148Q-Htt cells expressing no shRNA (see Figures 19A&G) or non-targeting shRNA (Figures B&H) displayed distinct phenotypes. Upon differentiation, 23Q-Htt cells became highly polarized with one or two long neurites, while 148Q-Htt cells were more often weakly polarized with multiple short neurites. Additionally, staining with MitoTracker Red

23Q-Htt/non-targeting shRNA

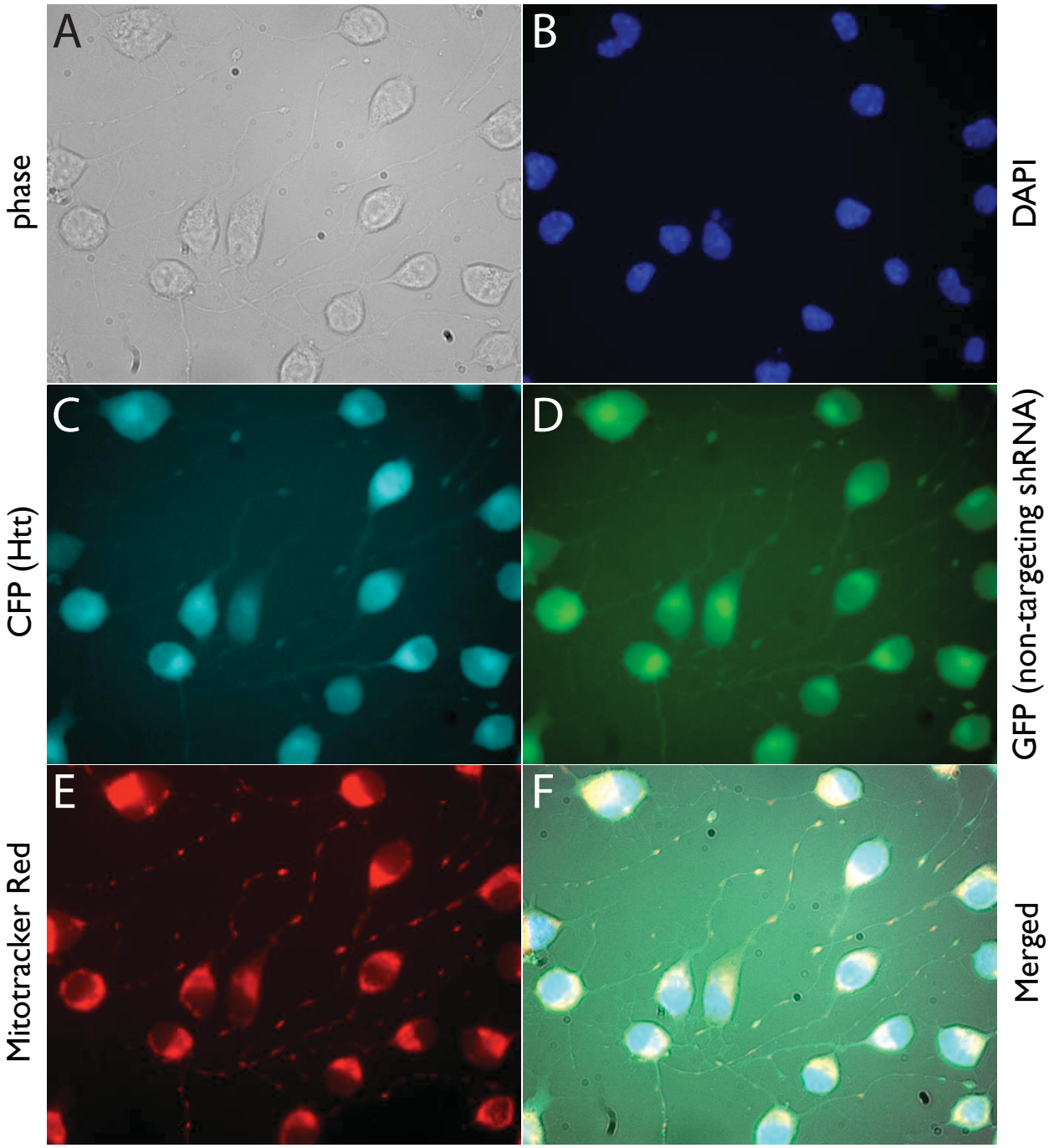

148Q -Htt/non-targeting shRNA

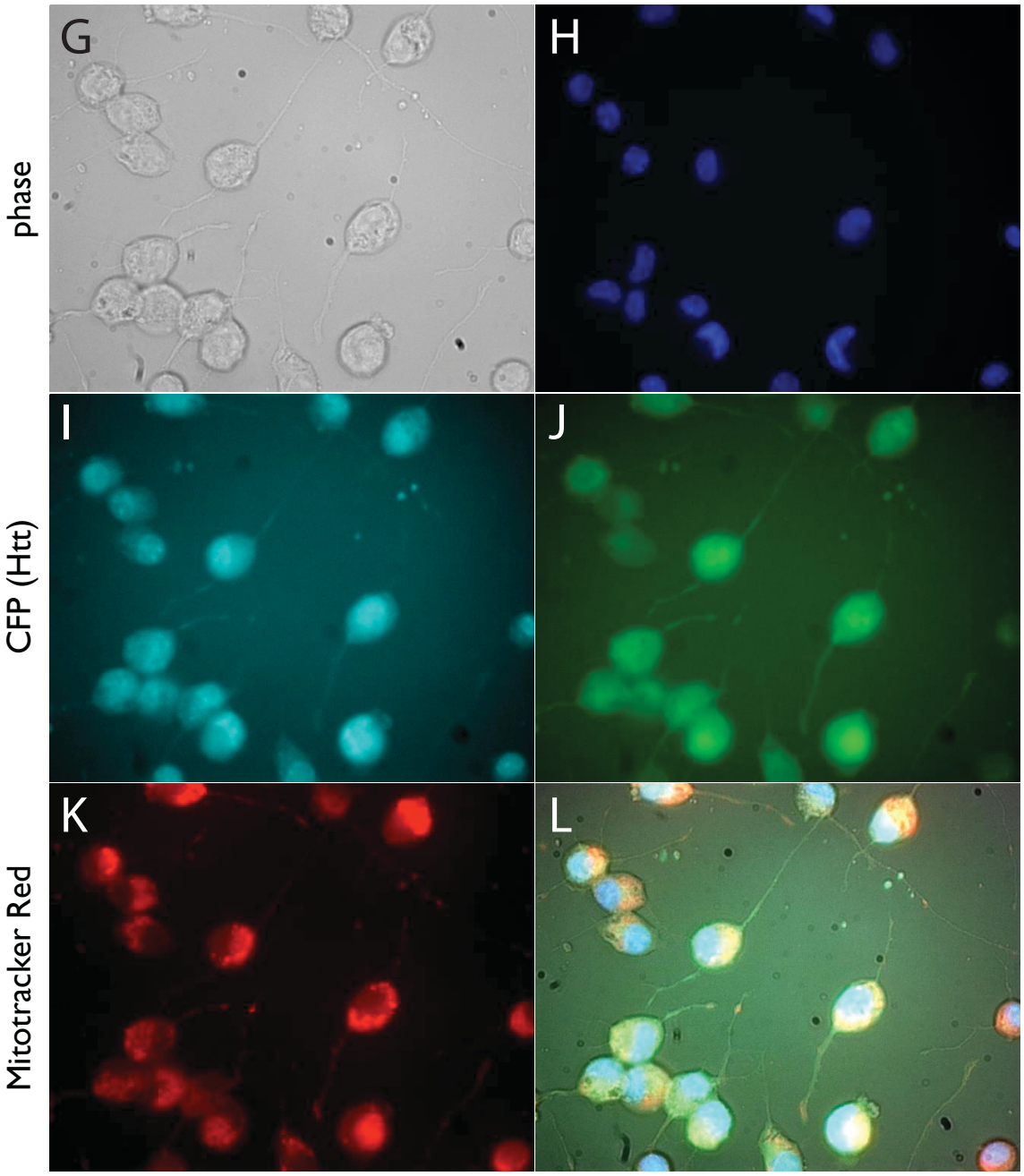

Figure 16. Fluorescent detection of exogenous Htt constructs and shRNA expression in differentiated N2a cells. Representative images of fluorescent detection of CFP for 23Q-Htt (C) or 148Q-Htt (I), GFP for expression of shRNA (D&J), and MitoTracker Red for assessment of mitochondrial density (E&K). Cells intended for neurite outgrowth analysis were immunostained with DM1a (α-tubulin) antibody (see Figure 19). The images here are for cells that stably express 23Q-Htt (A-F) or 148Q-Htt (G-L), and non-targeting shRNA (D&J). Note that CFP fluorescence does not show any bright inclusion spots in the neurites (C&I), indicating that neither of the Htt constructs formed neuritic aggregates. Images were acquired with a 40X, 1.3 N.A. objective.

revealed that, when present, neurites in 148Q-Htt cells had reduced fluorescence (see Figures and 22G&H)) compared to neurites of 23Q-Htt cells (see Figures 22A&B). Quantification and statistical analysis (by Student's t-test) of neurite outgrowth revealed no significant differences between 23Q-Htt/no shRNA and 23Q-Htt/non-targeting shRNA cells (see Figure 17), and no significant differences between 148Q-Htt/no shRNA and 148Q-Htt/non-targeting shRNA cells. This confirms that stable expression of non-targeting shRNA had no effect on neurite differentiation in either group. There was a significant difference ($p = 2.64 \times 10^{-30}$ by two-sample equal variance Student's t-test) between mean neurite length of cells expressing 23Q-Htt/ no shRNA (mean neurite length = 60.18μm, ±SEM= 1.58) and 148Q-Htt/no shRNA (mean neurite length = 39.41μm, ±SEM= 0.71), and also a significant difference ($p = 1.43 \times 10^{-25}$) between 23Q-Htt/non-targeting shRNA (mean neurite length = 59.82μm, ±SEM= 1.58) and 148Q-Htt/non-targeting shRNA (mean neurite length = 39.59μm, ±SEM= 0.94) groups. This confirms that stable expression of 148Q-Htt in N2a cells significantly inhibits neurite outgrowth compared to stable expression of 23Q-Htt. Likewise, neurite mitochondrial density revealed no differences between 23Q-Htt/no shRNA and 23Q-Htt/non-targeting shRNA cells, and no differences between 148Q-Htt/no shRNA and 148Q-Htt/non-targeting shRNA cells (see Figure 18), corroborating no effect by stable expression of non-targeting shRNA. There was a significant difference ($p = 1.42 \times 10^{-16}$) between mean neurite mitochondrial density of cells expressing 23Q-Htt/no shRNA (mean gray pixel density = 375.53, ±SEM= 28.49) and 148Q-Htt/ no shRNA (mean gray pixel density = 111.49, ±SEM= 6.61), and also a significant difference ($p = 2.45 \times 10^{-10}$) between 23Q-Htt/non-targeting shRNA (mean gray pixel density = 402.46, ±SEM= 38.83) and 148Q-Htt/non-targeting shRNA (mean gray pixel density = 125.64, ±SEM=

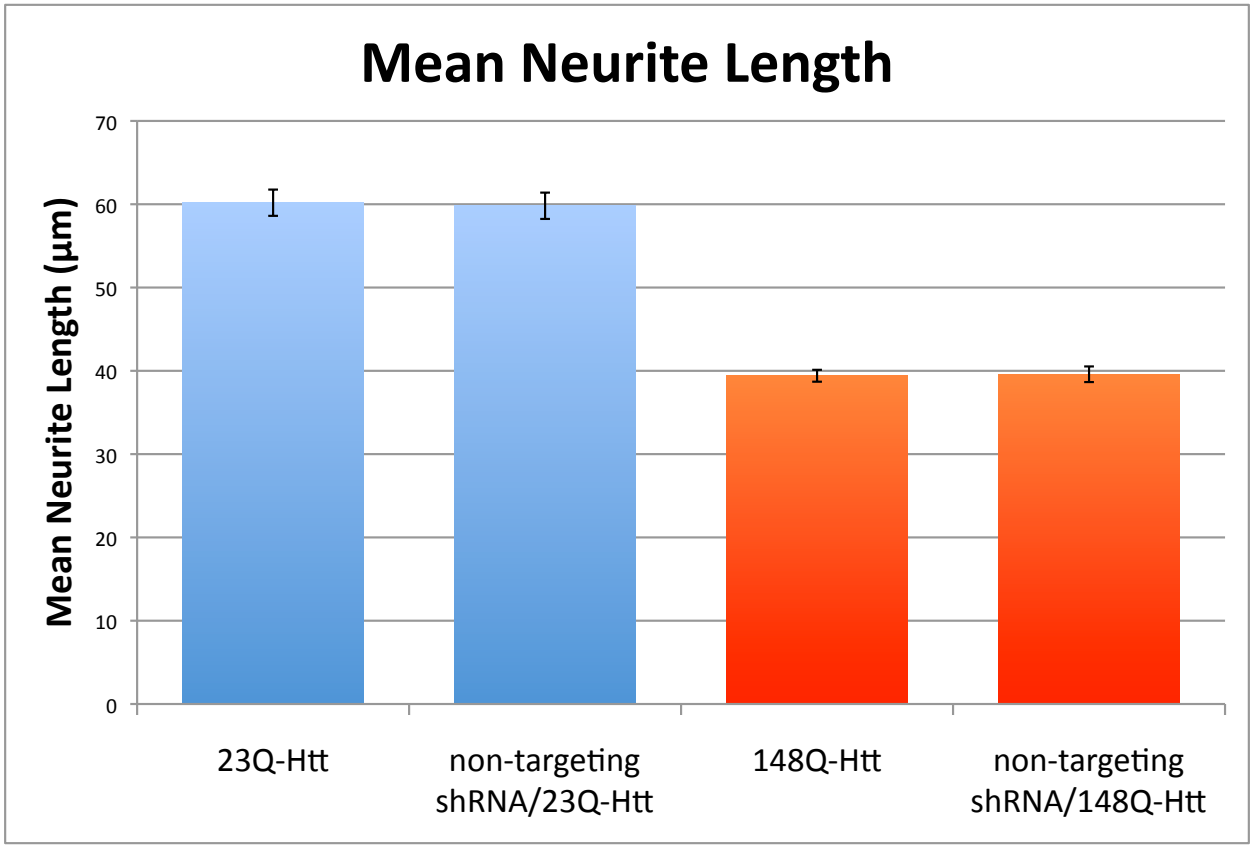

Figure 17. Neurite outgrowth analysis of Htt-expressing cells with no shRNA or non-targeting shRNA. Quantification and statistical analysis (by Student's t-test) of neurite outgrowth revealed no significant differences between 23Q-Htt/no shRNA and 23Q-Htt/non-targeting shRNA cells. There were also no significant differences between 148Q-Htt/no shRNA and 148Q-Htt/non-targeting shRNA cells. There was a significant difference ($p = 2.64 \times 10^{-30}$ by two-sample equal variance Student's t-test) between mean neurite length of cells expressing 23Q-Htt/no shRNA (mean neurite length = 60.18µm, ±SEM= 1.58) and 148Q-Htt/no shRNA (mean neurite length = 39.41µm, ±SEM= 0.71), and also a significant difference ($p = 1.43 \times 10^{-25}$) between 23Q-Htt/non-targeting shRNA (mean neurite length = 59.82µm, ±SEM= 1.58) and 148Q-Htt/non-targeting shRNA (mean neurite length = 39.59µm, ±SEM= 0.94) groups.

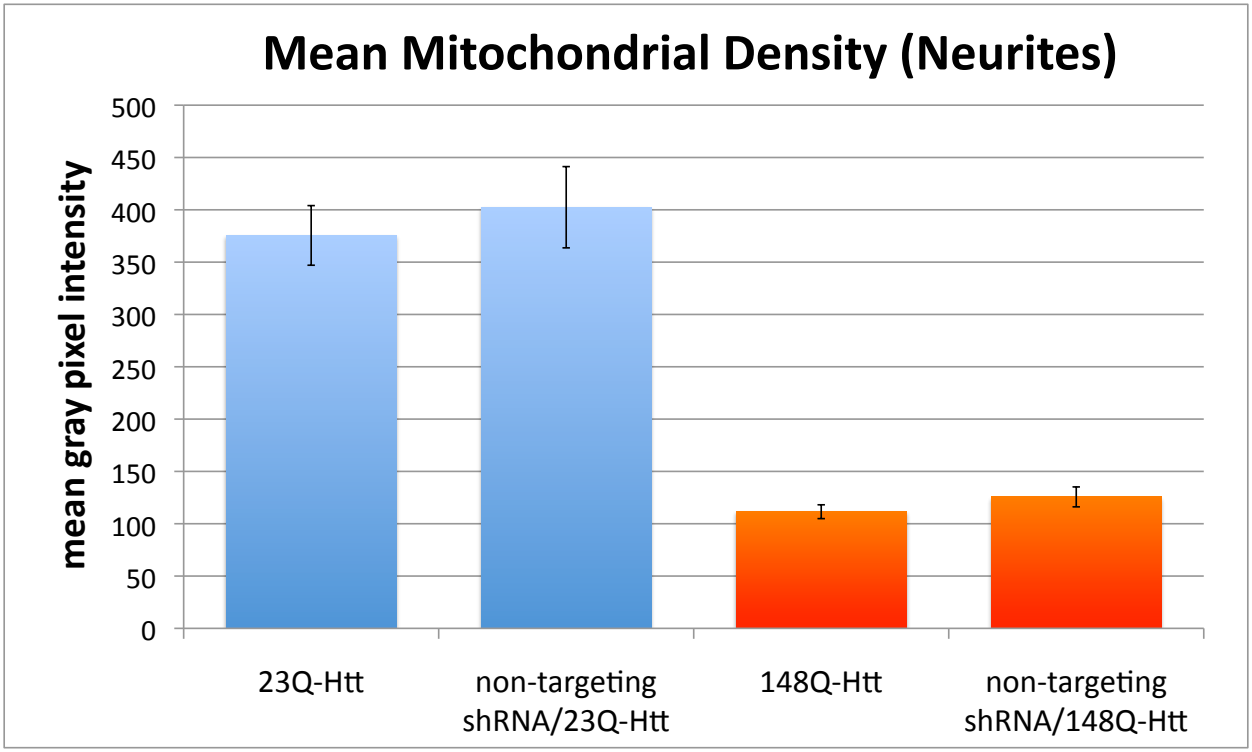

Figure 18. Neurite mitochondrial density analysis of Htt-expressing cells with no shRNA or non-targeting shRNA. Quantification and statistical analysis (by Student's t-test) revealed no differences between 23Q-Htt/no shRNA and 23Q-Htt/non-targeting shRNA cells, and no differences between 148Q-Htt/no shRNA and 148Q-Htt/non-targeting shRNA cells in mitochondrial density. There was a significant difference ($p = 1.42x10^{-16}$) between mean neurite mitochondrial density of cells expressing 23Q-Htt/no shRNA (mean gray pixel density = 375.53, ±SEM= 28.49) and 148Q-Htt/no shRNA (mean gray pixel density = 111.49, ±SEM= 6.61), and also a significant difference ($p = 2.45x10^{-10}$) between 23Q-Htt/non-targeting shRNA (mean gray pixel density = 402.46, ±SEM= 38.83) and 148Q-Htt/non-targeting shRNA (mean gray pixel density = 125.64, ±SEM= 9.52) groups.

9.52) groups. This confirms that stable expression of 148Q-Htt in N2a cells significantly reduces neurite mitochondrial density compared to stable expression of 23Q-Htt.

Combined with the above WB and qPCR data, these findings confirm our model for investigating the role of specific JNK isoforms in polyQ-Htt induced axonal dysfunction in N2a cells.

4.2. Evaluation of the Role of Specific JNK Isoforms in PolyQ-Htt Mediated Dysfunction of Axonal Transport

4.2.1. JNK3 Mediates PolyQ-Htt Induced Impairment of Neurite Outgrowth

While neurite outgrowth is not by any means the reverse process of dying back neuropathy, a number of studies indicate that neurite outgrowth is dependent on the ability of kinesins and dyneins to properly deliver specific cargoes via regulated travel along microtubules. Inhibition of kinesin with siRNA inhibits process formation in neurons, indicating a role for kinesin-dependent transport in neurite outgrowth **[326, 327]**. Likewise, properly functioning dynein is also necessary for neurite outgrowth **[260, 328]**. Any misregulation of transport by either kinesin or dynein, whether directly or via numerous accessory and adaptor proteins necessary for the proper transport of their cargoes, suffices to inhibit neurite outgrowth. Specific to the model used here, it has been previously shown that polyQ-Htt, but not wt-Htt, inhibits neurite outgrowth in N2a cells **[67]**. Therefore, neurite outgrowth analysis is a reasonable outcome measure for the toxic effects of polyQ-Htt on axonal transport in N2a cells.

23Q-Htt

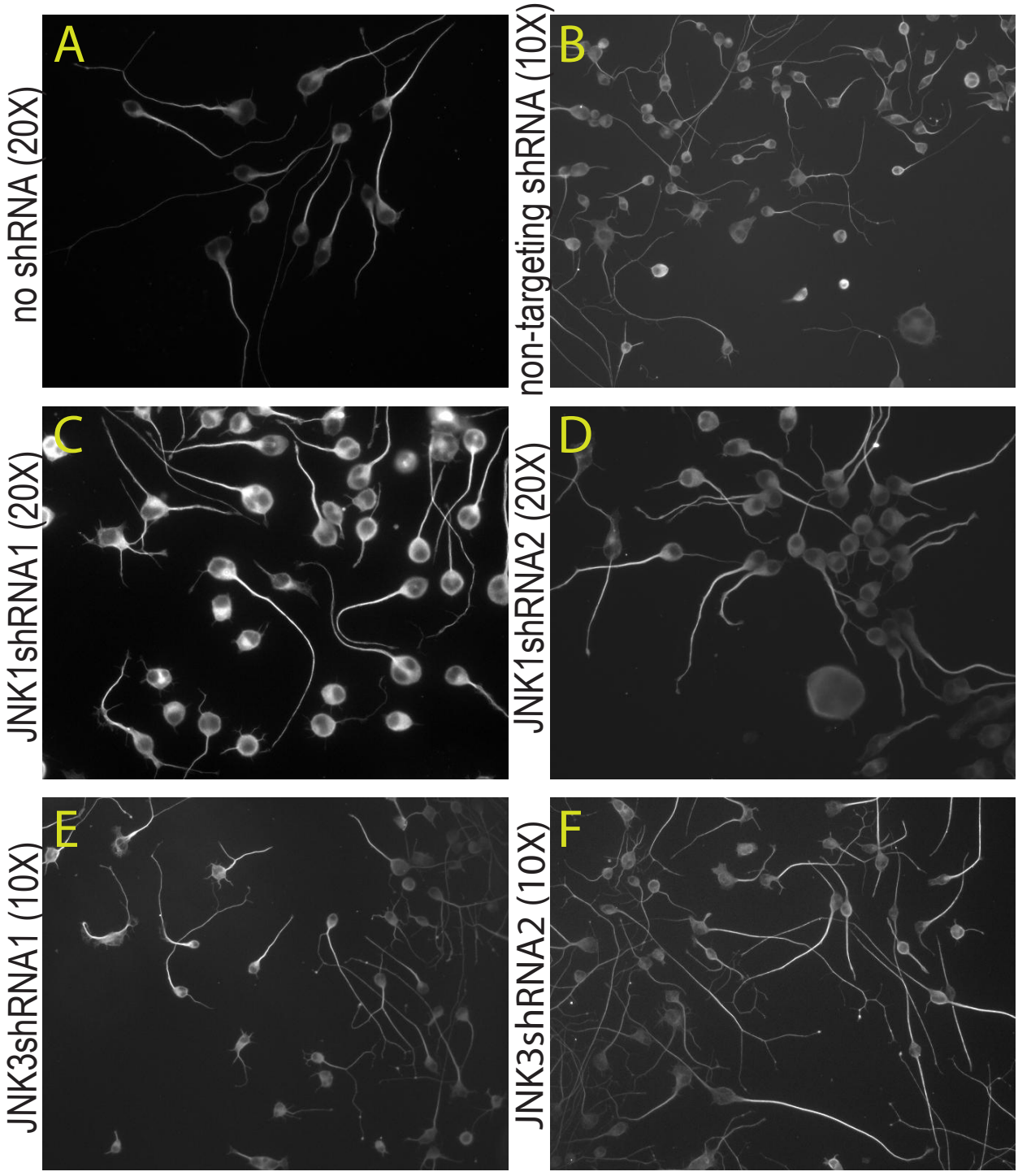
A
no shRNA (20X)
B
non-targeting shRNA (10X)
C
JNK1shRNA1 (20X)
D
JNK1shRNA2 (20X)
E
JNK3shRNA1 (10X)
F
JNK3shRNA2 (10X)

148Q-Htt

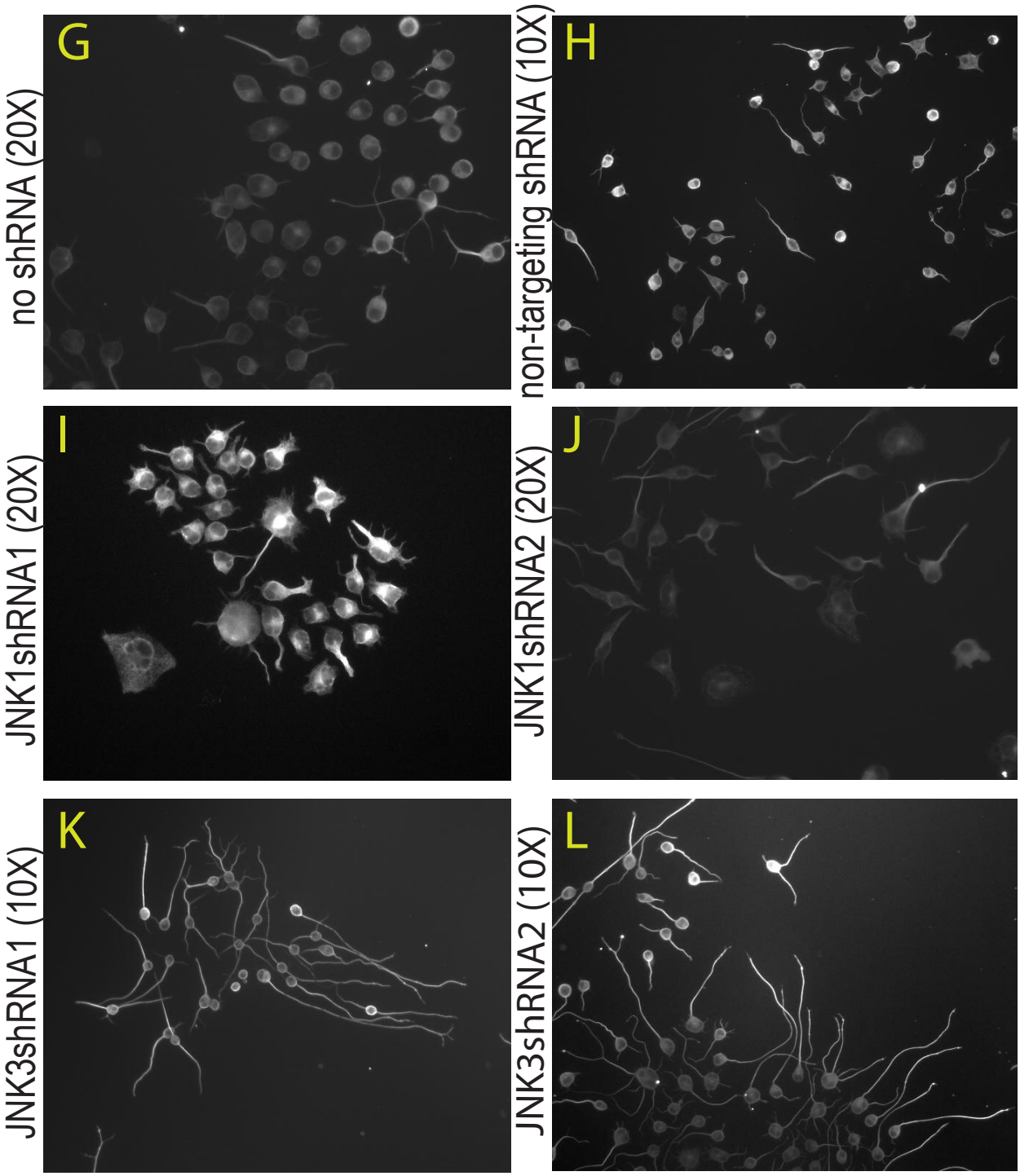
G
no shRNA (20X)
H
non-targeting shRNA (10X)
I
JNK1shRNA1 (20X)
J
JNK1shRNA2 (20X)
K
JNK3shRNA1 (10X)
L
JNK3shRNA2 (10X)

Figure 19. Representative images for neurite outgrowth analysis. Cells immunostained for α-tubulin (DM1a, Sigma) are shown 5 days after serum deprivation and RA treatment. Most 23Q-Htt cells in all groups (A-F) were elongated with one or two very long neurites, whereas cells in 148Q-Htt groups with no shRNA (G), non-targeting shRNA (H), JNK1shRNA1 (I), or JNK1shRNA2 (J) were more often shorter and less polarized, often sprouting multiple short neurites. 148Q-Htt/JNK3shRNA1 (K) and 148-Htt/JNK3shRNA2 (L) cells resembled those in 23Q-Htt expressing groups (A-F), distinct from all other 148Q-Htt groups (G-J). Images were acquired with either a 20X, 0.5 N.A., or 10X, 0.3 N.A. objective as specified.

Cell cultures for all groups were differentiated for 5 days by serum withdrawal in conjunction with RA(10uM) treatment, then immunostained for α-tubulin (DM1a, Sigma) to facilitate the assessment of neurite outgrowth. Cells from all groups expressing 23Q-Htt (see Figure 16A-F) were highly polarized, with one or two long neurites. Cells expressing 148Q-Htt in conjunction with no knockdown (see Figure 16G&H) or JNK1 knockdown (see Figure 16I&J) had short neurites, and were often poorly polarized, sprouting several short neurites. In contrast, cells expressing 148Q-Htt in conjunction with either JNK3shRNA (see Figure 16K&L) closely resembled cells from 23Q-Htt groups (A-F).

For quantitative analysis, neurite lengths were measured for at least 260 cells per group (see Appendix A). Using ImageJ software (NIH), measurements were taken from the middle of the soma to the tip of the longest measurable neurite. In order to maintain consistency with cells used in mitochondrial density analysis, cells with neurites less than 1.5x cell body diameter were excluded. All statistical outcomes were determined by MANOVA followed by post-hoc Tukey's HSD analysis. MANOVA performs multiple comparisons simultaneously, and also takes into account multiple dependent variables, as is the case in our experimental model. While a robust statistical test for its intended purpose, Student's t-test is capable of comparing 2 data sets with 1 dependent variable, and performing numerous t-tests across pairs of group data in lieu of the MANOVA increases the chance of type 1 error. Tukey's HSD analysis output differs from the Student's t-test in that the level of significance is pre-set at the alpha value, in this case, at $p = 0.05$, and any outcomes are deemed significant or not based on this p-value. While the use of MANOVA and post-hoc Tukey's HSD entails the loss of degrees of freedom, and is therefore a more stringent test, our data still yielded significant differences with $p < 0.05$.

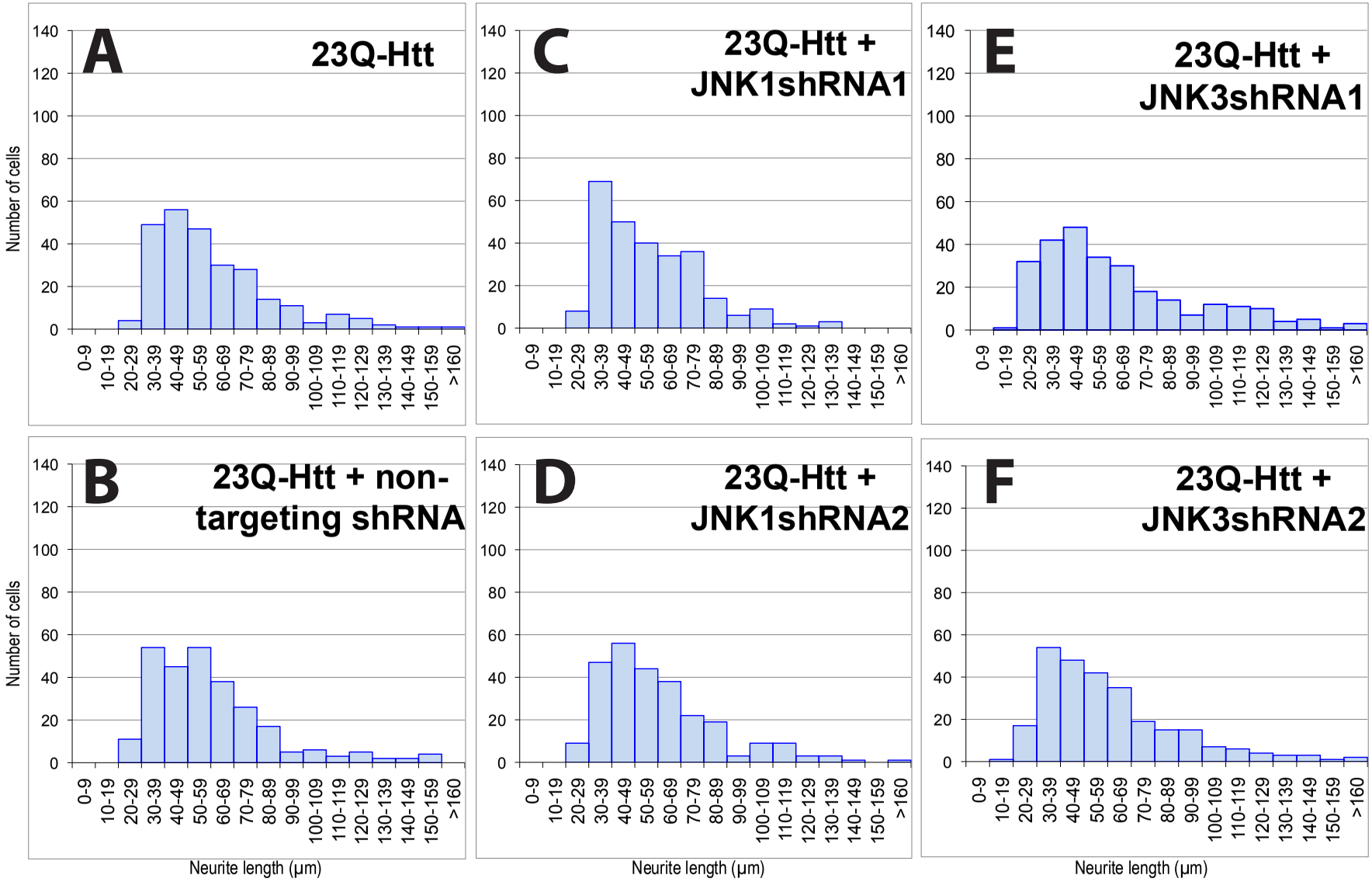
A
23Q-Htt
B
23Q-Htt + non-targeting shRNA
C
23Q-Htt + JNK1shRNA1
D
23Q-Htt + JNK1shRNA2
E
23Q-Htt + JNK3shRNA1
F
23Q-Htt + JNK3shRNA2
Number of cells
Neurite length (µm)
0-9
10-19
20-29
30-39
40-49
50-59
60-69
70-79
80-89
90-99
100-109
110-119
120-129
130-139
140-149
150-159
>160
0
20
40
60
80
100
120
140

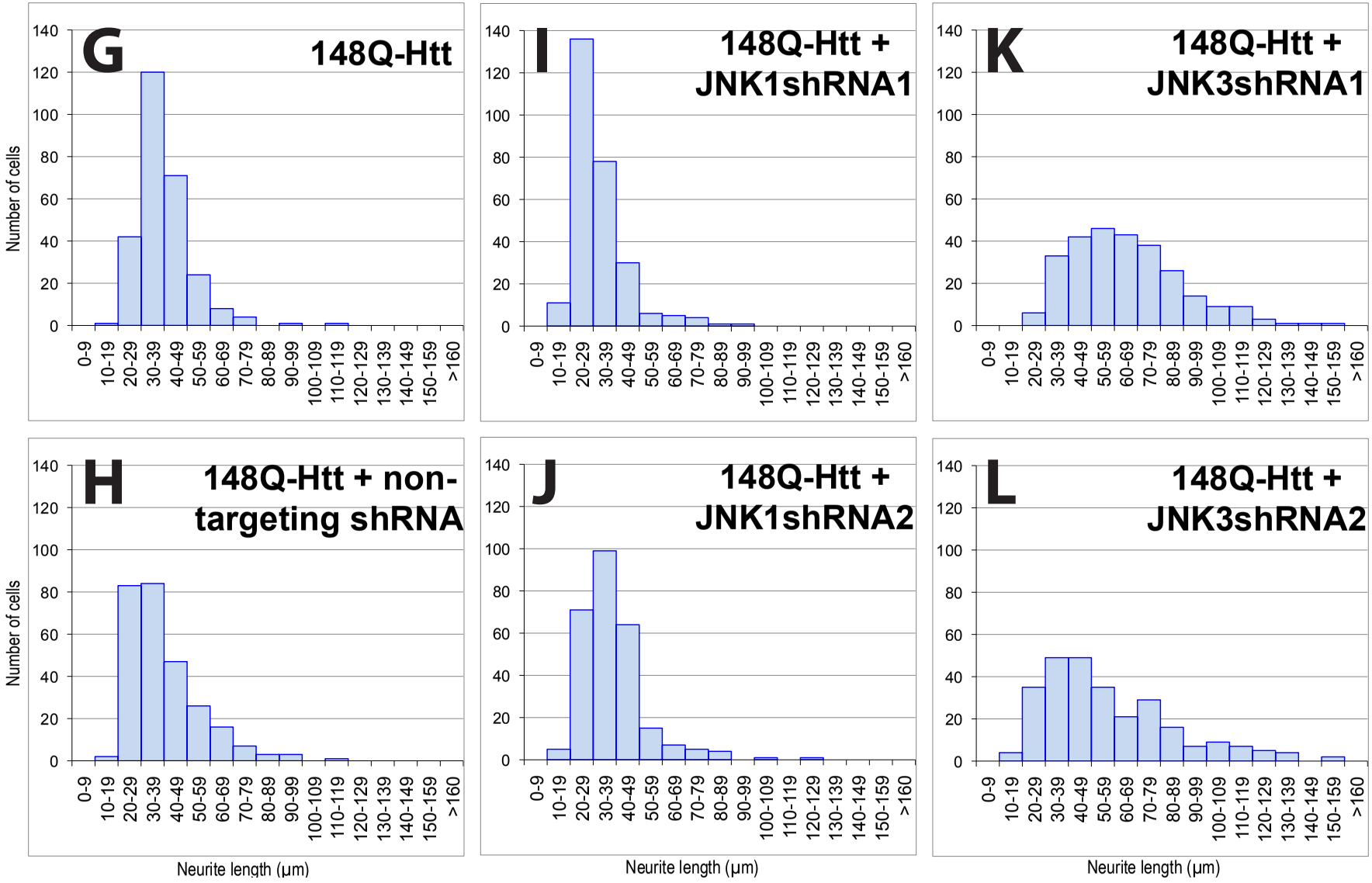
G
148Q-Htt
I
148Q-Htt + JNK1shRNA1
K
148Q-Htt + JNK3shRNA1
H
148Q-Htt + non-targeting shRNA
J
148Q-Htt + JNK1shRNA2
L
148Q-Htt + JNK3shRNA2
Number of cells
Neurite length (µm)
0-9
10-19
20-29
30-39
40-49
50-59
60-69
70-79
80-89
90-99
100-109
110-119
120-129
130-139
140-149
150-159
>160
0
20
40
60
80
100
120
140

Figure 20. Distribution of neurite lengths. The number of cells that fall within a given range of neurite lengths is plotted for all 23Q-Htt expressing groups (A-F) and 148Q-Htt expressing groups (G-L). Most cells in all 23Q-Htt groups had long neurites (>50μm), while most cells in 148Q-Htt groups with no knockdown (G&H) or JNK1 knockdown (I&J) had shorter neurites (<50μm). The number of cells with the shortest neurites (0-19μm) may have been even higher in 148Q-Htt groups with no knockdown (G&H) or JNK1 knockdown (I&J), but cells with neurites less than 1.5x the cell diameter were excluded. 148Q-Htt cells with JNK3 knockdown (K&L) had increased numbers of cells extending long neurites as compared to those with no knockdown or JNK1 knockdown, and showed similar distributions as 23Q-Htt groups (A-F).

Histograms in Figure 17 show the number of cells within a given range for neurite lengths for each test group. Most of the cells in all 23Q-Htt expressing groups had longer neurites, with over 50% with lengths over 50μm (see Figures 17A-F), and less than 30% of any given 23Q-Htt group had neurites under 40μm. In contrast, most cells in 148Q-Htt groups with no knockdown (see Figures 17G&H) or JNK1 knockdown (17I&J) were much shorter, with 20.6% or less of cells possessing neurites over 50μm, and over 60% of cells had neurite length under 40μm. There would have been more cells with even shorter neurites (0-19μm) in these groups, but cells with neurites with less than 1.5x the cell diameter were excluded. Knockdown of JNK3 in 148Q-Htt cells resulted in increased numbers of cells extending longer neurites (see Figures 17K&L) as compared to 148Q-Htt cells with no knockdown or JNK1 knockdown (17G-J), with distributions that closely resembled 23Q-Htt groups (17A-F). Statistical analysis corroborated observations from microscopic images (see Figure 16) and neurite length distributions (see Figure 17). The expression of JNK1shRNAs in 148Q-Htt cells showed no change compared to 148Q-Htt cells with no knockdown (see Figure 18). This indicates that JNK1 knockdown had no effect on neurite outgrowth of 148Q-Htt cells. On the other hand, 148Q-Htt cells with JNK3 specific knockdown had statistically significant longer neurite lengths than the 148Q-Htt groups with no shRNA or JNK1shRNAs. Furthermore, neurite lengths in JNK3shRNA expressing 148Q-Htt groups showed no differences compared to any of the 23Q-Htt expressing groups. Setting our lower limit of neurite length to exclude cells with the shortest neurites only reinforces the significance of our findings. These results demonstrate that JNK3, and not JNK1, mediates polyQ-Htt induced deficits in neurite outgrowth.

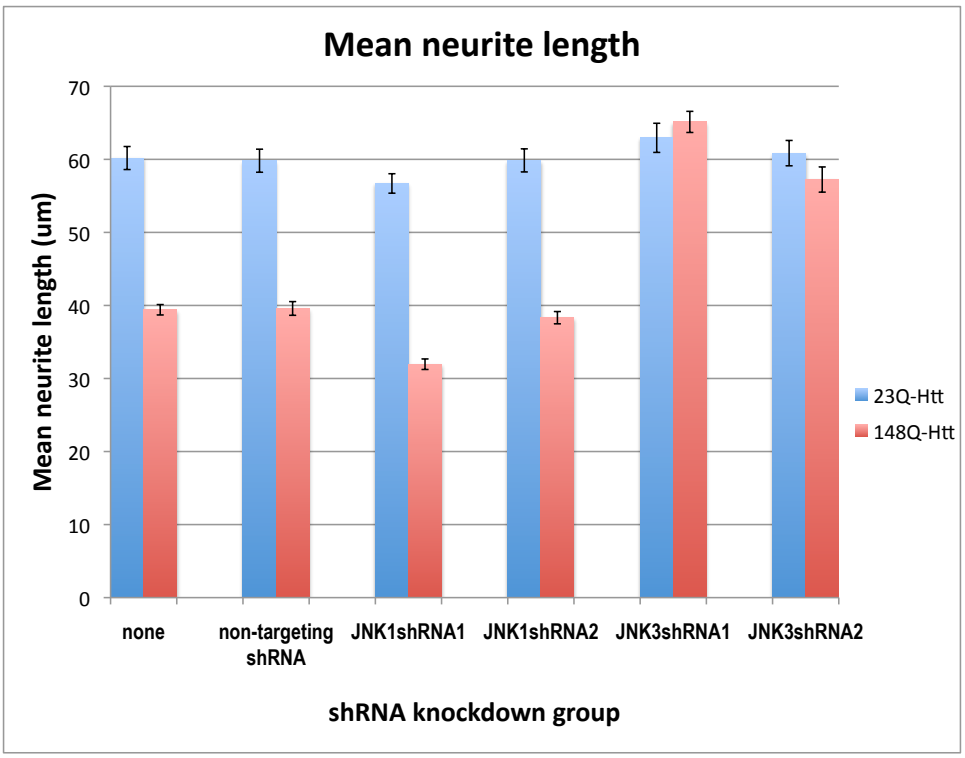

Figure 21. Neurite outgrowth analysis. N2a cells stably expressing either 23Q-Htt (Top, blue columns. Bottom, left panel) or 148Q-Htt (Top, red columns. Bottom, right panel) in conjunction with no shRNA, non-targeting shRNA, one of two JNK1 specific shRNAs, or one of two JNK3 specific shRNAs, were immunostained for α-tubulin (DM1a, Sigma) after 5 days of differentiation by serum deprivation and RA treatment. Using ImageJ software (NIH), neurite length was measured as the distance from the center of the cell body to the tip of the longest measurable neurite. At least 260 cells were measured per group, and potential differences were analyzed using MANOVA followed by post-hoc Tukey's HSD analysis. Neurite lengths of cells with knockdown with JNK1shRNA in 148Q-Htt cells were no different than those with no knockdown. 148Q-Htt expressing cells with JNK3shRNA knockdown showed significantly increased neurite length as compared to 148Q-Htt cells with no knockdown or JNK1shRNA knockdown. Also, 148Q-Htt cells with JNK3shRNA knockdown showed no differences in neurite length compared to cells in all 23Q-Htt groups. Error bars indicate ± SEM.

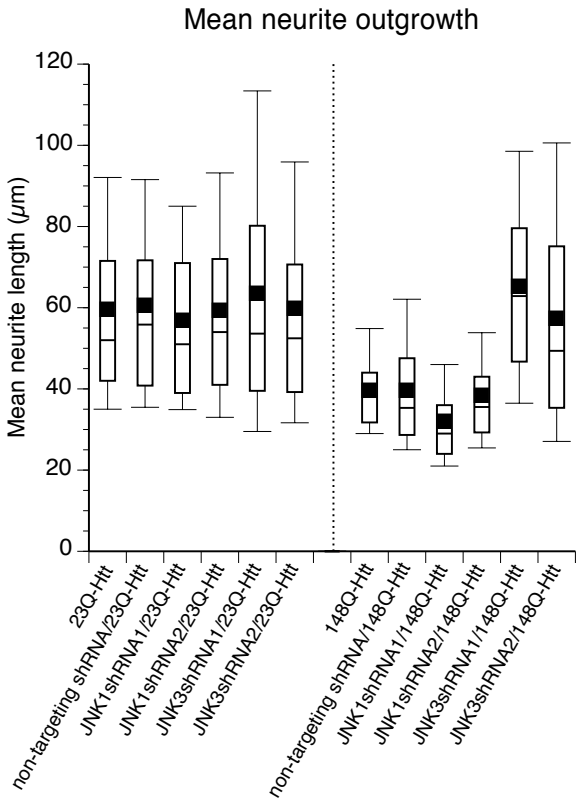

4.2.2. JNK3 Mediates PolyQ-Htt Induced Impairment in Axonal Transport of Mitochondria

Mitochondria are transported anterogradely by kinesin-I motors, and it has been demonstrated that disruption of mouse KHC by gene targeting leads to decreased mitochondrial density in neurites [329]. A number of studies have shown that polyQ-Htt impairs transport of mitochondria in neurites [165, 198, 199], and that reduced transport of mitochondria can lead to decreased ATP in areas of high demand such as axonal processes and synapses [199]. Furthermore, mitochondrial density was also reduced in neurites, but not cell bodies, of cultured neurons from a PS1 mutant mouse model of Alzheimer's Disease [16]. This line of research provided evidence that the reduction was a result of impaired mitochondrial transport due to mutant PS1-induced activation of GSK3β, which in turn phosphorylates kinesin light chain (KLC) resulting in the unwanted release of Kinesin-1 from MBO, in this case, mitochondria [16, 300]. This provides precedent that dysregulation of Kinesin-1 components via phosphorylation results in decreased mitochondrial density in neurites. In the model used here, we are proposing that polyQ-Htt disrupts Kinesin-1 transport through phosphorylation of KHC by JNK3, and that knockdown of JNK3 should ameliorate that disruption. Therefore, mitochondrial distribution is a reasonable measure of polyQ-Htt induced disruption to KHC-mediated transport in neural cells.

To assess the effects of isoform-specific JNK knockdown on polyQ-Htt induced deficits in axonal transport, we analyzed mitochondrial density in the somatic and neuritic compartments of differentiated cells. To detect mitochondria we used MitoTracker® Red CMXRos (Invitrogen, Grand Island, NY), a fluorescing dye that selectively accumulates in active mitochondria. As assessed by the intensity and distribution of fluorescence, mitochondrial density in the somatic

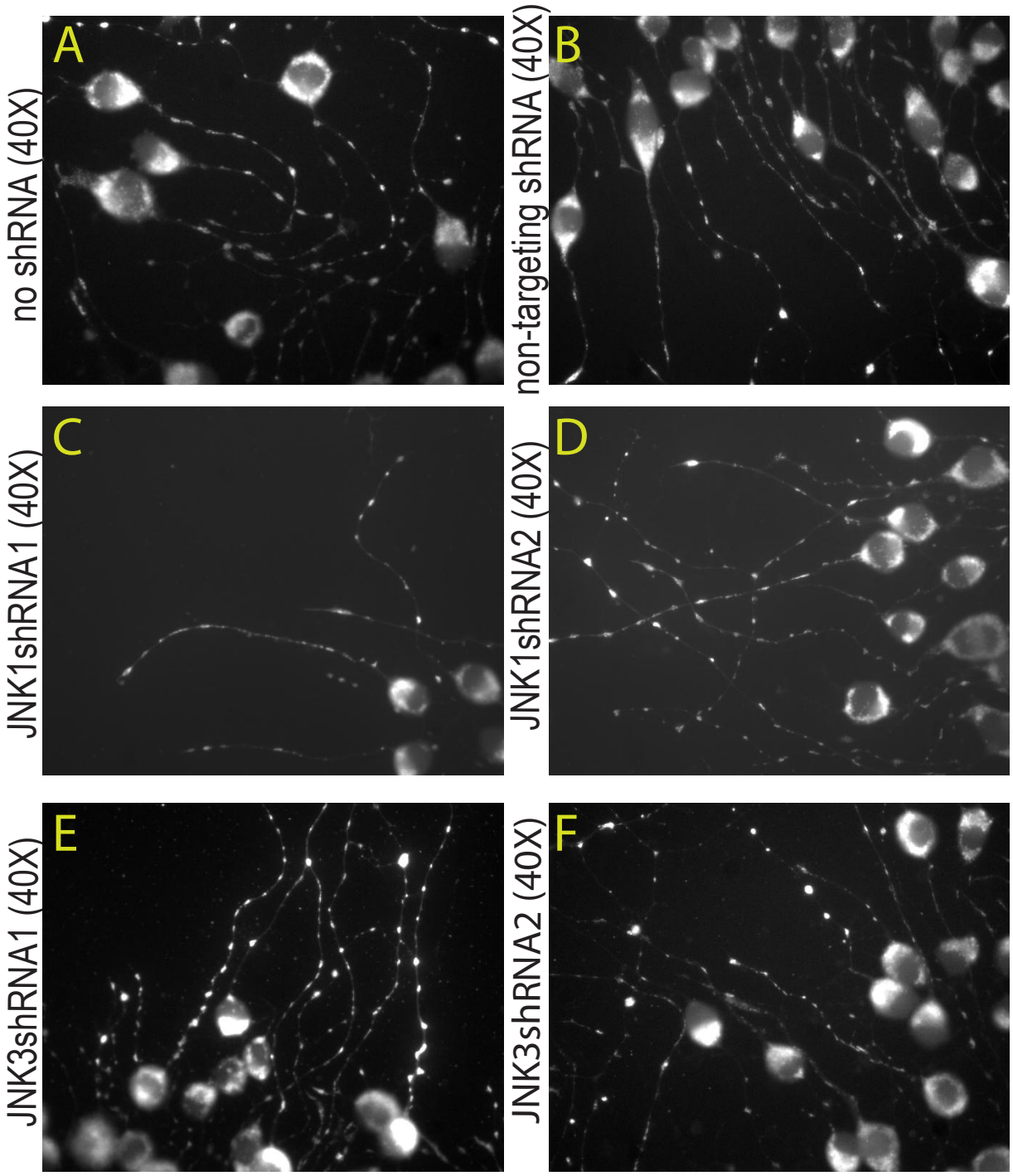
23Q-Htt
A
no shRNA (40X)
B
non-targeting shRNA (40X)
C
JNK1shRNA1 (40X)
D
JNK1shRNA2 (40X)
E
JNK3shRNA1 (40X)
F
JNK3shRNA2 (40X)

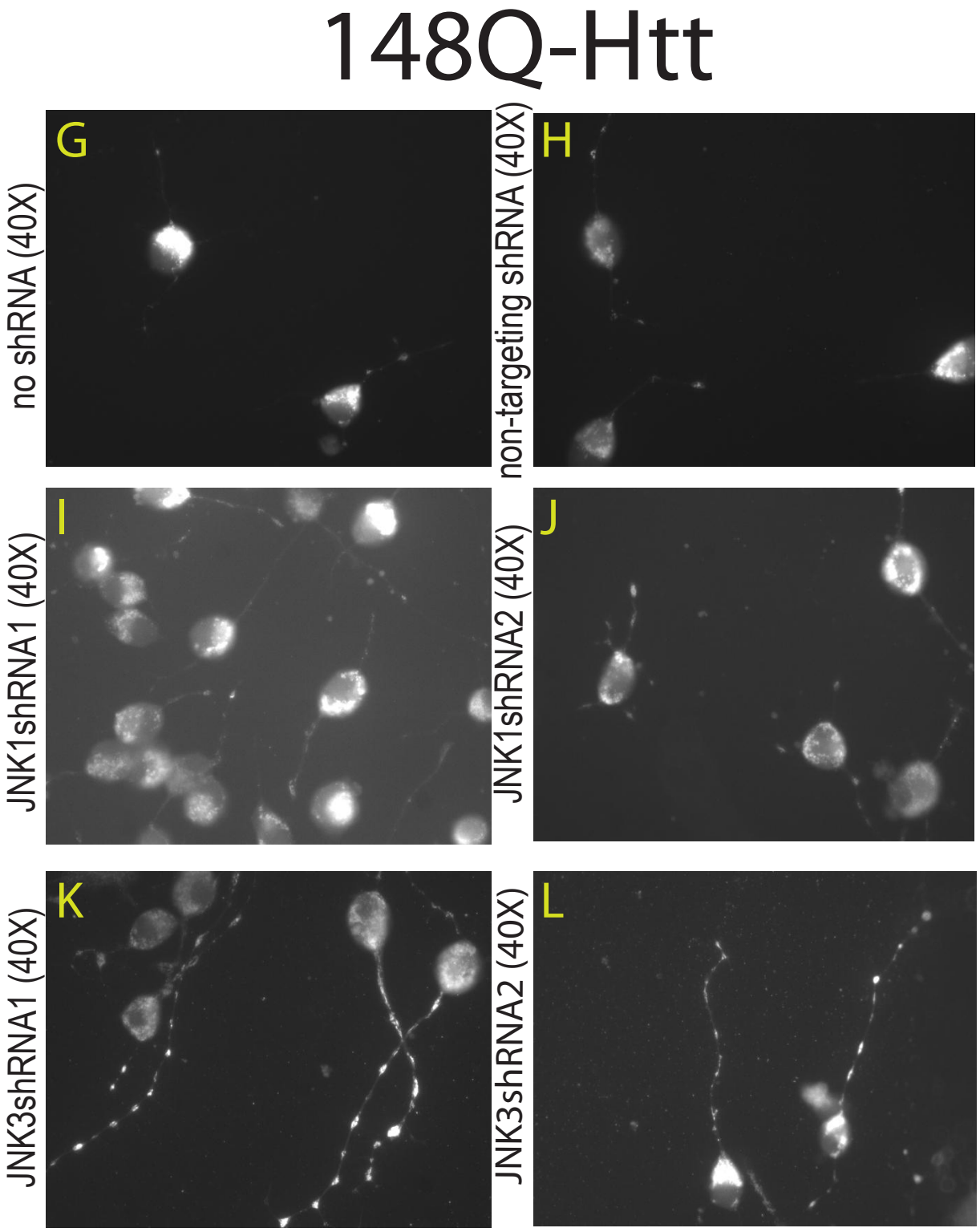
148Q-Htt
G
no shRNA (40X)
H
non-targeting shRNA (40X)
I
JNK1shRNA1 (40X)
J
JNK1shRNA2 (40X)
K
JNK3shRNA1 (40X)
L
JNK3shRNA2 (40X)

Figure 22. Representative images for mitochondrial density analysis. N2a cells stably expressing either 23Q-Htt (left panel) or 148Q-Htt (right panel) in conjunction with no shRNA (A&G), non-targeting shRNA(B&H), JNK1 specific shRNAs (C, D, I, &J), or JNK3 specific shRNAs (E, F, K, &L) were stained with MitoTracker® Red CMXRos after 5 days of differentiation by serum deprivation and RA treatment. Most 23Q-Htt cells in all groups (A-F) show bright fluorescence along the entire length of the neurite. Cells from 148Q-Htt groups with no shRNA (G), non-targeting shRNA (H), JNK1shRNA1 (I), or JNK1shRNA2 (J) had faint fluorescence along the length of neurites where present. Fluorescence in the cells of 148Q-Htt/ JNK3shRNA1 (K) and 148-Htt/JNK3shRNA2 (L) groups more closely resembled that seen in 23Q-Htt expressing groups (A-F). Fluorescence in soma were comparable across all groups. Images were acquired with a 40X, 1.3 N.A. objective.

compartment appeared similar across all groups, whether they expressed 23Q-Htt or 148Q-Htt (see Figures 19A-L). Cells from all groups expressing 23Q-Htt showed strong areas of fluorescence along the entire length of neurites (see Figure 19A-F). In contrast, neurites from cells expressing 148Q-Htt in conjunction with no shRNA (see Figure 19G), non-targeting shRNA (19H), JNK1shRNA1 (19I), and JNK1shRNA2 (19J) showed weak fluorescence in neurites. However, neurites in cells expressing 148Q-Htt in conjunction with JNK3shRNA1 (see Figure 19K) and JNK3shRNA2 (19L) appeared to have similar amount and distribution of fluorescence as in the 23Q-Htt expressing groups (A-F).

For quantitative analysis, the entire soma, neurite, and adjacent non-cell area (for background) were traced for a minimum of 60 cells per group (see Appendix A). ImageJ software (NIH) was used to calculate the mean gray pixel intensity of traced areas. Because many of the cells in 148Q-Htt groups had extremely short neurites, we excluded cells with neurites less than 1.5x cell body diameter to ensure that density of mitochondria in neurites could be measured. Prior to statistical analysis, measured soma and neurite gray pixel intensities were corrected for background. Data was analyzed by MANOVA with post-hoc Tukey's HSD as with neurite outgrowth analysis above. Analysis by MANOVA found that other than a very slight elevation in the 23Q-Htt/no shRNA group (see Figure 20), there were no significant differences in the somal mitochondrial densities across all groups. In contrast, the neurites of 148Q-Htt groups with no knockdown or JNK1 knockdown showed significantly decreased mitochondrial density as compared to all 23Q-Htt groups. This decrease was >50% in all comparisons. Also, there were no differences between 148Q-Htt groups with no knockdown or JNK1 knockdown, demonstrating that JNK1 knockdown had no effect on the transport of mitochondria.

Figure 23. Somatic mitochondrial density. N2a cells stably expressing either 23Q-Htt (Top, blue columns. Bottom, left panel) or 148Q-Htt (Top, red columns. Bottom, right panel) in conjunction with no shRNA, non-targeting shRNA, one of two JNK1 specific shRNAs, or one of two JNK3 specific shRNAs, were stained with MitoTracker® Red CMXRos after 5 days of differentiation by serum deprivation and RA treatment. Mean gray pixel density of entire somal compartment and adjacent cell-free area for background were measured using ImageJ software (NIH). At least 60 cells were measured per group, and potential differences were analyzed using MANOVA. Other than a slight elevation in the 23Q-Htt/no shRNA group, there were no significant differences in the somal mitochondrial densities across all groups. Error bars indicate ± SEM.

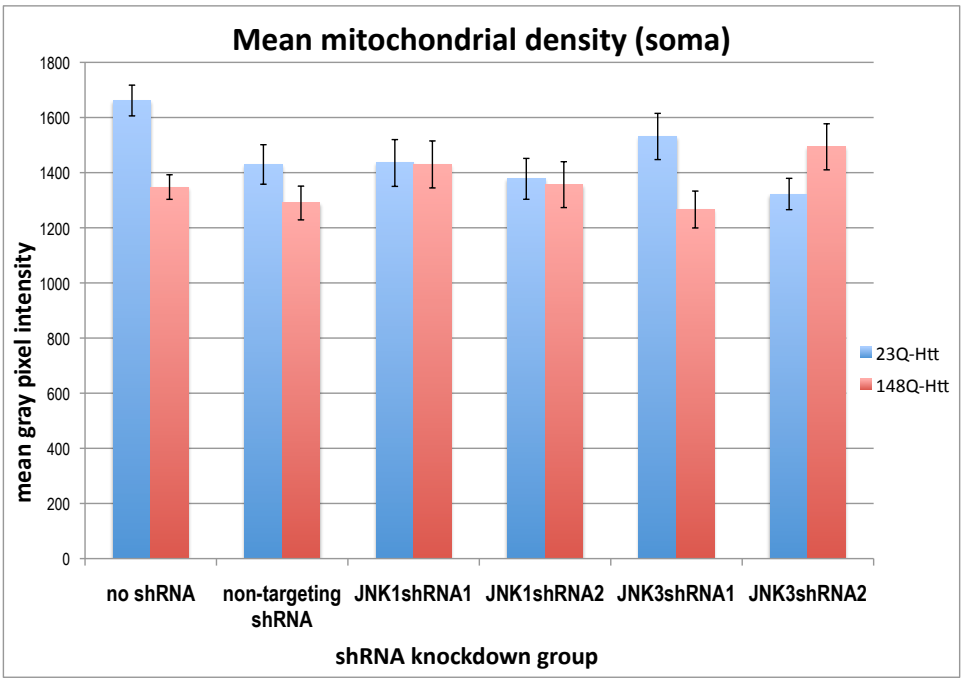

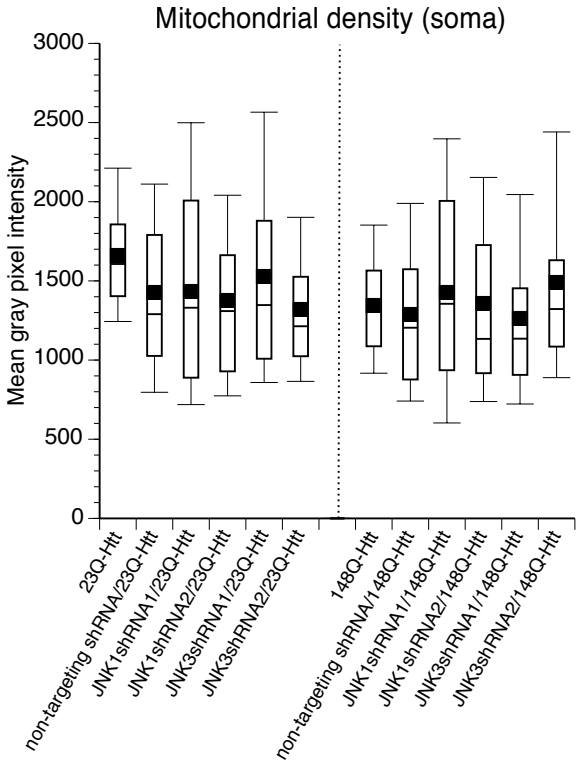

Figure 24. Neuritic mitochondrial density. N2a cells stably expressing either 23Q-Htt (A, blue columns. B, left panel) or 148Q-Htt (A, red columns. B, right panel) in conjunction with no shRNA, non-targeting shRNA, one of two JNK1 specific shRNAs, or one of two JNK3 specific shRNAs, were stained with MitoTracker® Red CMXRos after 5 days of differentiation by serum deprivation and RA treatment. Mean gray pixel density of entire neuritic compartment and adjacent cell-free area for background were measured using ImageJ software (NIH). At least 60 cells were measured per group, and potential differences were analyzed using MANOVA followed by post-hoc Tukey's HSD analysis. Mitochondrial density in neurites of 148Q-Htt cells expressing 1) no shRNA, 2) non-targeting shRNA, 3) JNK1shRNA1, or 4) JNK1shRNA2 were significantly lower than all 23Q-Htt groups. There were no differences between 148Q-Htt groups with 1) no shRNA, 2) non-targeting shRNA, 3) JNK1shRNA1, and 4) JNK1shRNA2. Mitochondrial density in neurites of 148Q-Htt cells expressing either JNK3shRNA1 or JNK3shRNA2 were significantly higher than in 148Q-Htt cells expressing 1) no shRNA, 2) non-targeting shRNA, 3) JNK1shRNA1, and 4) JNK1shRNA2. Mitochondrial density in neurites of 148Q-Htt cells expressing either JNK3shRNA were no different than those of any 23Q-Htt group, regardless of shRNA expressed. Error bars indicate ± SEM.

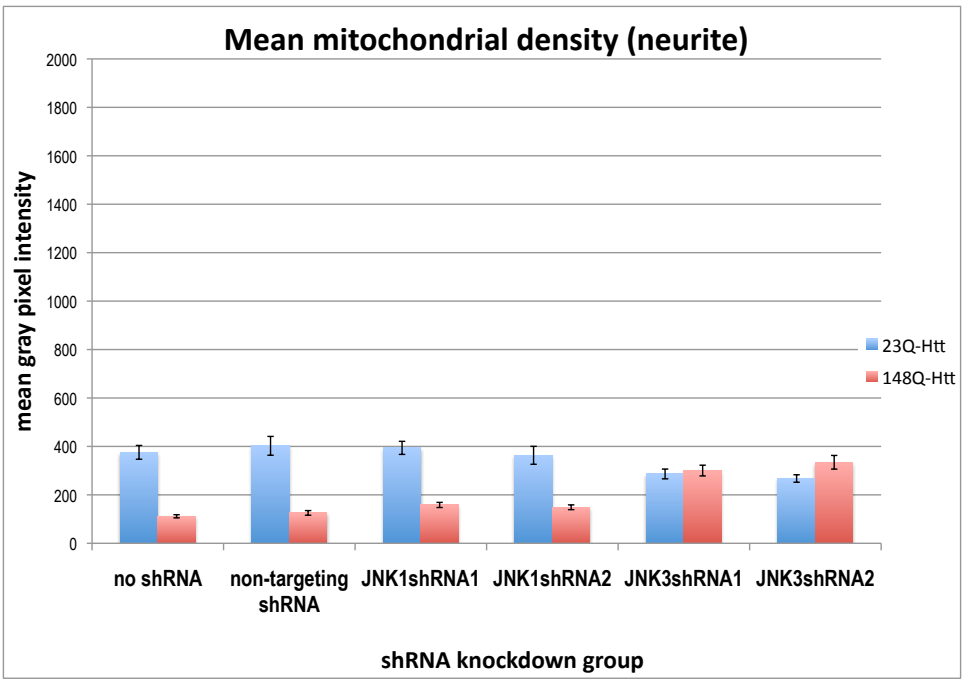

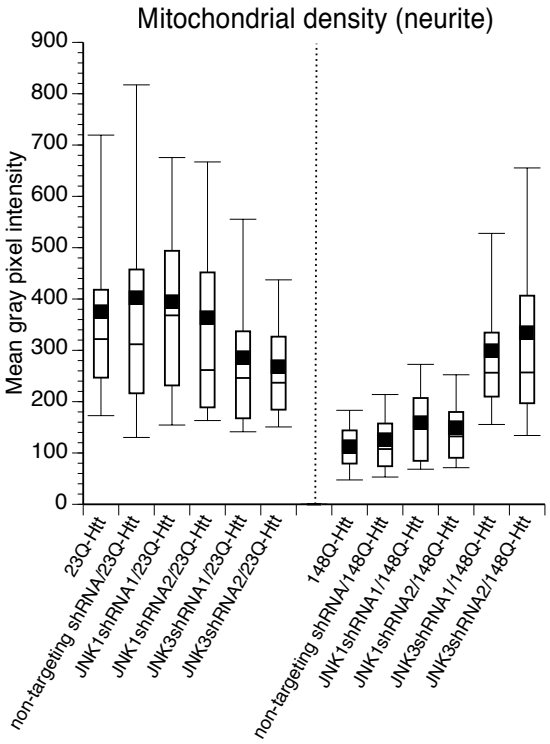

Importantly, JNK3 knockdown in 148Q-Htt cells significantly increased neurite mitochondrial density compared to 148Q-Htt cells with no knockdown or JNK1 knockdown. Furthermore, the neurite density in the 148Q-Htt JNK3 knockdown cells were restored to levels with no significant difference from any of the 23Q-Htt groups. This outcome held true with both JNK3shRNA1 and JNK3shRNA2, making it unlikely that any effect was specific to one shRNA sequence, and probable that the effects were due to knockdown of JNK3. These results indicate that polyQ-Htt deficits in axonal transport of mitochondria are mediated by JNK3, and not JNK1.

CHAPTER 5

DISCUSSION

5.1. SIGNIFICANCE OF RESULTS TO A PATHOGENIC MECHANISM FOR HD

Previous data from our lab identified axon-autonomous effects of polyQ-Htt on JNK activity and impaired axonal transport of MBO [18]. Studies using a knock-in HD mouse revealed differential phosphorylation of certain JNK isoforms [20], specifically a greater relative increase in phosphorylation of JNKs 2 and 3, leading to the investigation of each isoform's contribution to polyQ-Htt induced deficits in axonal transport. Perfusion of active recombinant JNKs into squid axoplasm revealed that JNK3, but not JNK1, mimicked the effects of polyQ-Htt on anterograde and retrograde transport. While this could not take into account any effects that polyQ-Htt might have on other JNK regulating factors, it did reveal differential effects of JNK isoforms on MBO transport. Additional squid axoplasm experiments using pharmacological inhibitors showed that the JNK pathway is indeed involved in polyQ-Htt induced axonal transport impairments, and also suggested varying degrees of participation from specific JNK isoforms. However, due to the nature of the pharmacological agents used, off-target effects were inevitable [25-28], and any observations from these studies could not conclusively be attributed to any single JNK isoform. For example, SP600125, a pharmacological inhibitor of primarily JNKs, was used to selectively knock down JNKs. At the time, SP600125 was established to have a 420-fold greater selectivity for JNKs over a range of kinases. However, it has since been shown to inhibit phosphatidylinositol 3-kinase (PI3K) [26], which plays a role in axon formation and neuron polarization [330]. The JSAP1a and JSAP1d peptides were also used to differentially

inhibit activity of JNK isoforms, and prevention of polyQ-Htt effects on transport by use of JSAP1d yielded different results than use of JSAPa, as anticipated, but those results were difficult to attribute to any one JNK isoform. As stated [20], JSAP1d does indeed have reduced binding to JNK3 compared to JSAP1a, but it also has reduced binding to JNK1 [27]. The use of JIP inhibitors may also yield off-target consequences that are due not only due to competition with their endogenous counterparts, but also from unforeseen changes in regulation by competition with other scaffolding proteins that regulate JNKs. Nonetheless, these previous results certainly implicated specific JNK isoforms more than others, especially in conjunction with mass spectrometry data demonstrating that JNK3, but not JNK1, could phosphorylate the microtubule binding region of kinesin. These limitations, however, brought recognition of the need for a more definitive test model, leading to the work presented here.

The use of shRNA technology to specifically knock down individual JNK isoforms minimizes off-target effects. Results obtained from the cell model generated for the work put forth in this dissertation can be attributed to the knockdown of single isoforms of JNK with a high degree of confidence. Each shRNA used was shown to effectively knock down its respective JNK isoform at both the mRNA (see Figs. 8&10) and protein levels (see Figs 7&9), and did not change expression of the non-target JNK isoform. All shRNA sequences were also validated using the NIH Basic Local Alignment Search Tool (BLAST) to ensure a 100% match with its intended JNK isoform target, and to minimize sequence recognition of non-target JNK isoforms and other unintended targets. Additionally, each isoform was knocked down by two different shRNA sequences as a separate test condition, further decreasing the probability of spurious effects. Previous studies have established that impairments to kinesin-1 function cause

deficits in neurite outgrowth [326, 327] and mitochondrial transport [329]. It has independently been shown that polyQ-Htt inhibits neurite outgrowth in N2a cells [67], and also impairs mitochondrial transport in neurites [165, 198, 199]. Mass spectrometry studies demonstrate that recombinant active JNK3, but not JNK1, phosphorylates KHC within the microtubule-binding region [20] . JNK3 and KHC are highly conserved across species, so it is quite possible that activation of endogenous JNK3 in our N2a cells could phosphorylate endogenous KHC, resulting in dissociation of kinesin-1 from microtubules, thereby disrupting kinesin-1 function. Sequence-specific silencing by shRNA demonstrated that knockdown of JNK3, but not JNK1, prevented polyQ-Htt induced deficits in both neurite outgrowth and mitochondrial distribution to neurites. Within this experimental model, we can conclude with high confidance that JNK1 did not have any effect on polyQ-Htt induced deficits in neurite outgrowth or mitochondrial density in neurites. We can also conclude that, in our model, JNK3 is a mediator of polyQ-Htt induced impairment of neurite outgrowth and mitochondrial density in neurites. Alternate proposals claim that axonal transport deficits observed in HD models are due to physical impedence by Htt aggregates, but microscopic analysis in our study did not reveal any Htt aggregates (see Figure 15). These results, combined with evidence from previous studies from our lab, strongly suggest that neuronal JNK3, and not ubiquitous JNK1, mediates polyQ-Htt induced deficits by phosphorylating Ser176 on KHC.

In the context of prior work [331] from the Brady Laboratory, a pathogenic molecular mechanism for HD can be proposed. Abnormally expanded polyglutamine repeats alter the conformation of the Htt protein, exposing a normally hidden proline rich domain (PRD). Polyproline tandem repeats within the PRD can then interact with SH3 domains in mixed lineage

kinase 3 (MLK3), which results in the activation of MLK3. Active MLK3, an upstream regulator of the JNK pathway, then phosphorylates mitogen-activated protein kinase kinase (MKK)4 or MKK7, which in turn phosphorylate and activate JNK3. Activated JNK can then phosphorylate Ser176 on KHC, causing KHC to dissociate from microtubules, and thereby render kinesin unable to carry out its function. Ensuing impairments in delivery of essential materials and organelles to where they are needed result in dying back neuropathy underlying HD.

5.2. SIGNIFICANCE OF RESULTS TO PREFERENTIAL VULNERABILITY IN HD

The evidence indicates that deficits in axonal transport play a role in the degeneration of neurons observed in HD, but not why deficits in axonal transport in HD would affect projection neurons in the striatum and the cortex to a greater extent than projection neurons in different brain structures. Several possibilities exist. Among these, MSNs and cortical projection neurons affected in HD may have unique axonal transport requirements or specializations that makes them more vulnerable to polyQ-Htt-induced toxicity. Consistent with this idea, cytotypic differences in axonal transport have been documented *in vivo* for different neuronal populations[332]. Reinforcing the idea that differential vulnerabilities between cell types to the same polyQ-Htt induced deficits contributes to preferential loss of striatal MSNs, microarray analysis of pre-symptomatic knock-in HD mouse tissues show that changes in gene expression of striatal and cerebellar tissues are qualitatively similar, but quantitatively different [333].

One example of cell-type specific vulnerability to polyQ-Htt could be the synergy between JNK3 and neurotransmitters. Cumulative evidence indicates that DA, and perhaps other

neurotransmitters as well, might modulate the toxic effects of polyQ-Htt in a manner consistent with the differential vulnerabilities of striatal neurons in HD. Most studies on neurotransmitter signaling in HD have focused on altered calcium homeostasis and induction of apoptosis as a consequence of abnormal signaling [56, 241], but little emphasis has been placed on well-established events downstream of neurotransmitter receptor activation, including the modulation of kinase-dependent signaling pathways [334, 335]. Indeed, it is plausible that specific neurotransmitters and neuropeptides could act synergistically with polyQ-Htt-induced pathogenic JNK activation to increase the vulnerability of specific neuronal populations[31]. Consistent with this idea, activation of the JNK pathway induced by polyQ-Htt [20, 274, 296] was reportedly exacerbated by activation of D2 receptors [246, 334], which are specifically expressed in the most affected neuron population in HD - MSNs of the indirect pathway.

Another mechanism in play might be that one or more components mediating the effects of polyQ-Htt on axonal transport is expressed at higher levels and/or is more crucial to maintenance and survival of neurons affected in HD. Htt itself has been implicated to have physiological functions related to vesicle transport, and is expressed at varying levels in different brain structures in both humans [336] and mice [337], with some indication of higher expression levels in structures affected in HD. There is also evidence that striatal lysates from homozygous knock-in HD mice showed higher levels of activated JNK than heterozygous knock-in HD mice [20], suggesting that activation of JNK by polyQ-Htt is dose-dependent. Relative expression of JNK isoforms in different areas of the brain, and also importantly in different cell types within the same area of the brain, have not been extensively characterized, but there is some evidence that there are regional differences [287]. Of note, microarray data shows increased expression of

JNK3 in striatal and cortical areas affected in HD [338]. A molecular basis underlying the increased vulnerability of MSNs and cortical projection neurons to polyQ-Htt induced axonal transport alterations is currently unknown, but could reflect unique axonal transport specializations of these neuronal cell types [19, 20, 332].

It is also altogether possible that higher physiologic expression of JNK3 may render certain cell populations more vulnerable to polyQ-Htt induced stresses, whether or not axonal transport is a crucial process in those cells. JNK3 is considered the "neural-specific" isoform of JNK, although it has been known for some time to be expressed in the heart in testes as well [339]. Relatively recently, JNK3 has also been found to be abundant in insulin-secreting pancreatic β-islet cells [340]. This is particularly interesting because pathology of pancreatic islets has been found in 3 different HD mouse models [341-343]. And while non-neuronal human HD tissue has not been available for adequate analysis, it has been established that HD patients develop diabetes mellitus 7 times more often than matched controls [344], and that diabetic HD patients also have decreased insulin secretion [345]. HD patients suffer profound weight loss despite normal to increased caloric intake, and there is also evidence of disturbances in cellular metabolism [170]. Subsequent in vivo studies in HD patients employing live imaging techniques report region-specific alterations in metabolic markers [172-174]. These alterations were also found in presymptomatic HD carriers [175-178], suggesting that metabolic defects are present early on in the disease process. The fact that polyQ-Htt induced pathology in the pancreas could share a common cause with pathology in the brain has been largely overlooked, and deserves more attention, as it could shed light on common mechanisms underlying polyQ-Htt pathogenicity more easily than comparisons between neuronal populations. This connection

also lends credence to our findings that polyQ-Htt pathology is mediated by JNK3, and suggests that the extent of pathology in any given tissue in a HD patient might be proportional to expression of JNK3.

5.3. FUTURE DIRECTIONS

Earlier studies in squid axoplasm demonstrated that perfusion of polyQ-Htt inhibits retrograde transport as well as anterograde transport [18]. While there is yet no evidence that JNK3 can directly phosphorylate dynein, it is likely that knockdown of JNK3 had prevented deficits in dynein-mediated retrograde transport. Like kinesin, the proper function of dynein is necessary for neurite outgrowth [260, 328]. Any misregulation of transport by either kinesin or dynein, whether directly or via numerous accessory and adaptor proteins necessary for the proper transport of their cargoes, suffices to inhibit neurite outgrowth. Therefore it is reasonable to conclude that knockdown of JNK3 also prevented impairments in dynein-mediated transport. While polyQ-Htt has been shown to decrease KHC binding to MTs, MT-binding assays demonstrate that polyQ-Htt does not cause DHC to dissociate from MTs [20]. However, dyneins are enormous complexes with no shortage of components, on any of which phosphorylation by JNK could result in impaired retrograde transport. Investigation of polyQ-Htt induced phosphorylation of dynein components could confirm that JNK3 mediates deficits in retrograde axonal transport, and potentially reveal a specific site on which phosphorylation could deregulate proper function of dynein.

The effects of JNK isoforms in polyQ-Htt induced pathogenesis should logically be extended to animal models. There are viable JNK1, 2, and 3 knockout animals which could be

of great utility in the investigation of individual JNK isoforms in polyQ-Htt pathogenesis. JNK2 and JNK3 knockout animals have shown resistance to a number of neural stressors, including toxicity from MPTP [282], a chemical used to mimic the pattern of cell death seen in Parkinson's Disease. JNK3 knockout mice in particular have shown resistance to a number of additional neural stressors including kainic acid [283], ischemia [284, 285], Alzheimer's disease-related protein β-amyloid [286], and 6-hydroxydopamine [287]. JNK knockout animals could potentially be cross-bred with any number of genetic HD mice, or alternatively receive delivery of polyQ-Htt by brain injections. Evidence from JNK3 animals have also implicated JNK3 in non-pathological roles in brain development processes [288], such as neurite formation and plasticity [289, 290], and in cognitive functions such as memory and learning [287, 291]. As deficits in these cognitive functions are also seen in HD patients, this reiterates the importance of working towards of a better understanding of the role of JNKs in normal brain physiology, in addition to the pathologic state induced by mutant Htt.

As discussed in the above section, differential expression of JNK3 and polyQ-Htt might contribute to preferential vulnerability of certain cell populations in HD. A detailed characterization of expression of JNK isoforms and Htt in different brain structures, in both wt and HD mice (assuming human tissue is not all that available) might reveal a correlation. Furthermore, single-cell RT-PCR techniques could be used to compare expression of JNK isoforms and Htt at the level of cell types, such as MSNs and striatal interneurons. In addition to JNK isoforms and Htt, expression levels of upstream JNK pathway activators could also be explored, and could further enhance our understanding of preferential vulnerabilities in HD.

5.4. Concluding Remarks

The ubiquitous expression of polyQ-Htt contrasts sharply with the pronounced vulnerability of projection neurons in the striatum and cerebral cortex observed in HD. The incontrovertible loss of these neurons had led to the use of the term "selective" vulnerability, which may inadvertently undermine the importance of non-striatal and non-cortical cells affected in HD. Degeneration to a lesser degree is nonetheless degeneration, and within the "differential" vulnerabilities of these neuronal populations is information that could elucidate mechanisms underlying HD. Experimental evidence showing toxic effects of polyQ-Htt in a variety of neuronal cell types suggests that the pattern of neuronal degeneration in HD could result from modulation of polyQ-Htt by cell-type specific features. The confluence of a cell's properties confer identity as well as specific weaknesses, which are in turn exploited by a multifactorial cascade of cellular insults initiated by mutant Htt. When compensatory mechanisms can no longer keep up with the additive toxic effects, the delicate balance shifts from survival to degeneration. Proposed pathogenic mechanisms for HD vary from excitotoxicity to energy impairments to axonal dysfunction, amongst others. These possibilities are not mutually exclusive, but the relative contribution of each will only be clarified with an understanding of molecular systems mediating toxicity in HD. We have provided but a link in a vast and complex puzzle that begins with a single mutation in a single gene, and culminates in the decline of a vital process resulting in dying back neurodegenerative disease. But while there may eventually be enough evidence to pursue JNK3 as a therapeutic target for HD, the multi-layered regulation of JNKs, and our lack of knowledge on how polyQ-Htt deregulates JNK activity, makes outright inhibition of JNK3 an unrealistic candidate at this point in time.

Recent clinical trials provide salient examples of how non-pathogenic phenomena become mistaken heralds for developing effective treatments for neurodegenerative disease. The Parkinson Research Examination of CEP-1347 Trial (PRECEPT) assessed the disease-modifying potential of CEP-1347, a mixed lineage kinase (MLK) inhibitor, in patients with early stage Parkinson's disease (PD). CEP-1347 was found to reduce apoptosis of neuronal cells in nonclinical PD models, and was found to be safe and well tolerated in PD patients. However, the PRECEPT trial was terminated early when it was clear that CEP-1347 was ineffective in modifying the progression of PD compared to placebo [346]. And just August 6, 2012, Pfizer and Johnson&Johnson announced a second failed Phase III clinical trial for bapineuzumab, an anti-amyloid antibody for the treatment of Alzheimer's disease (AD). While preclinical trials demonstrated that the antibody could clear amyloid plaques in animal models of AD, two Phase III trials failed to show any cognitive or functional improvement in early to moderate stage AD patients. As posited in this dissertation, neither Htt aggregates nor apoptosis is an appropriate target for disease treatment, as they are not root causes of HD. Along similar lines, these failed clinical trials demonstrate in actual patients that drugs that prevent amyloid plaques and apoptosis do not stave off progression of AD or PD. Discovery and understanding of pathogenic molecular mechanisms is crucial to the development of any therapeutic agent, as they should serve as the basis for drug design. Targeting subclinical pathology should translate into detectable slowing, halting, or reversal of progressive clinical symptoms. Failure to distinguish between disease causing events and epiphenomena can lead to enormous losses of effort and resources that could have been better spent towards developing meaningful treatments. While a definitive link between the Htt gene mutation and disease was established nearly 20 years ago,

the molecular mechanisms underlying HD pathogenesis remain elusive. It is our hope that our contribution here may help advance the understanding of this devastating disease towards a meaningful, disease-modifying therapy.

CITED LITERATURE

1. Cicchetti, F., et al., *Chemical anatomy of striatal interneurons in normal individuals and in patients with Huntington's disease.* Brain Res.Brain Res.Rev., 2000. **34**(1-2): p. 80-101.

2. Zuccato, C. and E. Cattaneo, *Role of brain-derived neurotrophic factor in Huntington's disease.* Prog.Neurobiol., 2007. **81**(5-6): p. 294-330.

3. HDCRG, *A novel gene containing a trinucleotide repeat that is expanded and unstable on Huntington's disease chromosomes. The Huntington's Disease Collaborative Research Group.* Cell, 1993. **72**(6): p. 971-983.

4. Brinkman, R.R., et al., *The likelihood of being affected with Huntington disease by a particular age, for a specific CAG size.* Am J Hum Genet, 1997. **60**(5): p. 1202-10.

5. Snell, R.G., et al., *Relationship between trinucleotide repeat expansion and phenotypic variation in Huntington's disease.* Nat.Genet., 1993. **4**(4): p. 393-397.

6. Walker, F.O., *Huntington's Disease.* Semin.Neurol., 2007. **27**(2): p. 143-150.

7. Reilmann, R., et al., *Objective assessment of progression in Huntington's disease: a 3-year follow-up study.* Neurology, 2001. **57**(5): p. 920-924.

8. Barbeau, A., et al., *Classification of extrapyramidal disorders. Proposal for an international classification and glossary of terms.* J Neurol Sci, 1981. **51**(2): p. 311-27.

9. Okun, M.S., *Huntington's disease: what we learned from the original essay.* Neurologist., 2003. **9**(4): p. 175-179.

10. Vonsattel, J.P., et al., *Neuropathological classification of Huntington's disease.* J.Neuropathol.Exp.Neurol., 1985. **44**(6): p. 559-577.

11. Reiner, A., et al., *Differential loss of striatal projection neurons in Huntington disease.* Proc Natl Acad Sci U S A, 1988. **85**(15): p. 5733-7.

12. Storey, E. and M.F. Beal, *Neurochemical substrates of rigidity and chorea in Huntington's disease.* Brain, 1993. **116 (Pt 5)**: p. 1201-1222.

13. Li, S.H., et al., *Huntington's disease gene (IT15) is widely expressed in human and rat tissues.* Neuron, 1993. **11**(5): p. 985-93.

14. Landwehrmeyer, G.B., et al., *Huntington's disease gene: regional and cellular expression in brain of normal and affected individuals.* Ann.Neurol., 1995. **37**(2): p. 218-230.

15. Strong, T.V., et al., *Widespread expression of the human and rat Huntington's disease gene in brain and nonneural tissues.* Nat.Genet., 1993. **5**(3): p. 259-265.

16. Pigino, G., et al., *Alzheimer's presenilin 1 mutations impair kinesin-based axonal transport.* J.Neurosci., 2003. **23**(11): p. 4499-4508.

17. Braunstein, K.E., et al., *A point mutation in the dynein heavy chain gene leads to striatal atrophy and compromises neurite outgrowth of striatal neurons.* Hum Mol Genet, 2010.

18. Szebenyi, G., et al., *Neuropathogenic forms of huntingtin and androgen receptor inhibit fast axonal transport.* Neuron, 2003. **40**(1): p. 41-52.

19. Her, L.S. and L.S. Goldstein, *Enhanced sensitivity of striatal neurons to axonal transport defects induced by mutant huntingtin.* J Neurosci, 2008. **28**(50): p. 13662-72.

20. Morfini, G., et al., *Inhibition of Fast Axonal Transport by Pathogenic Huntingtin Involves Activation of JNK3 and Phosphorylation of Kinesin-1.* Nature Neuroscience, 2009.

21. Reid, E., et al., *A kinesin heavy chain (KIF5A) mutation in hereditary spastic paraplegia (SPG10).* Am J Hum Genet, 2002. **71**(5): p. 1189-94.

22. Levine, M.S., et al., *Genetic mouse models of Huntington's and Parkinson's diseases: illuminating but imperfect.* Trends Neurosci., 2004. **27**(11): p. 691-697.

23. Tobin, A.J. and E.R. Signer, *Huntington's disease: the challenge for cell biologists.* Trends Cell Biol., 2000. **10**(12): p. 531-536.

24. Menalled, L.B., *Knock-in mouse models of Huntington's disease.* NeuroRx., 2005. **2**(3): p. 465-470.

25. Horiuchi, D., et al., *APLIP1, a kinesin binding JIP-1/JNK scaffold protein, influences the axonal transport of both vesicles and mitochondria in Drosophila.* Curr Biol, 2005. **15**(23): p. 2137-41.

26. Miyazawa, K., *Encountering unpredicted off-target effects of pharmacological inhibitors.* J Biochem, 2011. **150**(1): p. 1-3.

27. Ito, M., et al., *Isoforms of JSAP1 scaffold protein generated through alternative splicing.* Gene, 2000. **255**(2): p. 229-34.

28. Coffey, E.T., et al., *c-Jun N-terminal protein kinase (JNK) 2/3 is specifically activated by stress, mediating c-Jun activation, in the presence of constitutive JNK1 activity in cerebellar neurons.* J Neurosci, 2002. **22**(11): p. 4335-45.

29. Dunkel, P., et al., *Clinical utility of neuroprotective agents in neurodegenerative diseases: current status of drug development for Alzheimer's, Parkinson's and Huntington's diseases, and amyotrophic lateral sclerosis.* Expert Opin Investig Drugs, 2012.

30. MacDonald, M.E., et al., *Huntington's disease.* Neuromolecular.Med., 2003. **4**(1-2): p. 7-20.

31. Morfini, G., G. Pigino, and S.T. Brady, *Polyglutamine expansion diseases: failing to deliver.* Trends Mol.Med., 2005. **11**(2): p. 64-70.

32. Graybiel, A.M., *Neurotransmitters and neuromodulators in the basal ganglia.* Trends Neurosci, 1990. **13**(7): p. 244-54.

33. Mitchell, I.J., A.J. Cooper, and M.R. Griffiths, *The selective vulnerability of striatopallidal neurons.* Prog.Neurobiol., 1999. **59**(6): p. 691-719.

34. Parent, A. and L.N. Hazrati, *Functional anatomy of the basal ganglia. I. The cortico-basal ganglia-thalamo-cortical loop.* Brain Res Brain Res Rev, 1995. **20**(1): p. 91-127.

35. Vonsattel, J.P. and M. DiFiglia, *Huntington disease.* J Neuropathol Exp Neurol, 1998. **57**(5): p. 369-84.

36. Mann, D.M., R. Oliver, and J.S. Snowden, *The topographic distribution of brain atrophy in Huntington's disease and progressive supranuclear palsy.* Acta Neuropathol., 1993. **85**(5): p. 553-559.

37. Heinsen, H., et al., *Cortical and striatal neurone number in Huntington's disease.* Acta Neuropathol., 1994. **88**(4): p. 320-333.

38. DiFiglia, M., P. Pasik, and T. Pasik, *A Golgi study of neuronal types in the neostriatum of monkeys.* Brain Res, 1976. **114**(2): p. 245-56.

39. Difiglia, M., T. Pasik, and P. Pasik, *Ultrastructure of Golgi-impregnated and gold-toned spiny and aspiny neurons in the monkey neostriatum.* J Neurocytol, 1980. **9**(4): p. 471-92.

40. Parent, A., C. Csonka, and P. Etienne, *The occurrence of large acetylcholinesterase-containing neurons in human neostriatum as disclosed in normal and Alzheimer-diseased brains.* Brain Res, 1984. **291**(1): p. 154-8.

41. Gerfen, C.R., *Synaptic organization of the striatum.* J Electron Microsc Tech, 1988. **10**(3): p. 265-81.

42. Parent, A., J. O'Reilly-Fromentin, and R. Boucher, *Acetylcholinesterase-containing neurons in cat neostriatum: a morphological and quantitative analysis.* Neurosci Lett, 1980. **20**(3): p. 271-6.

43. Kawaguchi, Y., *Neostriatal cell subtypes and their functional roles.* Neurosci Res, 1997. **27**(1): p. 1-8.

44. Kawaguchi, Y., et al., *Striatal interneurones: chemical, physiological and morphological characterization.* Trends Neurosci, 1995. **18**(12): p. 527-35.

45. Mattson, M.P. and T. Magnus, *Ageing and neuronal vulnerability.* Nat Rev Neurosci, 2006. **7**(4): p. 278-94.

46. Morfini, G.A., et al., *Axonal transport defects in neurodegenerative diseases.* J Neurosci, 2009. **29**(41): p. 12776-86.

47. Smith, Y., et al., *Microcircuitry of the direct and indirect pathways of the basal ganglia.* Neuroscience, 1998. **86**(2): p. 353-87.

48. Albin, R.L., et al., *Preferential loss of striato-external pallidal projection neurons in presymptomatic Huntington's disease.* Ann.Neurol., 1992. **31**(4): p. 425-430.

49. Richfield, E.K., et al., *Preferential loss of preproenkephalin versus preprotachykinin neurons from the striatum of Huntington's disease patients.* Ann.Neurol., 1995. **38**(6): p. 852-861.

50. Crossman, A.R., *Primate models of dyskinesia: the experimental approach to the study of basal ganglia-related involuntary movement disorders.* Neuroscience, 1987. **21**(1): p. 1-40.

51. Crossman, A.R., et al., *Chorea and myoclonus in the monkey induced by gamma-aminobutyric acid antagonism in the lentiform complex. The site of drug action and a hypothesis for the neural mechanisms of chorea.* Brain, 1988. **111 (Pt 5)**: p. 1211-1233.

52. Berardelli, A., et al., *Pathophysiology of chorea and bradykinesia in Huntington's disease.* Mov Disord., 1999. **14**(3): p. 398-403.

53. Cudkowicz, M. and N.W. Kowall, *Degeneration of pyramidal projection neurons in Huntington's disease cortex.* Ann.Neurol., 1990. **27**(2): p. 200-204.

54. Hedreen, J.C., et al., *Neuronal loss in layers V and VI of cerebral cortex in Huntington's disease.* Neurosci.Lett., 1991. **133**(2): p. 257-261.

55. Sotrel, A., et al., *Morphometric analysis of the prefrontal cortex in Huntington's disease.* Neurology, 1991. **41**(7): p. 1117-1123.

56. Sieradzan, K.A. and D.M. Mann, *The selective vulnerability of nerve cells in Huntington's disease.* Neuropathol.Appl.Neurobiol., 2001. **27**(1): p. 1-21.

57. Perez-Navarro, E., et al., *Cellular and molecular mechanisms involved in the selective vulnerability of striatal projection neurons in Huntington's disease.* Histol.Histopathol., 2006. **21**(11): p. 1217-1232.

58. Cowan, C.M. and L.A. Raymond, *Selective neuronal degeneration in Huntington's disease.* Curr.Top.Dev.Biol., 2006. **75**: p. 25-71.

59. Lange, H., et al., *Morphometric studies of the neuropathological changes in choreatic diseases.* J Neurol Sci, 1976. **28**(4): p. 401-25.

60. Oyanagi, K., et al., *A quantitative investigation of the substantia nigra in Huntington's disease.* Ann.Neurol., 1989. **26**(1): p. 13-19.

61. Heinsen, H., et al., *Nerve cell loss in the thalamic mediodorsal nucleus in Huntington's disease.* Acta Neuropathol., 1999. **97**(6): p. 613-622.

62. Byers, R.K., F.H. Gilles, and C. Fung, *Huntington's disease in children. Neuropathologic study of four cases.* Neurology, 1973. **23**(6): p. 561-569.

63. Rodda, R.A., *Cerebellar atrophy in Huntington's disease.* J.Neurol.Sci., 1981. **50**(1): p. 147-157.

64. Senut, M.C., et al., *Intraneuronal aggregate formation and cell death after viral expression of expanded polyglutamine tracts in the adult rat brain.* J Neurosci, 2000. **20**(1): p. 219-29.

65. de Almeida, L.P., et al., *Lentiviral-mediated delivery of mutant huntingtin in the striatum of rats induces a selective neuropathology modulated by polyglutamine repeat size, huntingtin expression levels, and protein length.* J.Neurosci., 2002. **22**(9): p. 3473-3483.

66. Sassone, J., et al., *Huntington's disease: the current state of research with peripheral tissues.* Exp Neurol, 2009. **219**(2): p. 385-97.

67. Ye, C., et al., *Inhibition of neurite outgrowth and promotion of cell death by cytoplasmic soluble mutant huntingtin stably transfected in mouse neuroblastoma cells.* Neurosci Lett, 2008. **442**(1): p. 63-8.

68. Lunkes, A. and J.L. Mandel, *A cellular model that recapitulates major pathogenic steps of Huntington's disease.* Hum.Mol.Genet., 1998. **7**(9): p. 1355-1361.

69. Carmichael, J., et al., *Glycogen synthase kinase-3beta inhibitors prevent cellular polyglutamine toxicity caused by the Huntington's disease mutation.* J.Biol.Chem., 2002. **277**(37): p. 33791-33798.

70. Carmichael, J., C. Vacher, and D.C. Rubinsztein, *The bacterial chaperonin GroEL requires GroES to reduce aggregation and cell death in a COS-7 cell model of Huntington's disease.* Neurosci.Lett., 2002. **330**(3): p. 270-274.

71. Li, S.H., et al., *Cellular defects and altered gene expression in PC12 cells stably expressing mutant huntingtin.* J Neurosci, 1999. **19**(13): p. 5159-72.

72. Vila, M. and S. Przedborski, *Targeting programmed cell death in neurodegenerative diseases.* Nat Rev Neurosci, 2003. **4**(5): p. 365-75.

73. Portera-Cailliau, C., et al., *Evidence for apoptotic cell death in Huntington disease and excitotoxic animal models.* J.Neurosci., 1995. **15**(5 Pt 2): p. 3775-3787.

74. Ramaswamy, S., J.L. McBride, and J.H. Kordower, *Animal models of Huntington's disease.* ILAR.J., 2007. **48**(4): p. 356-373.

75. Vonsattel, J.P., *Huntington disease models and human neuropathology: similarities and differences.* Acta Neuropathol, 2008. **115**(1): p. 55-69.

76. Lione, L.A., et al., *Selective discrimination learning impairments in mice expressing the human Huntington's disease mutation.* J.Neurosci., 1999. **19**(23): p. 10428-10437.

77. Luesse, H.G., et al., *Evaluation of R6/2 HD transgenic mice for therapeutic studies in Huntington's disease: behavioral testing and impact of diabetes mellitus.* Behav.Brain Res., 2001. **126**(1-2): p. 185-195.

78. Murphy, K.P., et al., *Abnormal synaptic plasticity and impaired spatial cognition in mice transgenic for exon 1 of the human Huntington's disease mutation.* J.Neurosci., 2000. **20**(13): p. 5115-5123.

79. Klivenyi, P., et al., *Behaviour changes in a transgenic model of Huntington's disease.* Behav.Brain Res., 2006. **169**(1): p. 137-141.

80. von Horsten, S., et al., *Transgenic rat model of Huntington's disease.* Hum Mol Genet, 2003. **12**(6): p. 617-24.

81. Davies, S.W. and E. Scherzinger, *Nuclear inclusions in Huntington's disease.* Trends Cell Biol., 1997. **7**(11): p. 422.

82. Davies, S.W., et al., *Formation of neuronal intranuclear inclusions underlies the neurological dysfunction in mice transgenic for the HD mutation.* Cell, 1997. **90**(3): p. 537-548.

83. DiFiglia, M., et al., *Aggregation of huntingtin in neuronal intranuclear inclusions and dystrophic neurites in brain.* Science, 1997. **277**(5334): p. 1990-1993.

84. Sapp, E., et al., *Axonal transport of N-terminal huntingtin suggests early pathology of corticostriatal projections in Huntington disease.* J Neuropathol Exp Neurol, 1999. **58**(2): p. 165-73.

85. DiProspero, N.A., et al., *Early changes in Huntington's disease patient brains involve alterations in cytoskeletal and synaptic elements.* J.Neurocytol., 2004. **33**(5): p. 517-533.

86. Cepeda, C., et al., *Transient and progressive electrophysiological alterations in the corticostriatal pathway in a mouse model of Huntington's disease.* J.Neurosci., 2003. **23**(3): p. 961-969.

87. Mizuno, H., et al., *An autopsy case with clinically and molecular genetically diagnosed Huntington's disease with only minimal non-specific neuropathological findings.* Clin.Neuropathol., 2000. **19**(2): p. 94-103.

88. Vis, J.C., et al., *Expression pattern of apoptosis-related markers in Huntington's disease.* Acta Neuropathol., 2005. **109**(3): p. 321-328.

89. Reading, S.A., et al., *Functional brain changes in presymptomatic Huntington's disease.* Ann.Neurol., 2004. **55**(6): p. 879-883.

90. Rosenblatt, A., et al., *Predictors of neuropathological severity in 100 patients with Huntington's disease.* Ann.Neurol., 2003. **54**(4): p. 488-493.

91. Li, H., et al., *Huntingtin aggregate-associated axonal degeneration is an early pathological event in Huntington's disease mice.* J.Neurosci., 2001. **21**(21): p. 8473-8481.

92. Klapstein, G.J., et al., *Electrophysiological and morphological changes in striatal spiny neurons in R6/2 Huntington's disease transgenic mice.* J.Neurophysiol., 2001. **86**(6): p. 2667-2677.

93. Bibb, J.A., et al., *Severe deficiencies in dopamine signaling in presymptomatic Huntington's disease mice.* Proc.Natl.Acad.Sci.U.S.A, 2000. **97**(12): p. 6809-6814.

94. Cepeda, C., et al., *NMDA receptor function in mouse models of Huntington disease.* J Neurosci Res, 2001. **66**(4): p. 525-39.

95. Laforet, G.A., et al., *Changes in cortical and striatal neurons predict behavioral and electrophysiological abnormalities in a transgenic murine model of Huntington's disease.* J.Neurosci., 2001. **21**(23): p. 9112-9123.

96. Rosas, H.D., et al., *Altered white matter microstructure in the corpus callosum in Huntington's disease: implications for cortical "disconnection".* Neuroimage, 2010. **49**(4): p. 2995-3004.

97. Weaver, K.E., et al., *Longitudinal diffusion tensor imaging in Huntington's Disease.* Exp Neurol, 2009. **216**(2): p. 525-9.

98. Ferrante, R.J., N.W. Kowall, and E.P. Richardson, Jr., *Proliferative and degenerative changes in striatal spiny neurons in Huntington's disease: a combined study using the section-Golgi method and calbindin D28k immunocytochemistry.* J.Neurosci., 1991. **11**(12): p. 3877-3887.

99. Wade, A., P. Jacobs, and A.J. Morton, *Atrophy and degeneration in sciatic nerve of presymptomatic mice carrying the Huntington's disease mutation.* Brain Res., 2008. **1188**: p. 61-68.

100. White, J.K., et al., *Huntingtin is required for neurogenesis and is not impaired by the Huntington's disease CAG expansion.* Nat.Genet., 1997. **17**(4): p. 404-410.

101. Zeitlin, S., et al., *Increased apoptosis and early embryonic lethality in mice nullizygous for the Huntington's disease gene homologue.* Nat.Genet., 1995. **11**(2): p. 155-163.

102. Dragatsis, I., P. Dietrich, and S. Zeitlin, *Expression of the Huntingtin-associated protein 1 gene in the developing and adult mouse.* Neurosci.Lett., 2000. **282**(1-2): p. 37-40.

103. Harjes, P. and E.E. Wanker, *The hunt for huntingtin function: interaction partners tell many different stories.* Trends Biochem.Sci., 2003. **28**(8): p. 425-433.

104. Nasir, J., et al., *Targeted disruption of the Huntington's disease gene results in embryonic lethality and behavioral and morphological changes in heterozygotes.* Cell, 1995. **81**(5): p. 811-823.

105. MacDonald, M.E., et al., *Targeted inactivation of the mouse Huntington's disease gene homolog Hdh.* Cold Spring Harb.Symp.Quant.Biol., 1996. **61**: p. 627-638.

106. Orr, H.T. and H.Y. Zoghbi, *Trinucleotide repeat disorders.* Annu Rev Neurosci, 2007. **30**: p. 575-621.

107. Cepeda, C., et al., *The corticostriatal pathway in Huntington's disease.* Prog.Neurobiol., 2007. **81**(5-6): p. 253-271.

108. Trottier, Y., et al., *Cellular localization of the Huntington's disease protein and discrimination of the normal and mutated form.* Nat.Genet., 1995. **10**(1): p. 104-110.

109. Fusco, F.R., et al., *Cellular localization of huntingtin in striatal and cortical neurons in rats: lack of correlation with neuronal vulnerability in Huntington's disease.* J.Neurosci., 1999. **19**(4): p. 1189-1202.

110. Bhide, P.G., et al., *Expression of normal and mutant huntingtin in the developing brain.* J.Neurosci., 1996. **16**(17): p. 5523-5535.

111. DiFiglia, M., et al., *Huntingtin is a cytoplasmic protein associated with vesicles in human and rat brain neurons.* Neuron, 1995. **14**(5): p. 1075-1081.

112. Gutekunst, C.A., et al., *Identification and localization of huntingtin in brain and human lymphoblastoid cell lines with anti-fusion protein antibodies.* Proc.Natl.Acad.Sci.U.S.A, 1995. **92**(19): p. 8710-8714.

113. Ide, K., et al., *Abnormal gene product identified in Huntington's disease lymphocytes and brain.* Biochem.Biophys.Res.Commun., 1995. **209**(3): p. 1119-1125.

114. Shelbourne, P.F., et al., *Triplet repeat mutation length gains correlate with cell-type specific vulnerability in Huntington disease brain.* Hum.Mol.Genet., 2007. **16**(10): p. 1133-1142.

115. Ishiguro, H., et al., *Age-dependent and tissue-specific CAG repeat instability occurs in mouse knock-in for a mutant Huntington's disease gene.* J.Neurosci.Res., 2001. **65**(4): p. 289-297.

116. Kennedy, L., et al., *Dramatic tissue-specific mutation length increases are an early molecular event in Huntington disease pathogenesis.* Hum.Mol.Genet., 2003. **12**(24): p. 3359-3367.

117. Kennedy, L. and P.F. Shelbourne, *Dramatic mutation instability in HD mouse striatum: does polyglutamine load contribute to cell-specific vulnerability in Huntington's disease?* Hum.Mol.Genet., 2000. **9**(17): p. 2539-2544.

118. Lopes-Cendes, I., et al., *Somatic mosaicism in the central nervous system in spinocerebellar ataxia type 1 and Machado-Joseph disease.* Ann Neurol, 1996. **40**(2): p. 199-206.

119. Watase, K., et al., *Regional differences of somatic CAG repeat instability do not account for selective neuronal vulnerability in a knock-in mouse model of SCA1.* Hum.Mol.Genet., 2003. **12**(21): p. 2789-2795.

120. Gray, M., et al., *Full-length human mutant huntingtin with a stable polyglutamine repeat can elicit progressive and selective neuropathogenesis in BACHD mice.* J Neurosci, 2008. **28**(24): p. 6182-95.

121. Lee, J.M., et al., *Quantification of age-dependent somatic CAG repeat instability in Hdh CAG knock-in mice reveals different expansion dynamics in striatum and liver.* PLoS One, 2011. **6**(8): p. e23647.

122. Li, S.H. and X.J. Li, *Aggregation of N-terminal huntingtin is dependent on the length of its glutamine repeats.* Hum.Mol.Genet., 1998. **7**(5): p. 777-782.

123. Li, H., et al., *Ultrastructural localization and progressive formation of neuropil aggregates in Huntington's disease transgenic mice.* Hum.Mol.Genet., 1999. **8**(7): p. 1227-1236.

124. Kuemmerle, S., et al., *Huntington aggregates may not predict neuronal death in Huntington's disease.* Ann.Neurol., 1999. **46**(6): p. 842-849.

125. Li, S.H. and X.J. Li, *Huntingtin and its role in neuronal degeneration.* Neuroscientist., 2004. **10**(5): p. 467-475.

126. Perutz, M.F., *Glutamine repeats and neurodegenerative diseases: molecular aspects.* Trends Biochem Sci, 1999. **24**(2): p. 58-63.

127. Rubinsztein, D.C. and J. Carmichael, *Huntington's disease: molecular basis of neurodegeneration.* Expert.Rev.Mol.Med., 2003. **5**(20): p. 1-21.

128. Cooper, J.K., et al., *Truncated N-terminal fragments of huntingtin with expanded glutamine repeats form nuclear and cytoplasmic aggregates in cell culture.* Hum.Mol.Genet., 1998. **7**(5): p. 783-790.

129. Hackam, A.S., et al., *The influence of huntingtin protein size on nuclear localization and cellular toxicity.* J Cell Biol, 1998. **141**(5): p. 1097-105.

130. Arrasate, M., et al., *Inclusion body formation reduces levels of mutant huntingtin and the risk of neuronal death.* Nature, 2004. **431**(7010): p. 805-810.

131. Perrin, V., et al., *Implication of the JNK pathway in a rat model of Huntington's disease.* Exp Neurol, 2009. **215**(1): p. 191-200.

132. Truant, R., et al., *Huntington's disease: revisiting the aggregation hypothesis in polyglutamine neurodegenerative diseases.* FEBS J, 2008. **275**(17): p. 4252-62.

133. Wang, C.E., et al., *Suppression of neuropil aggregates and neurological symptoms by an intracellular antibody implicates the cytoplasmic toxicity of mutant huntingtin.* J.Cell Biol., 2008. **181**(5): p. 803-816.

134. La Spada, A.R. and J.P. Taylor, *Polyglutamines placed into context.* Neuron, 2003. **38**(5): p. 681-4.

135. Michalik, A. and B.C. Van, *Pathogenesis of polyglutamine disorders: aggregation revisited.* Hum.Mol.Genet., 2003. **12 Spec No 2**: p. R173-R186.

136. Saudou, F., et al., *Huntingtin acts in the nucleus to induce apoptosis but death does not correlate with the formation of intranuclear inclusions.* Cell, 1998. **95**(1): p. 55-66.

137. Becher, M.W., et al., *Intranuclear neuronal inclusions in Huntington's disease and dentatorubral and pallidoluysian atrophy: correlation between the density of inclusions and IT15 CAG triplet repeat length.* Neurobiol.Dis., 1998. **4**(6): p. 387-397.

138. Gutekunst, C.A., et al., *Nuclear and neuropil aggregates in Huntington's disease: relationship to neuropathology.* J.Neurosci., 1999. **19**(7): p. 2522-2534.

139. Thomas, E.A., *Striatal specificity of gene expression dysregulation in Huntington's disease.* J.Neurosci.Res., 2006. **84**(6): p. 1151-1164.

140. Cha, J.H., *Transcriptional signatures in Huntington's disease.* Prog.Neurobiol., 2007. **83**(4): p. 228-248.

141. Cha, J.H., *Transcriptional dysregulation in Huntington's disease.* Trends Neurosci., 2000. **23**(9): p. 387-392.

142. Sugars, K.L. and D.C. Rubinsztein, *Transcriptional abnormalities in Huntington disease.* Trends Genet, 2003. **19**(5): p. 233-8.

143. Courey, A.J., et al., *Synergistic activation by the glutamine-rich domains of human transcription factor Sp1.* Cell, 1989. **59**(5): p. 827-36.

144. Gerber, H.P., et al., *Transcriptional activation modulated by homopolymeric glutamine and proline stretches.* Science, 1994. **263**(5148): p. 808-11.

145. McCampbell, A., et al., *CREB-binding protein sequestration by expanded polyglutamine.* Hum Mol Genet, 2000. **9**(14): p. 2197-202.

146. Nucifora, F.C., Jr., et al., *Interference by huntingtin and atrophin-1 with cbp-mediated transcription leading to cellular toxicity.* Science, 2001. **291**(5512): p. 2423-2428.

147. Steffan, J.S., et al., *Histone deacetylase inhibitors arrest polyglutamine-dependent neurodegeneration in Drosophila.* Nature, 2001. **413**(6857): p. 739-743.

148. Glass, M., M. Dragunow, and R.L. Faull, *The pattern of neurodegeneration in Huntington's disease: a comparative study of cannabinoid, dopamine, adenosine and GABA(A) receptor alterations in the human basal ganglia in Huntington's disease.* Neuroscience, 2000. **97**(3): p. 505-519.

149. Mantamadiotis, T., et al., *Disruption of CREB function in brain leads to neurodegeneration.* Nat Genet, 2002. **31**(1): p. 47-54.

150. Obrietan, K. and K.R. Hoyt, *CRE-mediated transcription is increased in Huntington's disease transgenic mice.* J.Neurosci., 2004. **24**(4): p. 791-796.

151. Huang, C.C., et al., *Amyloid formation by mutant huntingtin: threshold, progressivity and recruitment of normal polyglutamine proteins.* Somat.Cell Mol.Genet., 1998. **24**(4): p. 217-233.

152. Stevanin, G., et al., *Huntington's disease-like phenotype due to trinucleotide repeat expansions in the TBP and JPH3 genes.* Brain, 2003. **126**(Pt 7): p. 1599-1603.

153. Dunah, A.W., et al., *Sp1 and TAFII130 transcriptional activity disrupted in early Huntington's disease.* Science, 2002. **296**(5576): p. 2238-2243.

154. Yu, Z.X., et al., *Huntingtin inclusions do not deplete polyglutamine-containing transcription factors in HD mice.* Hum.Mol.Genet., 2002. **11**(8): p. 905-914.

155. Luthi-Carter, R., et al., *Polyglutamine and transcription: gene expression changes shared by DRPLA and Huntington's disease mouse models reveal context-independent effects.* Hum.Mol.Genet., 2002. **11**(17): p. 1927-1937.

156. Kita, H., et al., *Modulation of polyglutamine-induced cell death by genes identified by expression profiling.* Hum.Mol.Genet., 2002. **11**(19): p. 2279-2287.

157. Sipione, S., et al., *Early transcriptional profiles in huntingtin-inducible striatal cells by microarray analyses.* Hum.Mol.Genet., 2002. **11**(17): p. 1953-1965.

158. Zuccato, C., et al., *Widespread disruption of repressor element-1 silencing transcription factor/neuron-restrictive silencer factor occupancy at its target genes in Huntington's disease.* J.Neurosci., 2007. **27**(26): p. 6972-6983.

159. Baquet, Z.C., J.A. Gorski, and K.R. Jones, *Early striatal dendrite deficits followed by neuron loss with advanced age in the absence of anterograde cortical brain-derived neurotrophic factor.* J.Neurosci., 2004. **24**(17): p. 4250-4258.

160. Mufson, E.J., et al., *Distribution and retrograde transport of trophic factors in the central nervous system: functional implications for the treatment of neurodegenerative diseases.* Prog.Neurobiol., 1999. **57**(4): p. 451-484.

161. Zuccato, C., et al., *Huntingtin interacts with REST/NRSF to modulate the transcription of NRSE-controlled neuronal genes.* Nat.Genet., 2003. **35**(1): p. 76-83.

162. Zuccato, C., et al., *Loss of huntingtin-mediated BDNF gene transcription in Huntington's disease.* Science, 2001. **293**(5529): p. 493-498.

163. Canals, J.M., et al., *Expression of brain-derived neurotrophic factor in cortical neurons is regulated by striatal target area.* J.Neurosci., 2001. **21**(1): p. 117-124.

164. Gauthier, L.R., et al., *Huntingtin controls neurotrophic support and survival of neurons by enhancing BDNF vesicular transport along microtubules.* Cell, 2004. **118**(1): p. 127-138.

165. Trushina, E., et al., *Mutant huntingtin impairs axonal trafficking in mammalian neurons in vivo and in vitro.* Mol.Cell Biol., 2004. **24**(18): p. 8195-8209.

166. Strand, A.D., et al., *Expression profiling of Huntington's disease models suggests that brain-derived neurotrophic factor depletion plays a major role in striatal degeneration.* J.Neurosci., 2007. **27**(43): p. 11758-11768.

167. Ricci, A., et al., *Neurotrophin and neurotrophin receptor protein expression in the human lung.* Am J Respir Cell Mol Biol, 2004. **30**(1): p. 12-9.

168. Kurihara, H., et al., *Neurotrophins in cultured cells from periodontal tissues.* J Periodontol, 2003. **74**(1): p. 76-84.

169. McBride, H.M., M. Neuspiel, and S. Wasiak, *Mitochondria: more than just a powerhouse.* Curr Biol, 2006. **16**(14): p. R551-60.

170. Djousse, L., et al., *Weight loss in early stage of Huntington's disease.* Neurology, 2002. **59**(9): p. 1325-1330.

171. Gu, M., et al., *Mitochondrial defect in Huntington's disease caudate nucleus.* Ann.Neurol., 1996. **39**(3): p. 385-389.

172. Kuwert, T., et al., *Cortical and subcortical glucose consumption measured by PET in patients with Huntington's disease.* Brain, 1990. **113 (Pt 5)**: p. 1405-1423.

173. Jenkins, B.G., et al., *Evidence for impairment of energy metabolism in vivo in Huntington's disease using localized 1H NMR spectroscopy.* Neurology, 1993. **43**(12): p. 2689-2695.

174. Sanchez-Pernaute, R., et al., *Clinical correlation of striatal 1H MRS changes in Huntington's disease.* Neurology, 1999. **53**(4): p. 806-12.

175. Ciarmiello, A., et al., *Brain white-matter volume loss and glucose hypometabolism precede the clinical symptoms of Huntington's disease.* J.Nucl.Med., 2006. **47**(2): p. 215-222.

176. Saft, C., et al., *Mitochondrial impairment in patients and asymptomatic mutation carriers of Huntington's disease.* Mov Disord., 2005. **20**(6): p. 674-679.

177. Reynolds, N.C., Jr., R.W. Prost, and L.P. Mark, *Heterogeneity in 1H-MRS profiles of presymptomatic and early manifest Huntington's disease.* Brain Res., 2005. **1031**(1): p. 82-89.

178. Feigin, A., et al., *Thalamic metabolism and symptom onset in preclinical Huntington's disease.* Brain, 2007. **130**(Pt 11): p. 2858-2867.

179. Ludolph, A.C., et al., *3-Nitropropionic acid-exogenous animal neurotoxin and possible human striatal toxin.* Can J Neurol Sci, 1991. **18**(4): p. 492-8.

180. Beal, M.F., et al., *Neurochemical and histologic characterization of striatal excitotoxic lesions produced by the mitochondrial toxin 3-nitropropionic acid.* J.Neurosci., 1993. **13**(10): p. 4181-4192.

181. Palfi, S., et al., *Chronic 3-nitropropionic acid treatment in baboons replicates the cognitive and motor deficits of Huntington's disease.* J.Neurosci., 1996. **16**(9): p. 3019-3025.

182. Saulle, E., et al., *Neuronal vulnerability following inhibition of mitochondrial complex II: a possible ionic mechanism for Huntington's disease.* Mol.Cell Neurosci., 2004. **25**(1): p. 9-20.

183. Bonsi, P., et al., *Mitochondrial toxins in Basal Ganglia disorders: from animal models to therapeutic strategies.* Curr Neuropharmacol, 2006. **4**(1): p. 69-75.

184. Clark, D.S.L., *Basic Neurochemistry: Molecular, Cellular and Medical Aspects.*, in *Basic Neurochemistry: Molecular, Cellular and Medical Aspects.*, A.B. Siegel GJ, Albers RW, Fisher SK, Uhler MD, Editor 1999, Lippincott: Philadelphia. p. 637-70.

185. Hollenbeck, P.J. and W.M. Saxton, *The axonal transport of mitochondria.* J Cell Sci, 2005. **118**(Pt 23): p. 5411-9.

186. Vande Velde, C., et al., *Selective association of misfolded ALS-linked mutant SOD1 with the cytoplasmic face of mitochondria.* Proc Natl Acad Sci U S A, 2008. **105**(10): p. 4022-7.

187. Choo, Y.S., et al., *Mutant huntingtin directly increases susceptibility of mitochondria to the calcium-induced permeability transition and cytochrome c release.* Hum.Mol.Genet., 2004. **13**(14): p. 1407-1420.

188. Kegel, K.B., et al., *Polyglutamine expansion in huntingtin alters its interaction with phospholipids.* J Neurochem, 2009. **110**(5): p. 1585-97.

189. Acevedo-Torres, K., et al., *Mitochondrial DNA damage is a hallmark of chemically induced and the R6/2 transgenic model of Huntington's disease.* DNA Repair (Amst), 2009. **8**(1): p. 126-36.

190. Milakovic, T. and G.V. Johnson, *Mitochondrial respiration and ATP production are significantly impaired in striatal cells expressing mutant huntingtin.* J Biol Chem, 2005. **280**(35): p. 30773-82.

191. Gines, S., et al., *Specific progressive cAMP reduction implicates energy deficit in presymptomatic Huntington's disease knock-in mice.* Hum.Mol.Genet., 2003. **12**(5): p. 497-508.

192. Brustovetsky, N., et al., *Age-dependent changes in the calcium sensitivity of striatal mitochondria in mouse models of Huntington's Disease.* J.Neurochem., 2005. **93**(6): p. 1361-1370.

193. Oliveira, J.M., et al., *Mitochondrial dysfunction in Huntington's disease: the bioenergetics of isolated and in situ mitochondria from transgenic mice.* J.Neurochem., 2007. **101**(1): p. 241-249.

194. Lee, J.M., et al., *Unbiased gene expression analysis implicates the huntingtin polyglutamine tract in extra-mitochondrial energy metabolism.* PLoS.Genet., 2007. **3**(8): p. e135.

195. McGuire, J.R., et al., *Interaction of Huntingtin-associated protein-1 with kinesin light chain: implications in intracellular trafficking in neurons.* J Biol Chem, 2006. **281**(6): p. 3552-9.

196. Fransson, S., A. Ruusala, and P. Aspenstrom, *The atypical Rho GTPases Miro-1 and Miro-2 have essential roles in mitochondrial trafficking.* Biochem Biophys Res Commun, 2006. **344**(2): p. 500-10.

197. Glater, E.E., et al., *Axonal transport of mitochondria requires milton to recruit kinesin heavy chain and is light chain independent.* J Cell Biol, 2006. **173**(4): p. 545-57.

198. Gunawardena, S., et al., *Disruption of axonal transport by loss of huntingtin or expression of pathogenic polyQ proteins in Drosophila.* Neuron, 2003. **40**(1): p. 25-40.

199. Orr, A.L., et al., *N-terminal mutant huntingtin associates with mitochondria and impairs mitochondrial trafficking.* J.Neurosci., 2008. **28**(11): p. 2783-2792.

200. Gerfen, C.R., *The neostriatal mosaic: multiple levels of compartmental organization.* Trends Neurosci, 1992. **15**(4): p. 133-9.

201. Hedreen, J.C. and S.E. Folstein, *Early loss of neostriatal striosome neurons in Huntington's disease.* J.Neuropathol.Exp.Neurol., 1995. **54**(1): p. 105-120.

202. Luthi-Carter, R., et al., *Decreased expression of striatal signaling genes in a mouse model of Huntington's disease.* Hum.Mol.Genet., 2000. **9**(9): p. 1259-1271.

203. Cha, J.H., et al., *Altered brain neurotransmitter receptors in transgenic mice expressing a portion of an abnormal human huntington disease gene.* Proc Natl Acad Sci U S A, 1998. **95**(11): p. 6480-5.

204. Holt, D.J., A.M. Graybiel, and C.B. Saper, *Neurochemical architecture of the human striatum.* J Comp Neurol, 1997. **384**(1): p. 1-25.

205. Angulo, J.A. and B.S. McEwen, *Molecular aspects of neuropeptide regulation and function in the corpus striatum and nucleus accumbens.* Brain Res Brain Res Rev, 1994. **19**(1): p. 1-28.

206. Gerfen, C.R. and W.S. Young, 3rd, *Distribution of striatonigral and striatopallidal peptidergic neurons in both patch and matrix compartments: an in situ hybridization histochemistry and fluorescent retrograde tracing study.* Brain Res, 1988. **460**(1): p. 161-7.

207. Ferrante, R.J., et al., *Selective sparing of a class of striatal neurons in Huntington's disease.* Science, 1985. **230**(4725): p. 561-563.

208. Gerfen, C.R., K.G. Baimbridge, and J.J. Miller, *The neostriatal mosaic: compartmental distribution of calcium-binding protein and parvalbumin in the basal ganglia of the rat and monkey.* Proc Natl Acad Sci U S A, 1985. **82**(24): p. 8780-4.

209. Mitchell, I.J. and M.R. Griffiths, *The differential susceptibility of specific neuronal populations: insights from Huntington's disease.* IUBMB.Life, 2003. **55**(6): p. 293-298.

210. Aizman, O., et al., *Anatomical and physiological evidence for D1 and D2 dopamine receptor colocalization in neostriatal neurons.* Nat Neurosci, 2000. **3**(3): p. 226-30.

211. Surmeier, D.J., W.J. Song, and Z. Yan, *Coordinated expression of dopamine receptors in neostriatal medium spiny neurons.* J Neurosci, 1996. **16**(20): p. 6579-91.

212. Rudinskiy, N., et al., *Diminished hippocalcin expression in Huntington's disease brain does not account for increased striatal neuron vulnerability as assessed in primary neurons.* J Neurochem, 2009. **111**(2): p. 460-72.

213. Gasic, G.P. and M. Hollmann, *Molecular neurobiology of glutamate receptors.* Annu Rev Physiol, 1992. **54**: p. 507-36.

214. Aarts, M.M. and M. Tymianski, *Molecular mechanisms underlying specificity of excitotoxic signaling in neurons.* Curr Mol Med, 2004. **4**(2): p. 137-47.

215. Bouyer, J.J., et al., *Chemical and structural analysis of the relation between cortical inputs and tyrosine hydroxylase-containing terminals in rat neostriatum.* Brain Res, 1984. **302**(2): p. 267-75.

216. Wilson, C.J. and Y. Kawaguchi, *The origins of two-state spontaneous membrane potential fluctuations of neostriatal spiny neurons.* J Neurosci, 1996. **16**(7): p. 2397-410.

217. McGeer, E.G. and P.L. McGeer, *Duplication of biochemical changes of Huntington's chorea by intrastriatal injections of glutamic and kainic acids.* Nature, 1976. **263**(5577): p. 517-9.

218. Coyle, J.T. and R. Schwarcz, *Lesion of striatal neurones with kainic acid provides a model for Huntington's chorea.* Nature, 1976. **263**(5574): p. 244-6.

219. Figueredo-Cardenas, G., et al., *Relative survival of striatal projection neurons and interneurons after intrastriatal injection of quinolinic acid in rats.* Exp.Neurol., 1994. **129**(1): p. 37-56.

220. Rigby, M., et al., *The messenger RNAs for the N-methyl-D-aspartate receptor subunits show region-specific expression of different subunit composition in the human brain.* Neuroscience, 1996. **73**(2): p. 429-47.

221. Goebel, D.J. and M.S. Poosch, *NMDA receptor subunit gene expression in the rat brain: a quantitative analysis of endogenous mRNA levels of NR1Com, NR2A, NR2B, NR2C, NR2D and NR3A.* Brain Res Mol Brain Res, 1999. **69**(2): p. 164-70.

222. Schoepfer, R., et al., *Molecular biology of glutamate receptors.* Prog Neurobiol, 1994. **42**(2): p. 353-7.

223. Landwehrmeyer, G.B., et al., *NMDA receptor subunit mRNA expression by projection neurons and interneurons in rat striatum.* J Neurosci, 1995. **15**(7 Pt 2): p. 5297-307.

224. Kuppenbender, K.D., et al., *Expression of NMDA receptor subunit mRNAs in neurochemically identified projection and interneurons in the human striatum.* J Comp Neurol, 2000. **419**(4): p. 407-21.

225. Laurie, D.J., et al., *Regional, developmental and interspecies expression of the four NMDAR2 subunits, examined using monoclonal antibodies.* Brain Res Mol Brain Res, 1997. **51**(1-2): p. 23-32.

226. Kieburtz, K., et al., *A controlled trial of remacemide hydrochloride in Huntington's disease.* Mov Disord., 1996. **11**(3): p. 273-277.

227. Bonelli, R.M., et al., *Neuroprotection in Huntington's disease: a 2-year study on minocycline.* Int.Clin.Psychopharmacol., 2004. **19**(6): p. 337-342.

228. Handley, O.J., et al., *Pharmaceutical, cellular and genetic therapies for Huntington's disease.* Clin.Sci. (Lond), 2006. **110**(1): p. 73-88.

229. Estrada Sanchez, A.M., J. Mejia-Toiber, and L. Massieu, *Excitotoxic neuronal death and the pathogenesis of Huntington's disease.* Arch.Med.Res., 2008. **39**(3): p. 265-276.

230. Albin, R.L., A.B. Young, and J.B. Penney, *The functional anatomy of basal ganglia disorders.* Trends Neurosci, 1989. **12**(10): p. 366-75.

231. Joyce, J.N., et al., *Organization of dopamine D1 and D2 receptors in human striatum: receptor autoradiographic studies in Huntington's disease and schizophrenia.* Synapse, 1988. **2**(5): p. 546-557.

232. Filloux, F., et al., *Nigral dopamine type-1 receptors are reduced in Huntington's disease: a postmortem autoradiographic study using [3H]SCH 23390 and correlation with [3H]forskolin binding.* Exp.Neurol., 1990. **110**(2): p. 219-227.

233. Richfield, E.K., et al., *Heterogeneous dopamine receptor changes in early and late Huntington's disease.* Neurosci.Lett., 1991. **132**(1): p. 121-126.

234. Augood, S.J., R.L. Faull, and P.C. Emson, *Dopamine D1 and D2 receptor gene expression in the striatum in Huntington's disease.* Ann.Neurol., 1997. **42**(2): p. 215-221.

235. Sedvall, G., et al., *Dopamine D1 receptor number--a sensitive PET marker for early brain degeneration in Huntington's disease.* Eur.Arch.Psychiatry Clin.Neurosci., 1994. **243**(5): p. 249-255.

236. Turjanski, N., et al., *Striatal D1 and D2 receptor binding in patients with Huntington's disease and other choreas. A PET study.* Brain, 1995. **118 (Pt 3)**: p. 689-696.

237. Antonini, A., et al., *Striatal glucose metabolism and dopamine D2 receptor binding in asymptomatic gene carriers and patients with Huntington's disease.* Brain, 1996. **119 (Pt 6)**: p. 2085-2095.

238. Weeks, R.A., et al., *Striatal D1 and D2 dopamine receptor loss in asymptomatic mutation carriers of Huntington's disease.* Ann.Neurol., 1996. **40**(1): p. 49-54.

239. Ginovart, N., et al., *PET study of the pre- and post-synaptic dopaminergic markers for the neurodegenerative process in Huntington's disease.* Brain, 1997. **120 (Pt 3)**: p. 503-514.

240. Cass, W.A., *Decreases in evoked overflow of dopamine in rat striatum after neurotoxic doses of methamphetamine.* J Pharmacol Exp Ther, 1997. **280**(1): p. 105-13.

241. Tang, T.S., et al., *Dopaminergic signaling and striatal neurodegeneration in Huntington's disease.* J.Neurosci., 2007. **27**(30): p. 7899-7910.

242. Jakel, R.J. and W.F. Maragos, *Neuronal cell death in Huntington's disease: a potential role for dopamine.* Trends Neurosci., 2000. **23**(6): p. 239-245.

243. Gerfen, C.R., et al., *D1 and D2 dopamine receptor-regulated gene expression of striatonigral and striatopallidal neurons.* Science, 1990. **250**(4986): p. 1429-32.

244. Surmeier, D.J., et al., *D1 and D2 dopamine-receptor modulation of striatal glutamatergic signaling in striatal medium spiny neurons.* Trends Neurosci, 2007. **30**(5): p. 228-35.

245. Borgkvist, A. and G. Fisone, *Psychoactive drugs and regulation of the cAMP/PKA/DARPP-32 cascade in striatal medium spiny neurons.* Neurosci Biobehav Rev, 2007. **31**(1): p. 79-88.

246. Charvin, D., et al., *Unraveling a role for dopamine in Huntington's disease: the dual role of reactive oxygen species and D2 receptor stimulation.* Proc.Natl.Acad.Sci.U.S.A, 2005. **102**(34): p. 12218-12223.

247. Ferre, S., et al., *The striopallidal neuron: a main locus for adenosine-dopamine interactions in the brain.* J Neurosci, 1993. **13**(12): p. 5402-6.

248. Ferre, S., P. Snaprud, and K. Fuxe, *Opposing actions of an adenosine A2 receptor agonist and a GTP analogue on the regulation of dopamine D2 receptors in rat neostriatal membranes.* Eur J Pharmacol, 1993. **244**(3): p. 311-5.

249. Hirokawa, N. and R. Takemura, *Molecular motors and mechanisms of directional transport in neurons.* Nat Rev Neurosci, 2005. **6**(3): p. 201-14.

250. Duncan, J.E. and L.S. Goldstein, *The genetics of axonal transport and axonal transport disorders.* PLoS Genet, 2006. **2**(9): p. e124.

251. Hirokawa, N., *Kinesin and dynein superfamily proteins and the mechanism of organelle transport.* Science, 1998. **279**(5350): p. 519-26.

252. Brady, S.T., *A novel brain ATPase with properties expected for the fast axonal transport motor.* Nature, 1985. **317**(6032): p. 73-75.

253. Vale, R.D., T.S. Reese, and M.P. Sheetz, *Identification of a novel force-generating protein, kinesin, involved in microtubule-based motility.* Cell, 1985. **42**(1): p. 39-50.

254. Cyr, J.L., et al., *Molecular genetics of kinesin light chains: generation of isoforms by alternative splicing.* Proc Natl Acad Sci U S A, 1991. **88**(22): p. 10114-8.

255. Hirokawa, N., et al., *Submolecular domains of bovine brain kinesin identified by electron microscopy and monoclonal antibody decoration.* Cell, 1989. **56**(5): p. 867-78.

256. Asai, D.J. and M.P. Koonce, *The dynein heavy chain: structure, mechanics and evolution.* Trends Cell Biol, 2001. **11**(5): p. 196-202.

257. King, S.M., *The dynein microtubule motor.* Biochim Biophys Acta, 2000. **1496**(1): p. 60-75.

258. Roy, S., et al., *Axonal transport defects: a common theme in neurodegenerative diseases.* Acta Neuropathol, 2005. **109**(1): p. 5-13.

259. Zhao, C., et al., *Charcot-Marie-Tooth disease type 2A caused by mutation in a microtubule motor KIF1Bbeta.* Cell, 2001. **105**(5): p. 587-97.

260. Hafezparast, M., et al., *Mutations in dynein link motor neuron degeneration to defects in retrograde transport.* Science, 2003. **300**(5620): p. 808-12.

261. Sinadinos, C., et al., *Live axonal transport disruption by mutant huntingtin fragments in Drosophila motor neuron axons.* Neurobiol Dis, 2009.

262. Lee, W.C., M. Yoshihara, and J.T. Littleton, *Cytoplasmic aggregates trap polyglutamine-containing proteins and block axonal transport in a Drosophila model of Huntington's disease.* Proc.Natl.Acad.Sci.U.S.A, 2004. **101**(9): p. 3224-3229.

263. Wang, X., A. Destrument, and C. Tournier, *Physiological roles of MKK4 and MKK7: insights from animal models.* Biochim Biophys Acta, 2007. **1773**(8): p. 1349-57.

264. Asaoka, Y. and H. Nishina, *Diverse physiological functions of MKK4 and MKK7 during early embryogenesis.* J Biochem, 2010. **148**(4): p. 393-401.

265. Haeusgen, W., T. Herdegen, and V. Waetzig, *The bottleneck of JNK signaling: molecular and functional characteristics of MKK4 and MKK7.* Eur J Cell Biol, 2011. **90**(6-7): p. 536-44.

266. Cuevas, B.D., A.N. Abell, and G.L. Johnson, *Role of mitogen-activated protein kinase kinase kinases in signal integration.* Oncogene, 2007. **26**(22): p. 3159-71.

267. Yasuda, J., et al., *The JIP group of mitogen-activated protein kinase scaffold proteins.* Mol Cell Biol, 1999. **19**(10): p. 7245-54.

268. Ito, M., et al., *JSAP1, a novel jun N-terminal protein kinase (JNK)-binding protein that functions as a Scaffold factor in the JNK signaling pathway.* Mol Cell Biol, 1999. **19**(11): p. 7539-48.

269. Kelkar, N., et al., *Interaction of a mitogen-activated protein kinase signaling module with the neuronal protein JIP3.* Mol Cell Biol, 2000. **20**(3): p. 1030-43.

270. Yamasaki, T., H. Kawasaki, and H. Nishina, *Diverse Roles of JNK and MKK Pathways in the Brain.* J Signal Transduct, 2012. **2012**: p. 459265.

271. Pulverer, B.J., et al., *Phosphorylation of c-jun mediated by MAP kinases.* Nature, 1991. **353**(6345): p. 670-4.

272. Hibi, M., et al., *Identification of an oncoprotein- and UV-responsive protein kinase that binds and potentiates the c-Jun activation domain.* Genes Dev, 1993. **7**(11): p. 2135-48.

273. Zhang, Y., L. Zhou, and C.A. Miller, *A splicing variant of a death domain protein that is regulated by a mitogen-activated kinase is a substrate for c-Jun N-terminal kinase in the human central nervous system.* Proc Natl Acad Sci U S A, 1998. **95**(5): p. 2586-91.

274. Phelan, D.R., et al., *Activated JNK phosphorylates the c-terminal domain of MLK2 that is required for MLK2-induced apoptosis.* J.Biol.Chem., 2001. **276**(14): p. 10801-10810.

275. Donovan, N., et al., *JNK phosphorylation and activation of BAD couples the stress-activated signaling pathway to the cell death machinery.* J Biol Chem, 2002. **277**(43): p. 40944-9.

276. Bjorkblom, B., et al., *Constitutively active cytoplasmic c-Jun N-terminal kinase 1 is a dominant regulator of dendritic architecture: role of microtubule-associated protein 2 as an effector.* J Neurosci, 2005. **25**(27): p. 6350-61.

277. Westerlund, N., et al., *Phosphorylation of SCG10/stathmin-2 determines multipolar stage exit and neuronal migration rate.* Nat Neurosci, 2011. **14**(3): p. 305-13.

278. Chang, L., et al., *JNK1 is required for maintenance of neuronal microtubules and controls phosphorylation of microtubule-associated proteins.* Dev Cell, 2003. **4**(4): p. 521-33.

279. Unger, E.K., et al., *Functional role of c-Jun-N-terminal kinase in feeding regulation.* Endocrinology, 2010. **151**(2): p. 671-82.

280. Hirosumi, J., et al., *A central role for JNK in obesity and insulin resistance.* Nature, 2002. **420**(6913): p. 333-6.

281. Nishina, H., et al., *Defective liver formation and liver cell apoptosis in mice lacking the stress signaling kinase SEK1/MKK4.* Development, 1999. **126**(3): p. 505-16.

282. Hunot, S., et al., *JNK-mediated induction of cyclooxygenase 2 is required for neurodegeneration in a mouse model of Parkinson's disease.* Proc Natl Acad Sci U S A, 2004. **101**(2): p. 665-70.

283. Yang, D.D., et al., *Absence of excitotoxicity-induced apoptosis in the hippocampus of mice lacking the Jnk3 gene.* Nature, 1997. **389**(6653): p. 865-70.

284. Kuan, C.Y., et al., *A critical role of neural-specific JNK3 for ischemic apoptosis.* Proc Natl Acad Sci U S A, 2003. **100**(25): p. 15184-9.

285. Pirianov, G., et al., *Deletion of the c-Jun N-terminal kinase 3 gene protects neonatal mice against cerebral hypoxic-ischaemic injury.* J Cereb Blood Flow Metab, 2007. **27**(5): p. 1022-32.

286. Morishima, Y., et al., *Beta-amyloid induces neuronal apoptosis via a mechanism that involves the c-Jun N-terminal kinase pathway and the induction of Fas ligand.* J Neurosci, 2001. **21**(19): p. 7551-60.

287. Brecht, S., et al., *Specific pathophysiological functions of JNK isoforms in the brain.* Eur J Neurosci, 2005. **21**(2): p. 363-77.

288. Kuan, C.Y., et al., *The Jnk1 and Jnk2 protein kinases are required for regional specific apoptosis during early brain development.* Neuron, 1999. **22**(4): p. 667-76.

289. Eminel, S., et al., *c-Jun N-terminal kinases trigger both degeneration and neurite outgrowth in primary hippocampal and cortical neurons.* J Neurochem, 2008. **104**(4): p. 957-69.

290. Waetzig, V., Y. Zhao, and T. Herdegen, *The bright side of JNKs-Multitalented mediators in neuronal sprouting, brain development and nerve fiber regeneration.* Prog Neurobiol, 2006. **80**(2): p. 84-97.

291. Bevilaqua, L.R., et al., *Inhibition of hippocampal Jun N-terminal kinase enhances short-term memory but blocks long-term memory formation and retrieval of an inhibitory avoidance task.* Eur J Neurosci, 2003. **17**(4): p. 897-902.

292. Barnat, M., et al., *Distinct roles of c-Jun N-terminal kinase isoforms in neurite initiation and elongation during axonal regeneration.* J Neurosci, 2010. **30**(23): p. 7804-16.

293. Liu, Y.F., D. Dorow, and J. Marshall, *Activation of MLK2-mediated signaling cascades by polyglutamine-expanded huntingtin.* J Biol Chem, 2000. **275**(25): p. 19035-40.

294. Merienne, K., et al., *Polyglutamine expansion induces a protein-damaging stress connecting heat shock protein 70 to the JNK pathway.* J.Biol.Chem., 2003. **278**(19): p. 16957-16967.

295. Garcia, M., D. Charvin, and J. Caboche, *Expanded huntingtin activates the c-Jun terminal kinase/c-Jun pathway prior to aggregate formation in striatal neurons in culture.* Neuroscience, 2004. **127**(4): p. 859-870.

296. Apostol, B.L., et al., *Mutant huntingtin alters MAPK signaling pathways in PC12 and striatal cells: ERK1/2 protects against mutant huntingtin-associated toxicity.* Hum.Mol.Genet., 2006. **15**(2): p. 273-285.

297. Apostol, B.L., et al., *CEP-1347 reduces mutant huntingtin-associated neurotoxicity and restores BDNF levels in R6/2 mice.* Mol Cell Neurosci, 2008. **39**(1): p. 8-20.

298. Matsuura, H., et al., *Phosphorylation-dependent scaffolding role of JSAP1/JIP3 in the ASK1-JNK signaling pathway. A new mode of regulation of the MAP kinase cascade.* J Biol Chem, 2002. **277**(43): p. 40703-9.

299. Morfini, G., et al., *Fast axonal transport misregulation and Alzheimer's disease.* Neuromolecular.Med., 2002. **2**(2): p. 89-99.

300. Morfini, G., et al., *Glycogen synthase kinase 3 phosphorylates kinesin light chains and negatively regulates kinesin-based motility.* EMBO J., 2002. **21**(3): p. 281-293.

301. Morfini, G., et al., *A novel CDK5-dependent pathway for regulating GSK3 activity and kinesin-driven motility in neurons.* EMBO J., 2004. **23**(11): p. 2235-2245.

302. Nihei, K. and N.W. Kowall, *Neurofilament and neural cell adhesion molecule immunocytochemistry of Huntington's disease striatum.* Ann.Neurol., 1992. **31**(1): p. 59-63.

303. Lievens, J.C., et al., *Abnormal phosphorylation of synapsin I predicts a neuronal transmission impairment in the R6/2 Huntington's disease transgenic mice.* Mol.Cell Neurosci., 2002. **20**(4): p. 638-648.

304. Liu, Y.F., *Expression of polyglutamine-expanded Huntingtin activates the SEK1-JNK pathway and induces apoptosis in a hippocampal neuronal cell line.* J.Biol.Chem., 1998. **273**(44): p. 28873-28877.

305. Verhey, K.J., et al., *Cargo of kinesin identified as JIP scaffolding proteins and associated signaling molecules.* J Cell Biol, 2001. **152**(5): p. 959-70.

306. Kelkar, N., C.L. Standen, and R.J. Davis, *Role of the JIP4 scaffold protein in the regulation of mitogen-activated protein kinase signaling pathways.* Mol Cell Biol, 2005. **25**(7): p. 2733-43.

307. Bowman, A.B., et al., *Kinesin-dependent axonal transport is mediated by the sunday driver (SYD) protein.* Cell, 2000. **103**(4): p. 583-94.

308. Dajas-Bailador, F., E.V. Jones, and A.J. Whitmarsh, *The JIP1 scaffold protein regulates axonal development in cortical neurons.* Curr Biol, 2008. **18**(3): p. 221-6.

309. Brady, S.T., K.K. Pfister, and G.S. Bloom, *A monoclonal antibody against kinesin inhibits both anterograde and retrograde fast axonal transport in squid axoplasm.* Proc.Natl.Acad.Sci.U.S.A, 1990. **87**(3): p. 1061-1065.

310. Stenoien, D.L. and S.T. Brady, *Immunochemical analysis of kinesin light chain function.* Mol.Biol.Cell, 1997. **8**(4): p. 675-689.

311. Sack, S., et al., *X-ray structure of motor and neck domains from rat brain kinesin.* Biochemistry, 1997. **36**(51): p. 16155-65.

312. Collection), A.A.T.C. *ATCC Number CCL-131 Product Description*. 2012 [cited 2012 May 10]; Available from: http://www.atcc.org/ATCCAdvancedCatalogSearch/ProductDetails/tabid/452/Default.aspx?ATCCNum=CCL-131&Template=cellBiology.

313. Olmsted, J.B., et al., *Isolation of microtubule protein from cultured mouse neuroblastoma cells.* Proc Natl Acad Sci U S A, 1970. **65**(1): p. 129-36.

314. Dillon, C.P. *MIT Center for Cancer Research: LentiLox 3.7 (pLL3.7)*. 2005 [cited 2012 August 2]; Available from: http://web.mit.edu/jacks-lab/protocols/pll37.htm.

315. Kim, D. and J. Rossi, *RNAi mechanisms and applications.* Biotechniques, 2008. **44**(5): p. 613-6.

316. Rubinson, D.A., et al., *A lentivirus-based system to functionally silence genes in primary mammalian cells, stem cells and transgenic mice by RNA interference.* Nat Genet, 2003. **33**(3): p. 401-6.

317. OpenBiosystems. *GIPZ Lentiviral shRNA*. 2012 [cited 2012 August 2]; Available from: https://www.openbiosystems.com/RNAi/shRNAmirLibraries/GIPZLentiviralshRNAmir/.

318. Livak, K.J. and T.D. Schmittgen, *Analysis of relative gene expression data using real-time quantitative PCR and the 2(-Delta Delta C(T)) Method.* Methods, 2001. **25**(4): p. 402-8.

319. Davis, R.J., *Signal transduction by the JNK group of MAP kinases.* Cell, 2000. **103**(2): p. 239-52.

320. Mielke, K., et al., *Selective expression of JNK isoforms and stress-specific JNK activity in different neural cell lines.* Brain Res Mol Brain Res, 2000. **75**(1): p. 128-37.

321. Southwell, A.L. and P.H. Patterson, *Antibody therapy in neurodegenerative disease.* Rev Neurosci, 2010. **21**(4): p. 273-87.

322. Stathopulos, P.B., et al., *Sonication of proteins causes formation of aggregates that resemble amyloid.* Protein Sci., 2004. **13**(11): p. 3017-3027.

323. Davies, P., et al., *Consequences of poly-glutamine repeat length for the conformation and folding of the androgen receptor amino-terminal domain.* J Mol Endocrinol, 2008. **41**(5): p. 301-14.

324. Akins, R.E., P.M. Levin, and R.S. Tuan, *Cetyltrimethylammonium bromide discontinuous gel electrophoresis: Mr-based separation of proteins with retention of enzymatic activity.* Anal Biochem, 1992. **202**(1): p. 172-8.

325. Penney, J.B., Jr., et al., *CAG repeat number governs the development rate of pathology in Huntington's disease.* Ann.Neurol., 1997. **41**(5): p. 689-692.

326. Amaratunga, A., et al., *Inhibition of kinesin synthesis and rapid anterograde axonal transport in vivo by an antisense oligonucleotide.* J Biol Chem, 1993. **268**(23): p. 17427-30.

327. Feiguin, F., et al., *Kinesin-mediated organelle translocation revealed by specific cellular manipulations.* J Cell Biol, 1994. **127**(4): p. 1021-39.

328. Ferhat, L., et al., *Process formation results from the imbalance between motor-mediated forces.* J Cell Sci, 2001. **114**(Pt 21): p. 3899-904.

329. Tanaka, Y., et al., *Targeted disruption of mouse conventional kinesin heavy chain, kif5B, results in abnormal perinuclear clustering of mitochondria.* Cell, 1998. **93**(7): p. 1147-58.

330. Amato, S. and H.Y. Man, *AMPK signaling in neuronal polarization: Putting the brakes on axonal traffic of PI3-Kinase.* Commun Integr Biol, 2012. **5**(2): p. 152-5.

331. Pollema, S., *Mechanism of fast axonal transport inhibition by polyglutamine expanded huntingtin*, in *Anatomy and Cell Biology*2010, University of Illinois at Chicago: Chicago.

332. Oblinger, M.M., et al., *Cytotypic differences in the protein composition of the axonally transported cytoskeleton in mammalian neurons.* J.Neurosci., 1987. **7**(2): p. 453-462.

333. Fossale, E., et al., *Differential effects of the Huntington's disease CAG mutation in striatum and cerebellum are quantitative not qualitative.* Hum Mol Genet, 2011. **20**(21): p. 4258-67.

334. Luo, Y., et al., *D2 dopamine receptors stimulate mitogenesis through pertussis toxin-sensitive G proteins and Ras-involved ERK and SAP/JNK pathways in rat C6-D2L glioma cells.* J Neurochem, 1998. **71**(3): p. 980-90.

335. Zhen, X., et al., *D1 dopamine receptor agonists mediate activation of p38 mitogen-activated protein kinase and c-Jun amino-terminal kinase by a protein kinase A-dependent mechanism in SK-N-MC human neuroblastoma cells.* Mol Pharmacol, 1998. **54**(3): p. 453-8.

336. Science, A.I.f.B. 2012 [cited 2012 August 22]; Human Brain Microarray for HTT]. Available from: http://human.brain-map.org/microarray/search/show?exact_match=true&search_term=HTT&search_type=gene&page_num=0.

337. Science, A.I.f.B. 2012 2012 [cited 2012 August 22]; Mouse HTT ISH data]. Available from: http://mouse.brain-map.org/gene/show/14970.

338. Science, A.I.f.B. 2012 2012 [cited 2012 August 22]; Human Brain JNK3 Microarray]. Available from: http://human.brain-map.org/microarray/search/show?exact_match=false&search_term=JNK3&search_type=gene.

339. Resnick, L. and M. Fennell, *Targeting JNK3 for the treatment of neurodegenerative disorders.* Drug Discov Today, 2004. **9**(21): p. 932-9.

340. Abdelli, S., et al., *JNK3 is abundant in insulin-secreting cells and protects against cytokine-induced apoptosis.* Diabetologia, 2009. **52**(9): p. 1871-80.

341. Sathasivam, K., et al., *Formation of polyglutamine inclusions in non-CNS tissue.* Hum.Mol.Genet., 1999. **8**(5): p. 813-822.

342. Martin, B., et al., *Exendin-4 improves glycemic control, ameliorates brain and pancreatic pathologies, and extends survival in a mouse model of Huntington's disease.* Diabetes, 2009. **58**(2): p. 318-28.

343. Moffitt, H., et al., *Formation of polyglutamine inclusions in a wide range of non-CNS tissues in the HdhQ150 knock-in mouse model of Huntington's disease.* PLoS One, 2009. **4**(11): p. e8025.

344. Farrer, L.A., *Diabetes mellitus in Huntington disease.* Clin Genet, 1985. **27**(1): p. 62-7.

345. Lalic, N.M., et al., *Glucose homeostasis in Huntington disease: abnormalities in insulin sensitivity and early-phase insulin secretion.* Arch Neurol, 2008. **65**(4): p. 476-80.

346. *Mixed lineage kinase inhibitor CEP-1347 fails to delay disability in early Parkinson disease.* Neurology, 2007. **69**(15): p. 1480-90.

VITA

EDUCATION

08/04 - 05/14 University of Illinois at Chicago, College of Medicine, Medical Scientist Training Program, Chicago, IL
Doctor of Medicine, May 2014
Doctor of Philosophy, Neuroscience, May 2014

01/02 – 12/02 Johns Hopkins University, Baltimore, MD
Non-degree seeking student in the Masters of Biotechnology Program

08/95 - 05/99 University of California, Berkeley, Berkeley, CA
Bachelor of Arts: Molecular & Cell Biology, Neurobiology Emphasis, May 1999

AWARDS/HONORS

AY13- Association of Pathology Chairs Pathology Honor Society Membership
AY12 - 13 MSTP T32 Grant (GM079086-06)
AY10 - 12 CCTS-PECTS TL1 Fellowship (RR029877-02)
AY08 - 09 UIC Chancellor's Student Service and Leadership Awards
AY09 - 11 UIC Graduate Student Council Excellence in Service Award
AY06 - 07 Training Grant in the Neuroscience of Mental Health (T32MH067631)
AY95 - 98 UC Berkeley Alumni Leadership Scholarship

RESEARCH EXPERIENCE

12/08 - 9/12 *Graduate Student,* University of Illinois at Chicago, College of Medicine, Chicago, IL
• The Role of the c-Jun N-terminus kinase pathway in Huntington's Disease pathogenesis.
• Molecular pathogenic pathway in Amyotrophic Lateral Sclerosis.

06/06 - 12/08 *Graduate Student ,* University of Illinois at Chicago, College of Medicine/Rush University, Chicago, IL
•Viral vector delivery of neurotrophins for potential therapeutic use in Huntington's Disease

10/01 – 04/04 *Research Associate II,* Human Genome Sciences, Inc. Rockville, MD
• Toxicity and efficacy characterization of IND monoclonal antibody and chemotherapeutic agents for neuroblastoma and glioblastoma in vitro and in vivo

07/99 – 08/01 *Pre-doctoral Intramural Research Training Associate ,* DMNB/NINDS, NIH, Bethesda, MD
• Adeno-associated viral vector-mediated gene transfer results in long-term enzymatic and functional correction in multiple organs of Fabry mice.
• Intercellular delivery of VP22 fusion protein from cells infected with lentiviral vectors
• Design of an HIV-1 lentiviral-based gene trap vector to detect developmentally regulated genes in mammalian cells

EDUCATIONAL & PROFESSIONAL ORGANIZATIONS

AY13-	Association of Pathology Chairs Pathology Honor Society
AY08 - 09	Graduate Student Council, Secretary
AY06 - 11	Graduate Student Council, Graduate Program in Neuroscience Representative
AY09 - 12	Campus Care Student Health Plan Advisory Committee, Graduate College Representative
2010 -	American Physican Scientist Association, student member
2006 -	Society for Neuroscience, student member
2006 -	American Society for Neural Therapy and Repair, student member
2004 -	American Medical Student Association, member
2004 -	Asian Pacific American Medical Student Association, member

EXTRACURRICULAR ACTIVITIES

Graduate Student Council: governing Graduate Student Body consisting of representatives from all degree-granting programs in the UIC Graduate College; serves to advocate for, promote, and continually improve on academic and social aspects of graduate education.

Medical Scientist Training Program Student Advisory Committee: coordination and participation in multiple activities to enhance current and prospective UIC MSTP student experiences including creation of new MSTP Student Handbook, interviewee dinners, MSTP discussion coordinator/facilitator, speaker recruitment for student seminars, and fundraising for the Student Run Free Clinic.

Chicago Brain Bee: Annual event designed to expose high school students to primary neuroscience research and introduce students to professors and graduate students actively leading neuroscience research programs.

GirlTalk mentor/discussion facilitator: Mentor/intervention program targeting female juveniles at risk for incarceration.

Chinatown Free Clinic: Annual free medical screening clinic in Chicago Chinatown for uninsured and undocumented patients.

The Night Ministry: Chicago-based organization that provides healthcare, housing, and human connection to community members struggling with poverty or homelessness; specifically helped with free health screening and vaccinations.

Student Run Free Clinic: Privately funded community-based free clinic provides primary medical care to uninsured patients.

PUBLICATIONS

1. Lee, I.H., et al., *Calcinosis Cutis presenting in the context of long-term therapy for Chronic Myeloid Leukemia (CML): A Case Report and Review of the Literature.* International Wound Journal (submitted).
2. Han, I., et al., *Differential vulnerability of neurons in Huntington's disease: the role of cell type-specific features.* J Neurochem, 2010. 113(5): p. 1073-91.
3. Ramaswamy, S., et al., *Intrastriatal CERE-120 (AAV-Neurturin) protects striatal and cortical neurons and delays motor deficits in a transgenic mouse model of Huntington's disease.* Neurobiol Dis, 2009. 34(1): p. 40-50.

4. Lai, Z., et al., *Design of an HIV-1 lentiviral-based gene-trap vector to detect developmentally regulated genes in mammalian cells.* Proc Natl Acad Sci U S A, 2002. 99(6): p. 3651-6.
5. Jung, S.C., et al., *Adeno-associated viral vector-mediated gene transfer results in long-term enzymatic and functional correction in multiple organs of Fabry mice.* Proc Natl Acad Sci U S A, 2001. 98(5): p. 2676-81.
6. Lai, Z., et al., *Intercellular delivery of a herpes simplex virus VP22 fusion protein from cells infected with lentiviral vectors.* Proc Natl Acad Sci U S A, 2000. 97(21): p. 11297-302.
7. Han, I.P., *Physicians trade in paternalism for patient autonomy*. Issues Berkeley Medical Journal, 1996.

PRESENTATIONS/ABSTRACTS

1. Lee, I.H., Huang, E.D., and Morfini, G. *The role of specific c-jun N-terminus kinase isoforms in Huntington's disease pathogenesis.* American Physician Scientist Association annual meeting, Chicago, IL, 2013.
2. Lee, I.H., Huang, E.D., and Morfini, G. *The role of specific c-jun N-terminus kinase isoforms in Huntington's disease pathogenesis*. UIC College of Medicine Research Day Symposium, Chicago, IL, 2012.
3. Lee, I.H., Huang, E.D., and Morfini, G. *The role of the JNK kinase pathway in Huntington's disease pathogenesis*. Second Annual ApoE, ApoE Receptors & Neurodegeneration, Chicago, IL, 2011.
4. Lee, I.H., Huang, E.D., and Morfini, G. *The role of the JNK kinase pathway in Huntington's disease pathogenesis*. Brain Research Foundation Neuroscience Day, Chicago, IL, 2010.
5. Lee, I.H., Huang, E.D., and Morfini, G. T*he role of the JNK kinase pathway in Huntington's disease pathogenesis*. Chicago Biomedical Consortium, Chicago, IL, 2010.
6. Han, I.P., et al., *Protection of cortical neurons by AAV2-NTN (CERE-120) in the N171-82Q transgenic mouse model of Huntington's disease*. Society for Neuroscience, San Diego, CA, 2007.
7. Ramaswamy, S., Han, I.P., et al., *Effects of AAVNTN (CERE-120) in post-symptomatic and survival studies in a transgenic mouse model of Huntington's disease*. Society for Neuroscience, San Diego, CA, 2007.
8. Ramaswamy, S., Han, I.P., et al., *Gene therapy using AAV-Neurturin (Cere-120) in a transgenic mouse model of Huntington's disease.* Platform presentation at the Croucher Advanced Study Institute: Innovative Therapies of Movement Disorders: Basic and Clinical Sciences, Hong Kong, 2007.
9. Ramaswamy, S., Han, I.P., et al., *Gene therapy using AAV-Neurturin (Cere-120) in a transgenic mouse model of Huntington's disease – Pre-symptomatic, Post-symptomatic and Survival studies*. American Society for Neural Trasplantation and Repair, Clearwater, FL, 2008.

10. Alderson, R.F., et al., *TRAIL-R2 mAb, a human agonistic monoclonal antibody to tumor necrosis factor-related apoptosis inducing ligand receptor 2, induces apoptosis in human tumor cells*. 94th AACR Annual Meeting, Washington, D.C., 2003.
11. Lai, Z., Han, I., Park, M., and Brady, R.O., *Design of an HIV-1 lentiviral-based gene trap to detect developmentally regulated genes in mammalian cells*. The 5th Annual Meeting of the American Society of Gene Therapy, Boston, Massachusetts, 2002.
12. Lai Z.**,** Han, I., Reiser, J., and Brady, R.O., *Lentiviral vector-mediated gene delivery using a HIV-1 Tat fusion protein.* The 3rd Annual Meeting of the American Society of Gene Therapy, Denver, Colorado, 2000.
13. Lai, Z., Han, I., Reiser, J. and Brady, R.O., *Lentiviral vector-mediated gene delivery in vitro and in vivo using a herpes simplex virus VP22 fusion protein*. The 8th Annual Meeting of European Society of Gene Therapy, Stockholm, Sweden, 2000.

APPENDIX A
Reprint Permissions for Text

JOHN WILEY AND SONS LICENSE TERMS AND CONDITIONS

Mar 19, 2014

This is a License Agreement between Ina Han ("You") and John Wiley and Sons ("John Wiley and Sons") provided by Copyright Clearance Center ("CCC"). The license consists of your order details, the terms and conditions provided by John Wiley and Sons, and the payment terms and conditions.

All payments must be made in full to CCC. For payment instructions, please see information listed at the bottom of this form.

License Number	3352551296916
License date	Mar 19, 2014
Licensed content publisher	John Wiley and Sons
Licensed content publication	Journal of Neurochemistry
Licensed content title	Differential vulnerability of neurons in Huntington's disease: the role of cell type-specific features
Licensed copyright line	© 2010 The Authors. Journal Compilation © 2010 International Society for Neurochemistry
Licensed content author	Ina Han,YiMei You,Jeffrey H. Kordower,Scott T. Brady,Gerardo A. Morfini
Licensed content date	Mar 17, 2010
Start page	1073
End page	1091
Type of use	Dissertation/Thesis
Requestor type	Author of this Wiley article
Format	Electronic
Portion	Text extract
Number of Pages	12
Will you be translating?	No
Title of your thesis / dissertation	The Role of Specific c-Jun N-Terminus Kinase Isoforms in Huntington's Disease Pathogenesis
Expected completion date	May 2014
Expected size (number of pages)	130
Total	0.00 USD
Terms and Conditions	

TERMS AND CONDITIONS

APPENDIX A (continued)

This copyrighted material is owned by or exclusively licensed to John Wiley & Sons, Inc. or one of its group companies (each a "Wiley Company") or a society for whom a Wiley Company has exclusive publishing rights in relation to a particular journal (collectively "WILEY"). By clicking "accept" in connection with completing this licensing transaction, you agree that the following terms and conditions apply to this transaction (along with the billing and payment terms and conditions established by the Copyright Clearance Center Inc., ("CCC's Billing and Payment terms and conditions"), at the time that you opened your RightsLink account (these are available at any time at http://myaccount.copyright.com).

Terms and Conditions

1. The materials you have requested permission to reproduce (the "Materials") are protected by copyright.

2.You are hereby granted a personal, non-exclusive, non-sublicensable, non-transferable, worldwide, limited license to reproduce the Materials for the purpose specified in the licensing process. This license is for a one-time use only with a maximum distribution equal to the number that you identified in the licensing process. Any form of republication granted by this license must be completed within two years of the date of the grant of this license (although copies prepared before may be distributed thereafter). The Materials shall not be used in any other manner or for any other purpose. Permission is granted subject to an appropriate acknowledgement given to the author, title of the material/book/journal and the publisher. You shall also duplicate the copyright notice that appears in the Wiley publication in your use of the Material. Permission is also granted on the understanding that nowhere in the text is a previously published source acknowledged for all or part of this Material. Any third party material is expressly excluded from this permission.

3. With respect to the Materials, all rights are reserved. Except as expressly granted by the terms of the license, no part of the Materials may be copied, modified, adapted (except for minor reformatting required by the new Publication), translated, reproduced, transferred or distributed, in any form or by any means, and no derivative works may be made based on the Materials without the prior permission of the respective copyright owner. You may not alter, remove or suppress in any manner any copyright, trademark or other notices displayed by the Materials. You may not license, rent, sell, loan, lease, pledge, offer as security, transfer or assign the Materials, or any of the rights granted to you hereunder to any other person.

4. The Materials and all of the intellectual property rights therein shall at all times remain the exclusive property of John Wiley & Sons Inc or one of its related companies (WILEY) or their respective licensors, and your interest therein is only that of having possession of and the right to reproduce the Materials pursuant to Section 2 herein during the continuance of this Agreement. You agree that you own no right, title or interest in or to the Materials or any of the intellectual property rights therein. You shall have no rights hereunder other than the license as provided for above in Section 2. No right, license or interest to any trademark, trade name, service mark or other branding ("Marks") of WILEY or its licensors is granted hereunder, and you agree that you shall not assert any such right, license or interest with respect thereto.

5. NEITHER WILEY NOR ITS LICENSORS MAKES ANY WARRANTY OR REPRESENTATION OF ANY KIND TO YOU OR ANY THIRD PARTY, EXPRESS,

APPENDIX A (continued)

IMPLIED OR STATUTORY, WITH RESPECT TO THE MATERIALS OR THE ACCURACY OF ANY INFORMATION CONTAINED IN THE MATERIALS, INCLUDING, WITHOUT LIMITATION, ANY IMPLIED WARRANTY OF MERCHANTABILITY, ACCURACY, SATISFACTORY QUALITY, FITNESS FOR A PARTICULAR PURPOSE, USABILITY, INTEGRATION OR NON-INFRINGEMENT AND ALL SUCH WARRANTIES ARE HEREBY EXCLUDED BY WILEY AND ITS LICENSORS AND WAIVED BY YOU.

6. WILEY shall have the right to terminate this Agreement immediately upon breach of this Agreement by you.

7. You shall indemnify, defend and hold harmless WILEY, its Licensors and their respective directors, officers, agents and employees, from and against any actual or threatened claims, demands, causes of action or proceedings arising from any breach of this Agreement by you.

8. IN NO EVENT SHALL WILEY OR ITS LICENSORS BE LIABLE TO YOU OR ANY OTHER PARTY OR ANY OTHER PERSON OR ENTITY FOR ANY SPECIAL, CONSEQUENTIAL, INCIDENTAL, INDIRECT, EXEMPLARY OR PUNITIVE DAMAGES, HOWEVER CAUSED, ARISING OUT OF OR IN CONNECTION WITH THE DOWNLOADING, PROVISIONING, VIEWING OR USE OF THE MATERIALS REGARDLESS OF THE FORM OF ACTION, WHETHER FOR BREACH OF CONTRACT, BREACH OF WARRANTY, TORT, NEGLIGENCE, INFRINGEMENT OR OTHERWISE (INCLUDING, WITHOUT LIMITATION, DAMAGES BASED ON LOSS OF PROFITS, DATA, FILES, USE, BUSINESS OPPORTUNITY OR CLAIMS OF THIRD PARTIES), AND WHETHER OR NOT THE PARTY HAS BEEN ADVISED OF THE POSSIBILITY OF SUCH DAMAGES. THIS LIMITATION SHALL APPLY NOTWITHSTANDING ANY FAILURE OF ESSENTIAL PURPOSE OF ANY LIMITED REMEDY PROVIDED HEREIN.

9. Should any provision of this Agreement be held by a court of competent jurisdiction to be illegal, invalid, or unenforceable, that provision shall be deemed amended to achieve as nearly as possible the same economic effect as the original provision, and the legality, validity and enforceability of the remaining provisions of this Agreement shall not be affected or impaired thereby.

10. The failure of either party to enforce any term or condition of this Agreement shall not constitute a waiver of either party's right to enforce each and every term and condition of this Agreement. No breach under this agreement shall be deemed waived or excused by either party unless such waiver or consent is in writing signed by the party granting such waiver or consent. The waiver by or consent of a party to a breach of any provision of this Agreement shall not operate or be construed as a waiver of or consent to any other or subsequent breach by such other party.

11. This Agreement may not be assigned (including by operation of law or otherwise) by you without WILEY's prior written consent.

12. Any fee required for this permission shall be non-refundable after thirty (30) days from receipt

13. These terms and conditions together with CCC's Billing and Payment terms and conditions (which are incorporated herein) form the entire agreement between you and WILEY concerning this licensing transaction and (in the absence of fraud) supersedes all prior

APPENDIX A (continued)

agreements and representations of the parties, oral or written. This Agreement may not be amended except in writing signed by both parties. This Agreement shall be binding upon and inure to the benefit of the parties' successors, legal representatives, and authorized assigns.

14. In the event of any conflict between your obligations established by these terms and conditions and those established by CCC's Billing and Payment terms and conditions, these terms and conditions shall prevail.

15. WILEY expressly reserves all rights not specifically granted in the combination of (i) the license details provided by you and accepted in the course of this licensing transaction, (ii) these terms and conditions and (iii) CCC's Billing and Payment terms and conditions.

16. This Agreement will be void if the Type of Use, Format, Circulation, or Requestor Type was misrepresented during the licensing process.

17. This Agreement shall be governed by and construed in accordance with the laws of the State of New York, USA, without regards to such state's conflict of law rules. Any legal action, suit or proceeding arising out of or relating to these Terms and Conditions or the breach thereof shall be instituted in a court of competent jurisdiction in New York County in the State of New York in the United States of America and each party hereby consents and submits to the personal jurisdiction of such court, waives any objection to venue in such court and consents to service of process by registered or certified mail, return receipt requested, at the last known address of such party.

Wiley Open Access Terms and Conditions

Wiley publishes Open Access articles in both its Wiley Open Access Journals program [http://www.wileyopenaccess.com/view/index.html] and as Online Open articles in its subscription journals. The majority of Wiley Open Access Journals have adopted the Creative Commons Attribution License (CC BY) which permits the unrestricted use, distribution, reproduction, adaptation and commercial exploitation of the article in any medium. No permission is required to use the article in this way provided that the article is properly cited and other license terms are observed. A small number of Wiley Open Access journals have retained the Creative Commons Attribution Non Commercial License (CC BY-NC), which permits use, distribution and reproduction in any medium, provided the original work is properly cited and is not used for commercial purposes.

Online Open articles - Authors selecting Online Open are, unless particular exceptions apply, offered a choice of Creative Commons licenses. They may therefore select from the CC BY, the CC BY-NC and the Attribution-NoDerivatives (CC BY-NC-ND). The CC BY-NC-ND is more restrictive than the CC BY-NC as it does not permit adaptations or modifications without rights holder consent.

Wiley Open Access articles are protected by copyright and are posted to repositories and websites in accordance with the terms of the applicable Creative Commons license referenced on the article. At the time of deposit, Wiley Open Access articles include all changes made during peer review, copyediting, and publishing. Repositories and websites that host the article are responsible for incorporating any publisher-supplied amendments or retractions issued subsequently.
Wiley Open Access articles are also available without charge on Wiley's publishing platform, **Wiley Online Library** or any successor sites.

APPENDIX A (continued)

Conditions applicable to all Wiley Open Access articles:

- The authors' moral rights must not be compromised. These rights include the right of "paternity" (also known as "attribution" - the right for the author to be identified as such) and "integrity" (the right for the author not to have the work altered in such a way that the author's reputation or integrity may be damaged).

- Where content in the article is identified as belonging to a third party, it is the obligation of the user to ensure that any reuse complies with the copyright policies of the owner of that content.

- If article content is copied, downloaded or otherwise reused for research and other purposes as permitted, a link to the appropriate bibliographic citation (authors, journal, article title, volume, issue, page numbers, DOI and the link to the definitive published version on Wiley Online Library) should be maintained. Copyright notices and disclaimers must not be deleted.
    - Creative Commons licenses are copyright licenses and do not confer any other rights, including but not limited to trademark or patent rights.

- Any translations, for which a prior translation agreement with Wiley has not been agreed, must prominently display the statement: "This is an unofficial translation of an article that appeared in a Wiley publication. The publisher has not endorsed this translation."

Conditions applicable to non-commercial licenses (CC BY-NC and CC BY-NC-ND)

For non-commercial and non-promotional purposes individual non-commercial users may access, download, copy, display and redistribute to colleagues Wiley Open Access articles. In addition, articles adopting the CC BY-NC may be adapted, translated, and text- and data-mined subject to the conditions above.

Use by commercial "for-profit" organizations

Use of non-commercial Wiley Open Access articles for commercial, promotional, or marketing purposes requires further explicit permission from Wiley and will be subject to a fee. Commercial purposes include:

- Copying or downloading of articles, or linking to such articles for further redistribution, sale or licensing;

- Copying, downloading or posting by a site or service that incorporates advertising with such content;

- The inclusion or incorporation of article content in other works or services (other than normal quotations with an appropriate citation) that is then available for sale or licensing, for a fee (for example, a compilation produced for marketing purposes, inclusion in a sales pack)

APPENDIX A (continued)

- Use of article content (other than normal quotations with appropriate citation) by for-profit organizations for promotional purposes
- Linking to article content in e-mails redistributed for promotional, marketing or educational purposes;
- Use for the purposes of monetary reward by means of sale, resale, license, loan, transfer or other form of commercial exploitation such as marketing products
- Print reprints of Wiley Open Access articles can be purchased from: corporatesales@wiley.com

The modification or adaptation for any purpose of an article referencing the CC BY-NC-ND License requires consent which can be requested from RightsLink@wiley.com .

Other Terms and Conditions:

BY CLICKING ON THE "I AGREE..." BOX, YOU ACKNOWLEDGE THAT YOU HAVE READ AND FULLY UNDERSTAND EACH OF THE SECTIONS OF AND PROVISIONS SET FORTH IN THIS AGREEMENT AND THAT YOU ARE IN AGREEMENT WITH AND ARE WILLING TO ACCEPT ALL OF YOUR OBLIGATIONS AS SET FORTH IN THIS AGREEMENT.

v1.8

If you would like to pay for this license now, please remit this license along with your payment made payable to "COPYRIGHT CLEARANCE CENTER" otherwise you will be invoiced within 48 hours of the license date. Payment should be in the form of a check or money order referencing your account number and this invoice number RLNK501255365.
Once you receive your invoice for this order, you may pay your invoice by credit card. Please follow instructions provided at that time.

Make Payment To:
Copyright Clearance Center
Dept 001
P.O. Box 843006
Boston, MA 02284-3006

For suggestions or comments regarding this order, contact RightsLink Customer Support: customercare@copyright.com or +1-877-622-5543 (toll free in the US) or +1-978-646-2777.

Gratis licenses (referencing $0 in the Total field) are free. Please retain this printable license for your reference. No payment is required.

APPENDIX A (continued)

APPENDIX B
Reprint Permissions for Figures

JOHN WILEY AND SONS LICENSE TERMS AND CONDITIONS

Mar 19, 2014

This is a License Agreement between Ina Han ("You") and John Wiley and Sons ("John Wiley and Sons") provided by Copyright Clearance Center ("CCC"). The license consists of your order details, the terms and conditions provided by John Wiley and Sons, and the payment terms and conditions.

All payments must be made in full to CCC. For payment instructions, please see information listed at the bottom of this form.

License Number	3352550888554
License date	Mar 19, 2014
Licensed content publisher	John Wiley and Sons
Licensed content publication	Journal of Neurochemistry
Licensed content title	Differential vulnerability of neurons in Huntington's disease: the role of cell type-specific features
Licensed copyright line	© 2010 The Authors. Journal Compilation © 2010 International Society for Neurochemistry
Licensed content author	Ina Han,YiMei You,Jeffrey H. Kordower,Scott T. Brady,Gerardo A. Morfini
Licensed content date	Mar 17, 2010
Start page	1073
End page	1091
Type of use	Dissertation/Thesis
Requestor type	Author of this Wiley article
Format	Electronic
Portion	Figure/table
Number of figures/tables	2
Original Wiley figure/table number(s)	Figures 1 and 3
Will you be translating?	No
Title of your thesis / dissertation	The Role of Specific c-Jun N-Terminus Kinase Isoforms in Huntington's Disease Pathogenesis
Expected completion date	May 2014
Expected size (number of pages)	130
Total	0.00 USD
Terms and Conditions	

APPENDIX B (continued)

TERMS AND CONDITIONS

This copyrighted material is owned by or exclusively licensed to John Wiley & Sons, Inc. or one of its group companies (each a "Wiley Company") or a society for whom a Wiley Company has exclusive publishing rights in relation to a particular journal (collectively "WILEY"). By clicking "accept" in connection with completing this licensing transaction, you agree that the following terms and conditions apply to this transaction (along with the billing and payment terms and conditions established by the Copyright Clearance Center Inc., ("CCC's Billing and Payment terms and conditions"), at the time that you opened your RightsLink account (these are available at any time at http://myaccount.copyright.com).

Terms and Conditions

1. The materials you have requested permission to reproduce (the "Materials") are protected by copyright.

2.You are hereby granted a personal, non-exclusive, non-sublicensable, non-transferable, worldwide, limited license to reproduce the Materials for the purpose specified in the licensing process. This license is for a one-time use only with a maximum distribution equal to the number that you identified in the licensing process. Any form of republication granted by this license must be completed within two years of the date of the grant of this license (although copies prepared before may be distributed thereafter). The Materials shall not be used in any other manner or for any other purpose. Permission is granted subject to an appropriate acknowledgement given to the author, title of the material/book/journal and the publisher. You shall also duplicate the copyright notice that appears in the Wiley publication in your use of the Material. Permission is also granted on the understanding that nowhere in the text is a previously published source acknowledged for all or part of this Material. Any third party material is expressly excluded from this permission.

3. With respect to the Materials, all rights are reserved. Except as expressly granted by the terms of the license, no part of the Materials may be copied, modified, adapted (except for minor reformatting required by the new Publication), translated, reproduced, transferred or distributed, in any form or by any means, and no derivative works may be made based on the Materials without the prior permission of the respective copyright owner. You may not alter, remove or suppress in any manner any copyright, trademark or other notices displayed by the Materials. You may not license, rent, sell, loan, lease, pledge, offer as security, transfer or assign the Materials, or any of the rights granted to you hereunder to any other person.

4. The Materials and all of the intellectual property rights therein shall at all times remain the exclusive property of John Wiley & Sons Inc or one of its related companies (WILEY) or their respective licensors, and your interest therein is only that of having possession of and the right to reproduce the Materials pursuant to Section 2 herein during the continuance of this Agreement. You agree that you own no right, title or interest in or to the Materials or any of the intellectual property rights therein. You shall have no rights hereunder other than the license as provided for above in Section 2. No right, license or interest to any trademark, trade name, service mark or other branding ("Marks") of WILEY or its licensors is granted hereunder, and you agree that you shall not assert any such right, license or interest with respect thereto.

APPENDIX B (continued)

5. NEITHER WILEY NOR ITS LICENSORS MAKES ANY WARRANTY OR REPRESENTATION OF ANY KIND TO YOU OR ANY THIRD PARTY, EXPRESS, IMPLIED OR STATUTORY, WITH RESPECT TO THE MATERIALS OR THE ACCURACY OF ANY INFORMATION CONTAINED IN THE MATERIALS, INCLUDING, WITHOUT LIMITATION, ANY IMPLIED WARRANTY OF MERCHANTABILITY, ACCURACY, SATISFACTORY QUALITY, FITNESS FOR A PARTICULAR PURPOSE, USABILITY, INTEGRATION OR NON-INFRINGEMENT AND ALL SUCH WARRANTIES ARE HEREBY EXCLUDED BY WILEY AND ITS LICENSORS AND WAIVED BY YOU.

6. WILEY shall have the right to terminate this Agreement immediately upon breach of this Agreement by you.

7. You shall indemnify, defend and hold harmless WILEY, its Licensors and their respective directors, officers, agents and employees, from and against any actual or threatened claims, demands, causes of action or proceedings arising from any breach of this Agreement by you.

8. IN NO EVENT SHALL WILEY OR ITS LICENSORS BE LIABLE TO YOU OR ANY OTHER PARTY OR ANY OTHER PERSON OR ENTITY FOR ANY SPECIAL, CONSEQUENTIAL, INCIDENTAL, INDIRECT, EXEMPLARY OR PUNITIVE DAMAGES, HOWEVER CAUSED, ARISING OUT OF OR IN CONNECTION WITH THE DOWNLOADING, PROVISIONING, VIEWING OR USE OF THE MATERIALS REGARDLESS OF THE FORM OF ACTION, WHETHER FOR BREACH OF CONTRACT, BREACH OF WARRANTY, TORT, NEGLIGENCE, INFRINGEMENT OR OTHERWISE (INCLUDING, WITHOUT LIMITATION, DAMAGES BASED ON LOSS OF PROFITS, DATA, FILES, USE, BUSINESS OPPORTUNITY OR CLAIMS OF THIRD PARTIES), AND WHETHER OR NOT THE PARTY HAS BEEN ADVISED OF THE POSSIBILITY OF SUCH DAMAGES. THIS LIMITATION SHALL APPLY NOTWITHSTANDING ANY FAILURE OF ESSENTIAL PURPOSE OF ANY LIMITED REMEDY PROVIDED HEREIN.

9. Should any provision of this Agreement be held by a court of competent jurisdiction to be illegal, invalid, or unenforceable, that provision shall be deemed amended to achieve as nearly as possible the same economic effect as the original provision, and the legality, validity and enforceability of the remaining provisions of this Agreement shall not be affected or impaired thereby.

10. The failure of either party to enforce any term or condition of this Agreement shall not constitute a waiver of either party's right to enforce each and every term and condition of this Agreement. No breach under this agreement shall be deemed waived or excused by either party unless such waiver or consent is in writing signed by the party granting such waiver or consent. The waiver by or consent of a party to a breach of any provision of this Agreement shall not operate or be construed as a waiver of or consent to any other or subsequent breach by such other party.

11. This Agreement may not be assigned (including by operation of law or otherwise) by you without WILEY's prior written consent.

12. Any fee required for this permission shall be non-refundable after thirty (30) days from receipt

13. These terms and conditions together with CCC's Billing and Payment terms and conditions

APPENDIX B (continued)

(which are incorporated herein) form the entire agreement between you and WILEY concerning this licensing transaction and (in the absence of fraud) supersedes all prior agreements and representations of the parties, oral or written. This Agreement may not be amended except in writing signed by both parties. This Agreement shall be binding upon and inure to the benefit of the parties' successors, legal representatives, and authorized assigns.

14. In the event of any conflict between your obligations established by these terms and conditions and those established by CCC's Billing and Payment terms and conditions, these terms and conditions shall prevail.

15. WILEY expressly reserves all rights not specifically granted in the combination of (i) the license details provided by you and accepted in the course of this licensing transaction, (ii) these terms and conditions and (iii) CCC's Billing and Payment terms and conditions.

16. This Agreement will be void if the Type of Use, Format, Circulation, or Requestor Type was misrepresented during the licensing process.

17. This Agreement shall be governed by and construed in accordance with the laws of the State of New York, USA, without regards to such state's conflict of law rules. Any legal action, suit or proceeding arising out of or relating to these Terms and Conditions or the breach thereof shall be instituted in a court of competent jurisdiction in New York County in the State of New York in the United States of America and each party hereby consents and submits to the personal jurisdiction of such court, waives any objection to venue in such court and consents to service of process by registered or certified mail, return receipt requested, at the last known address of such party.

Wiley Open Access Terms and Conditions

Wiley publishes Open Access articles in both its Wiley Open Access Journals program [http://www.wileyopenaccess.com/view/index.html] and as Online Open articles in its subscription journals. The majority of Wiley Open Access Journals have adopted the Creative Commons Attribution License (CC BY) which permits the unrestricted use, distribution, reproduction, adaptation and commercial exploitation of the article in any medium. No permission is required to use the article in this way provided that the article is properly cited and other license terms are observed. A small number of Wiley Open Access journals have retained the Creative Commons Attribution Non Commercial License (CC BY-NC), which permits use, distribution and reproduction in any medium, provided the original work is properly cited and is not used for commercial purposes.

Online Open articles - Authors selecting Online Open are, unless particular exceptions apply, offered a choice of Creative Commons licenses. They may therefore select from the CC BY, the CC BY-NC and the Attribution-NoDerivatives (CC BY-NC-ND). The CC BY-NC-ND is more restrictive than the CC BY-NC as it does not permit adaptations or modifications without rights holder consent.

Wiley Open Access articles are protected by copyright and are posted to repositories and websites in accordance with the terms of the applicable Creative Commons license referenced on the article. At the time of deposit, Wiley Open Access articles include all changes made during peer review, copyediting, and publishing. Repositories and websites that host the article are responsible for incorporating any publisher-supplied amendments or retractions issued subsequently.

Wiley Open Access articles are also available without charge on Wiley's publishing platform,

APPENDIX B (continued)

Wiley Online Library or any successor sites.

Conditions applicable to all Wiley Open Access articles:

- The authors' moral rights must not be compromised. These rights include the right of "paternity" (also known as "attribution" - the right for the author to be identified as such) and "integrity" (the right for the author not to have the work altered in such a way that the author's reputation or integrity may be damaged).

- Where content in the article is identified as belonging to a third party, it is the obligation of the user to ensure that any reuse complies with the copyright policies of the owner of that content.

- If article content is copied, downloaded or otherwise reused for research and other purposes as permitted, a link to the appropriate bibliographic citation (authors, journal, article title, volume, issue, page numbers, DOI and the link to the definitive published version on Wiley Online Library) should be maintained. Copyright notices and disclaimers must not be deleted.
    - Creative Commons licenses are copyright licenses and do not confer any other rights, including but not limited to trademark or patent rights.

- Any translations, for which a prior translation agreement with Wiley has not been agreed, must prominently display the statement: "This is an unofficial translation of an article that appeared in a Wiley publication. The publisher has not endorsed this translation."

Conditions applicable to non-commercial licenses (CC BY-NC and CC BY-NC-ND)

For non-commercial and non-promotional purposes individual non-commercial users may access, download, copy, display and redistribute to colleagues Wiley Open Access articles. In addition, articles adopting the CC BY-NC may be adapted, translated, and text- and data-mined subject to the conditions above.

Use by commercial "for-profit" organizations

Use of non-commercial Wiley Open Access articles for commercial, promotional, or marketing purposes requires further explicit permission from Wiley and will be subject to a fee. Commercial purposes include:

- Copying or downloading of articles, or linking to such articles for further redistribution, sale or licensing;

- Copying, downloading or posting by a site or service that incorporates advertising with such content;

- The inclusion or incorporation of article content in other works or services (other than normal quotations with an appropriate citation) that is then available for sale or licensing, for a fee (for example, a compilation produced for marketing

APPENDIX B (continued)

purposes, inclusion in a sales pack)

- Use of article content (other than normal quotations with appropriate citation) by for-profit organizations for promotional purposes
- Linking to article content in e-mails redistributed for promotional, marketing or educational purposes;
- Use for the purposes of monetary reward by means of sale, resale, license, loan, transfer or other form of commercial exploitation such as marketing products
- Print reprints of Wiley Open Access articles can be purchased from: corporatesales@wiley.com

The modification or adaptation for any purpose of an article referencing the CC BY-NC-ND License requires consent which can be requested from RightsLink@wiley.com .

Other Terms and Conditions:

BY CLICKING ON THE "I AGREE..." BOX, YOU ACKNOWLEDGE THAT YOU HAVE READ AND FULLY UNDERSTAND EACH OF THE SECTIONS OF AND PROVISIONS SET FORTH IN THIS AGREEMENT AND THAT YOU ARE IN AGREEMENT WITH AND ARE WILLING TO ACCEPT ALL OF YOUR OBLIGATIONS AS SET FORTH IN THIS AGREEMENT.

v1.8

If you would like to pay for this license now, please remit this license along with your payment made payable to "COPYRIGHT CLEARANCE CENTER" otherwise you will be invoiced within 48 hours of the license date. Payment should be in the form of a check or money order referencing your account number and this invoice number RLNK501255350.
Once you receive your invoice for this order, you may pay your invoice by credit card. Please follow instructions provided at that time.

Make Payment To:
Copyright Clearance Center
Dept 001
P.O. Box 843006
Boston, MA 02284-3006

For suggestions or comments regarding this order, contact RightsLink Customer Support: customercare@copyright.com or +1-877-622-5543 (toll free in the US) or +1-978-646-2777.

Gratis licenses (referencing $0 in the Total field) are free. Please retain this printable

APPENDIX B (continued)

license for your reference. No payment is required.